

Possible roles of ULTRAPETALA in root development

Dissertation

zur Erlangung des Doktorgrades der
Mathematisch-Naturwissenschaftlichen Fakultät
der Christian-Albrechts-Universität
zu Kiel

vorgelegt von
Melanie Demuth
aus Erfurt

Kiel
2017

Possible roles of ULTRAPETALA in root development

Dissertation

zur Erlangung des Doktorgrades der
Mathematisch-Naturwissenschaftlichen Fakultät
der Christian-Albrechts-Universität
zu Kiel

vorgelegt von
Melanie Demuth
aus Erfurt

Kiel
2017

Referent/in: Prof. Dr. Margret Sauter

Korreferent/in: Prof. Dr. Eva H. Stukenbrock

Tag der mündlichen Prüfung: 13.06.2017

Zum Druck genehmigt:

CONTENTS

1	ABBREVIATIONS	5
2	ZUSAMMENFASSUNG	7
3	SUMMARY	9
4	INTRODUCTION.....	10
4.1	Genetic and hormonal control of root organogenesis	10
4.1.1	Specification and function of the primary root and its root cap.....	11
4.1.2	Lateral root formation	13
4.1.3	Adventitious root formation.....	14
4.2	Mechanical forces influence root growth and morphology	17
4.3	ULTRAPETALA functions in reprogramming of cell fate in shoot and flower meristem of <i>Arabidopsis thaliana</i> L.....	20
4.4	The Arabidopsis ALTERNATIVE NAD (P) H dehydrogenase A1 may balance reactive oxygen species homeostasis	22
5	MATERIALS AND METHODS	25
5.1	Plant material and growth conditions	25
5.2	Genotyping of T-DNA insertion lines.....	25
5.3	Isolation of total RNA	26
5.4	Polymerase chain reaction (PCR) and gel electrophoresis ...	27
5.5	Quantitative real time PCR (qPCR).....	28
5.6	Cloning and transformations	28
5.7	Plasmid isolation.....	32
5.8	Crossing of plants	33
5.9	Treatment with ethylene or 1-Methylcyclopropene (1-MCP) .	33
5.10	Growth measurements.....	33

5.11	Histochemical Lugol’s and GUS staining.....	34
5.12	mPSPI (modified pseudo-Schiff propidium iodide) staining...	34
5.13	Statistical evaluation of the data	35
5.14	Databases for bioinformatics.....	35
6	RESULTS	36
6.1	Sequence and expression analysis of ULTRAPETALA1 and ALTERNATIVE NAD (P) H DEHYDROGENASE A1	36
6.2	Root growth in response to mechanical stress and ethylene	51
6.3	A role for AtULT1 in root development.....	63
7	PERSPECTIVES.....	81
8	DISCUSSION.....	85
8.1	Rice epidermal cells change cell fate in response to mechanical and ROS signalling	85
8.1.1	In Arabidopsis mechanical signals have impacts on morphology and development of roots	85
8.1.2	ALTERNATIVE NAD (P) H DEHYDROGENASE A might act in reactive oxygen species homeostasis.....	87
8.2	Root organogenesis.....	91
8.2.1	Cell cycle regulation and meristem maintenance	91
8.2.2	ULTRAPETALA1 and auxin may act in converging regulatory networks	96
9	REFERENCES	101
10	SUPPLEMENTAL DATA.....	117
11	DECLARATION OF AUTHORSHIP	121
12	CURRICULUM VITAE.....	122

1 ABBREVIATIONS

1-MCP	1-Methylcyclopropene
<i>A. tumefaciens</i>	<i>Agrobacterium tumefaciens</i>
ABCB	ATP-binding cassette B
ACC	1-Aminocyclopropane-1-carboxylic acid
ACR	Arabidopsis crinkly
ACT	Actin
AG	Agamous
ARF	Auxin response factor
At	<i>Arabidopsis thaliana</i>
ATP	Adenosine triphosphate
ATX	Arabidopsis homolog of trithorax
AUX	Auxin resistant
bp	Base pairs
CDK	Cyclin-dependent kinase
cDNA	Complementary DNA
CLE	CLAVATA3/ESR-related
CLV	Clavata
CRL	Crown rootless
Ct	Cycle threshold
CYCD	Cyclin D
DAI	Days after seed imbibition
DNA	Deoxyribonucleic acid
E	Amplification efficiency
<i>E. coli</i>	<i>Escherichia coli</i>
ETC	Electron transport chain
EZ	Elongation zone
GAPC subunit	Glycerinaldehyde-3-phosphate dehydrogenase C
GOI	Gene of interest
GUS	Beta-glucuronidase
IAA	Indole-3-acetic acid
LAX	Like AUX
LB	Lysogeny broth
MIR	MicroRNA
mPSPI	Modified pseudo-Schiff propidium iodide
MS	Murashige-Skoog
MZ	Meristematic zone
NAA	1-Naphthaleneacetic acid

NCBI	National Center for Biotechnology Information
NDA	Alternative NAD (P) H dehydrogenase A
OD	Optical density
PCD	Programmed cell death
PcG	Polycomb group
PCR	Polymerase chain reaction
Pfu	<i>Pyrococcus furiosus</i>
PIN	Pin-formed
PLT	Plethora
PTS	Peroxisomal targeting signal
QC	Quiescence centre
qPCR	Quantitative real time PCR
R	Expression ratio
RAM	Root apical meristem
RCJ	Root cap junction
Ref	Reference gene
RGAP	MSU Rice Genome Annotation Project
RNA	Ribonucleic acid
ROS	Reactive oxygen species
RT	Room temperature
RT-PCR	Reverse transcription PCR
SAM	Shoot apical meristem
Sc	<i>Saccharomyces cerevisiae</i>
SCR	Scarecrow
SDS	Sodium dodecyl sulfate
SHR	Short root
SMB	Sombrero
TAIR	The Arabidopsis Information Resource
T-DNA	Transfer DNA
TrxG	Trithorax group
TZ	Transition zone
ULT	Ultrapetala
WOX	WUSCHEL related homeobox
WUS	Wuschel

2 ZUSAMMENFASSUNG

Das Ziel dieser Studie war Expressionen und *in vivo* Funktionen des transkriptionellen Anti-Repressors ULTRAPETALA1 (ULT1) und der mitochondrial lokalisierten ALTERNATIVE NAD (P) H DEHYDROGENASE A1 (NDA1) in Wurzeln von Arabidopsis zu beschreiben. Spezifische Expression von *AtNDA1* und *AtULT1* wurde in der Wurzelhaube von Primärwurzeln festgestellt. Zusätzlich wurde *AtULT1* Expression an Basis und Apex von Lateral- und Adventivwurzeln nachgewiesen. Für die Reishomologe, *OsULT1* und *OsNDA1*, wurde aufgrund differentieller Expression in Epidermiszellen, welche durch Widerstand und reaktive Sauerstoffspezies zum Zelltod programmiert werden, eine mögliche Beteiligung in mechanischer Signaltransduktion vermutet. Daran anknüpfend wurden in Arabidopsis an den Nullmutanten, *nda1-1* und *ult1-3*, Auswirkungen von mechanischen Belastungen auf Morphologie und Wuchsverhalten der Wurzeln analysiert. Es zeigte sich, dass *AtNDA1* und *AtULT1* Wachstum von Primärwurzeln beeinflussen. Die beobachteten Phänotypen schienen jedoch unabhängig von mechanischen Stress aufzutreten. Beim Reis erleichtert mechanisch-induzierter Zelltod der Epidermis das Auswachsen von darunterliegenden Adventivwurzeln (Steffens et al., 2012). In Arabidopsis bestätigten Studien, welche Untersuchungen an *ult1-3 ult2-1* und *AtULT1* überexprimierenden Keimlingen einschlossen, eine *AtULT1*-abhängige Hemmung der Adventivwurzelbildung und der Elongation des Hypokotyls, aus dem diese hervorgehen. Lateralwurzelbildung wurde hingegen durch *AtULT1* Expression begünstigt. In der Primärwurzel wirkte sich genetische Manipulation der *AtULT1* Expression negativ auf das Wachstum aus und führte zu Anomalien bei Teilungsverhalten und Differenzierung der zentralen Wurzelhaube. Gene, welche Erhaltung und Strukturierung des Wurzelmeristems oder Differenzierung der Kalyptra steuern waren jedoch nicht signifikant reguliert. Da Auxingabe zur verstärkten Störung der Wurzelhaubendifferenzierung in *AtULT1 loss-of-function* Keimlingen führte, wurde eine mit Auxin-assoziierte Funktion für *AtULT1* angenommen. In Reis wird *OsULT1* durch den Auxin-induzierbaren Transkriptionsfaktor CROWN ROOTLESS1 reguliert, was wiederum auf eine Beteiligung von *OsULT1* bei der Kronenwurzelnitiierung hindeutet (Coudert et al., 2015). Zusammenfassend zeigte die vorliegende Studie mögliche Rollen von

AtULT1 bei der Wurzelorganogenese auf. In Zukunft könnten Ansätze wie *ChIPseq* oder *RNAseq* dazu beitragen einen umfassenderen Einblick in die Funktion von AtULT1 in der Wurzelentwicklung zu erhalten.

3 SUMMARY

In this study, expression and *in vivo* roles of the transcriptional anti-repressor ULTRAPETALA1 (ULT1) and the mitochondrial complex I by-pass protein ALTERNATIVE NAD (P) H DEHYDROGENASE A1 (NDA1) were described in Arabidopsis roots. In primary roots *AtNDA1* and *AtULT1* were both expressed in a root cap-specific manner. *AtULT1* showed additional expression in lateral root tips and at the base of lateral and adventitious roots. Expression patterns of the rice homologs, *OsULT1* and *OsNDA1*, suggested an involvement in mechanical signal transduction that mediates epidermal cell death through reactive oxygen species (ROS) signalling. Hence, in the Arabidopsis *NDA1* and *ULT1* null mutants, *nda1-1* and *ult1-3*, the root response to mechanical stress was analysed. Lack of *AtNDA1* or *AtULT1* altered primary root growth. This phenotype, however, appeared to be independent of an applied force. In rice, mechanically induced cell death of the epidermis facilitates penetration of underlying adventitious roots (Steffens et al., 2012). Analysis of secondary root emergence in Arabidopsis suggested an involvement of *AtULT1* in adventitious root formation and penetration. Further studies that included *ult1-3 ult2-1* knockout and *AtULT1* overexpressing seedlings confirmed a negative effect of *AtULT1* on adventitious root formation and on elongation of the hypocotyl from which they emerge. Lateral root formation, in turn, was favoured by *AtULT1* expression. Furthermore, an unbalanced *AtULT1* expression in *ult1-3 ult2-1* and *ULT1ox* seedlings resulted in inhibition of primary root growth and anomalies in division planes and differentiation of the central root cap. However, genes responsible for root meristem maintenance, columella differentiation and radial patterning were not significantly regulated. Instead, an auxin-associated function of *AtULT1* was suggested by the observation that abnormal differentiation of the root cap was enhanced by auxin in *AtULT1* knockout seedlings. Interestingly, in rice *OsULT1* is regulated by the auxin-inducible transcription factor CROWN ROOTLESS1, indicating a possible involvement of *OsULT1* in crown root emergence (Coudert et al., 2015). In summary, the study revealed a function of *AtULT1* in root organogenesis. Future approaches using ChIPseq or RNAseq might help identify direct gene targets to provide a more comprehensive insight into ULTRAPETALA function in root development.

4 INTRODUCTION

Because of the sessile nature of plants their growing roots need to respond on a wide range of environmental conditions. The root is a dynamic system of permanent cell production, differentiation, displacement and release that needs to be coordinated. The most important region for growth, the root apical meristem, is protected from abrasive damage and pathogenic infection by the root cap or in more detail by border-like cells (Arnaud et al., 2010; Driouich et al., 2010). The root cap consists of several layers columella cells and the lateral root cap. Root cap cells secrete mucilage to aid the root in penetrating compact soil (Arnaud et al., 2010). However, physical barriers are not only an issue for primary root tips, also emerging secondary roots are forced to penetrate inner cell layer and the epidermis. In rice (*Oryza sativa* L.), emerging adventitious roots are protected from mechanical damage by programmed death of overlying epidermal cells (Mergemann and Sauter, 2000; Steffen et al., 2012). Reprogramming of their developmental fate is achieved by force from the growing root and reactive oxygen species (ROS) accumulation (Steffens et al., 2012). The transcriptional regulator *ULTRAPETALA1* (*OsULT1*) and the type II *NAD (P) H DEHYDROGENASE A1* (*OsNDA1*) were found to be upregulated by these two signals in rice (Sauter et al., unpublished). We used *Arabidopsis thaliana* L. to further study the function of AtULT1 and AtNDA1 with a focus on root organogenesis and the root response to mechanical stimulation.

4.1 Genetic and hormonal control of root organogenesis

Survival and development of a complex organism are highly dependent on the ability to perform cell identity changes. These changes are primarily induced by positional cues, hormonal inputs and chromatin state shifts that cause epigenetic and transcriptional reprogramming to drive asymmetric cell divisions, cell cycle re-entry, programmed cell death or de- and re-differentiation (van den Berg et al., 1995; Zhao et al., 2001; Zhao et al., 2008; Alatzas, 2013; Rosa et al., 2014; Pillitteri et al., 2016). Inducing signals can be of intrinsic or extrinsic nature. As part of normal development *Arabidopsis* specifies cell identity already in early embryogenesis. Later, reprogramming of cell fate occurs prior to germination, when cell cycle in

quiescent embryonic meristems becomes re-activated by a subset of D-type cyclins and major transcriptional changes are initiated (Masubelele et al., 2005).

4.1.1 Specification and function of the primary root and its root cap

During the seed to seedling transition, cells of the post-embryonic root apical meristem (RAM) become specified through a mutual established auxin and PLETHORA (PLT) gradient and the action of the transcription factor SCARECROW (SCR; Sabatini et al., 1999; Sabatini et al., 2003; Aida et al., 2004; Blilou et al., 2005). Maintenance of the resulting RAM is finally adopted by another transcription factor, namely WUSCHEL-RELATED HOMEBOX5 (WOX5). WOX5 defines the identity of the stem cell niche, as its expression keeps 4 central cells in a quiescent stage and adjacent cells in a stem cell state (Sarkar et al., 2007; Kong et al., 2015). However, for organ and tissue patterning stem cell divisions must be balanced with differentiation events. In the columella cell lineage this is achieved by a receptor-ligand signalling module that is capable to restrict WOX5 expression in the roots organiser region, the so called quiescence centre (QC; De Smet et al., 2008; Stahl et al., 2009, Stahl et al., 2013). At the more proximal site of the RAM cell fate specification is controlled by a transcription factor regulatory network and is strongly connected to formative asymmetric cell divisions (Di Laurenzio et al., 1996; Helariutta et al., 2000; Nakajima et al., 2001; Heidstra et al., 2004; Cui et al., 2007; Willemsen et al., 2008). To form the central root cap merely anticlinal divisions of columella initials are sufficient. In contrast, construction of the outermost lateral root cap requires additional periclinal divisions of corresponding initials, since its descendant also give rise to the epidermal layer. The same is true for initials of cortex and endodermis (Dolan et al., 1993). Due to its simple organisation the columella at the root apex is a suitable organ to study stem cell activity and differentiation. Another feature of the central root cap is that generation, differentiation and programmed cell death (PCD) of cells can be observed in a narrow spatial and temporal framework. Hence the main developmental transitions are united in just one organ (Kumpf and Nowack, 2015). A similar developmental gradient is also present at the longitudinal axis 1.5 mm proximal from the RAM.

Starting from the root cap junction this region comprises the meristematic zone (MZ), where new cells are produced to enter the adjacent transition zone (TZ). In the TZ cells slowly expand and acquire necessary cytoarchitectural and metabolic features for fast elongation in the homonymous elongation zone (EZ). Finally cells migrate in the growth terminating zone, where differentiation is completed and cells acquired their final fate (Verbelen et al., 2006). Nevertheless, some cells retain competence to divide and create a new meristem (Dubrovsky et al., 2000; Beeckman et al., 2001). Herein the lateral root cap, which covers MZ and TZ at the outside, takes over a special role. In the central root cap a source of auxin is created through local biosynthesis and primarily PIN-FORMED1 (PIN1)-driven acropetal transport towards the root tip (Blilou et al., 2005; Ljung et al., 2005). Auxin flow to the elongation zone is mediated by the combinatorial action of the efflux carrier PIN2 and the influx carriers AUXIN RESISTANT1 (AUX1) (Swarup et al., 2005; Blilou et al., 2005). PCD of lateral root cells at the onset of the EZ is capable to control auxin oscillation in the main root (Xuan et al., 2016). Transient accumulation of auxin in protoxylem cells of the TZ specifies lateral root founder cells (De Smet et al., 2007).

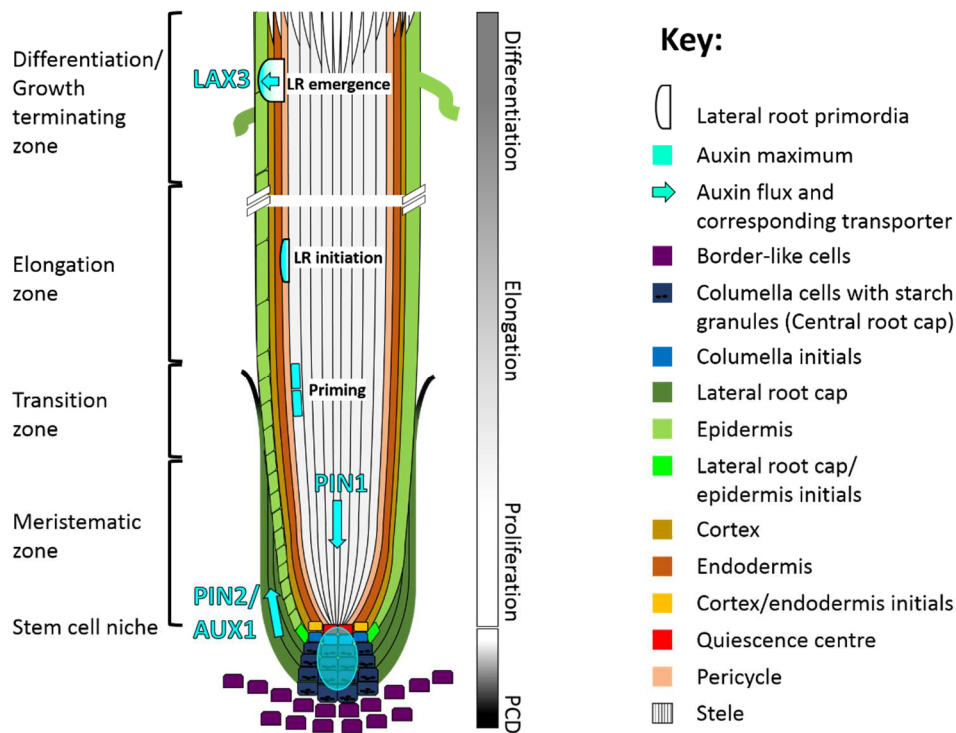


Figure 1: Schematic presentation of structure, cellular arrangement and developmental gradients of the Arabidopsis primary root (not to scale; according to Lavenus et

al. (2013) and De Smet et al. (2015)). Cells and cell layers of different origin are color-coded (right). Shading of bars (middle) refers to developmental state of distinct root zones (left). Auxin transport, accumulation and its role in lateral root formation is only partly presented. See text for accompanying explanations. AUX1, AUXIN RESISTANT 1; LAX3, LIKE AUX1; PCD, programmed cell death; PIN, PIN-FORMED; LR, lateral root.

4.1.2 Lateral root formation

Lateral root primordia always initiate from pericycle cells adjacent to the xylem poles (Casimiro et al., 2003). In contrast to phloem connected pericycle cells, which remain in G1-phase of the cell cycle, these cells advance to the G2-phase and keep mitotic competence (Beeckman et al., 2001). Hence pericycle cells at the xylem poles were considered to present a monolayered “extended meristem” (Casimiro et al., 2003). The periodic positioning of lateral roots along the primary root, however, is dependent on oscillation of auxin flux that is controlled by the lateral root cap (Dubrovsky et al., 2008; Xuan et al., 2015). After this priming, founder cells undergo a coordinated sequence of asymmetric divisions to form a primordium that finally emerges in the differentiation zone of the primary root. To facilitate lateral root emergence, production of cell-wall remodelling enzymes is induced by a LIKE AUX1 (LAX3)-established auxin maximum at the primordium tip (Swarup et al., 2008). In addition, auxin decreases cell turgor pressure in the outer tissue layers and primordium tips through regulation of aquaporin expression (Péret et al., 2012). Ultimately auxin also acts after root penetration in inducing meristems of lateral roots (Celenza et al., 1995). In summary auxin fluxes and maxima are directly or indirectly involved in every step of lateral root development, whereas sources of auxin can differ (Peret et al., 2009; Lavenus et al., 2013). While root tip derived auxin regulates lateral root initiation, auxin coming from the shoot functions in lateral root development and emergence (Bhalerao et al., 2002; Ljung et al., 2005; Wu et al., 2007; De Rybel et al., 2012).

4.1.3 Adventitious root formation

In contrast to the broad knowledge about lateral root development, mechanism driving adventitious root formation are elusive. In dicots like *Arabidopsis* the root system primarily consists of a main root that branches out lateral roots of several orders. This so called tap root system is preserved and important for their entire life. Monocots, in contrast, develop a small and short-living primary root that is only important for the young seedling stage. Naturally their root architecture is rather shaped by secondary roots, such as seminal and adventitious roots (Bellini et al., 2014). However, under certain circumstances induction of adventitious roots is also present in *Arabidopsis*. Adventitious roots develop from non-root tissue like stems, leaves and hypocotyls. While lateral root initiation at the main root is a rather developmental process, adventitious root formation requires environmental signals like wounding, flooding or continuous dark (Takahashi et al., 2003; Sorin et al., 2005; Steffens and Rasmussen, 2016).

***Arabidopsis thaliana* L.**

At the etiolated hypocotyl of *Arabidopsis*, adventitious roots, likewise to lateral roots, originate from pericycle cells. However, roots developing from excised leaves and hypocotyls were shown to initiate from vascular tissue (Da Rocha Correa et al., 2012). The primary root is a structure that continuously grows through production of new cells from the meristem. The hypocotyl, in contrast, is a determinate organ with a fixed number of cells whose growth is primarily driven by longitudinal cell expansion (Gendreau et al., 1997). Thus *de novo* organogenesis in non-root tissue strongly depends on cellular dedifferentiation and reprogramming (Verstraeten et al., 2014). However, in contrast to lateral roots only very limited knowledge about prebranch site establishment is available for adventitious roots. Auxin pulses that predestine pericycle cells to give birth to a new meristem are absent in hypocotyls. Nonetheless, stimulation of adventitious rooting by auxin is evident from several studies (De Klerk et al., 1999; Pop et al., 2011; Bellini et al., 2014). In root-excised hypocotyls, recent studies verified auxin synthesized in the shoot and the ATP-BINDING CASSETTE B19 (ABCB19) auxin efflux transporter as being essential for adventitious root induction in *Arabidopsis* (Sukumar et al., 2013). Moreover, during

early organogenesis, establishment and maintenance of an adventitious root meristem is achieved through PIN1- and LAX3-driven auxin accumulation at the adventitious root tip (Della Rovere et al., 2013). In intact hypocotyls AUXIN RESPONSE FACTOR17 (ARF17) has been shown to negatively affect adventitious root formation by repression of ARF6 and deregulation of auxin homeostasis (Sorin et al., 2005; Gutierrez et al., 2009). Expression of *ARF17* and *ARF6*, in turn, is light-dependent and under the control of microRNA (MIR)-induced silencing complexes (Rhoades et al., 2002; Mallory et al., 2005; Gutierrez et al., 2009). Other studies in Eucalyptus also identified auxin and light as influencing factors for adventitious root development. Experiments with stem cuttings from easy- and difficult-to-root species, led to the conclusion that light decreased auxin activity in the tissue and thereby reduced rooting capacity (Fett-Neto et al., 2001).

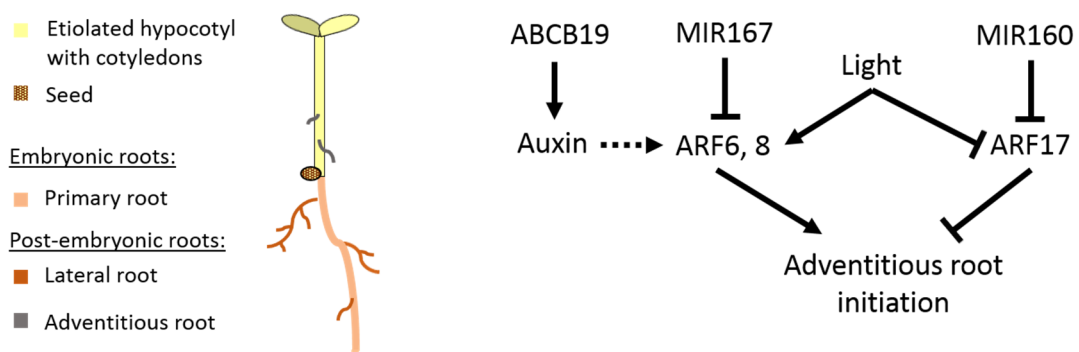


Figure 2: Schematic diagram of root system architecture of an etiolated Arabidopsis seedling (middle) and factors influencing adventitious root formation (right). Plant structures and root types are colour-coded (left). The dashed line indicates a causal coherence. Positive regulation is represented by arrow heads. Blunt-ended arrows point out negative regulation. ATP-BINDING CASSETTE B19 (ABCB19) directs auxin synthesized in the shoot to the position of adventitious root initiation at the hypocotyl (Sukumar et al., 2013). Auxin abundance prevents repression of *AUXIN RESPONSE FACTOR (ARF)* genes (Chapman and Estelle, 2009). ARF6 and ARF8 induce adventitious roots, ARF17 has a negative impact. Light exposure and ribonucleic acid (RNA) silencing through complementary microRNAs (MIR) fine-tunes ARF6, 8 and 17 expression (Gutierrez et al., 2009).

***Oryza sativa* L.**

In *Arabidopsis*, adventitious roots are initiated through reprogramming of differentiated cells. In rice, adventitious root primordia are pre-formed at the nodes of the stem. Emergence and growth of adventitious roots, in contrast to the initiation, requires environmental signals like flooding (Lorbiecke and Sauter, 1999; Steffens and Sauter, 2005). Moreover it is not auxin, but the gaseous phytohormone ethylene that causes cell cycle activation in quiescent primordia pre-existing at the stem (Lorbiecke and Sauter, 1999). However, initiation of adventitious roots, also called crown roots, is strongly dependent on auxin-inducible CROWN ROOTLESS (CRL) proteins. CRL4/GNOM1, for example, coordinates auxin transport through modulation of PIN proteins (Kitomi et al., 2008; Liu et al., 2009). *CRL1/ARL1* and *CRL5*, in turn, are both downstream targets of ARF-mediated auxin signalling (Inukai et al., 2005; Kitomi et al., 2011). Disruption of the *CRL1/ADVENTITIOUS ROOTLESS1 (ARL1)* gene caused depletion in crown root formation, auxin-insensitivity and reduced lateral root formation (Inukai et al., 2005; Liu et al., 2005). A microarray-based study identified 31 transcription factors that were regulated by CRL1/ARL1. In addition to NO APICAL MERISTEM (NAC), homeobox and APETALA2/ETHYLENE RESPONSE FACTOR (AP2/ERF) transcription factors that regulate transcriptional reprogramming in response to plant stress or determine cell identity, ULTRAPETALA1 (OsULT1, LOC_Os01g57240) was identified to possibly act downstream from CRL1/ARL1 in postembryonic root formation (Coudert et al., 2015). For the *Arabidopsis* homolog AtULT1 (At4g28190) a negative regulation of stem cell activity in shoot and floral meristems was observed, but a role in root development has not been described to date (Fletcher, 2001; Carles et al., 2004, 2005).

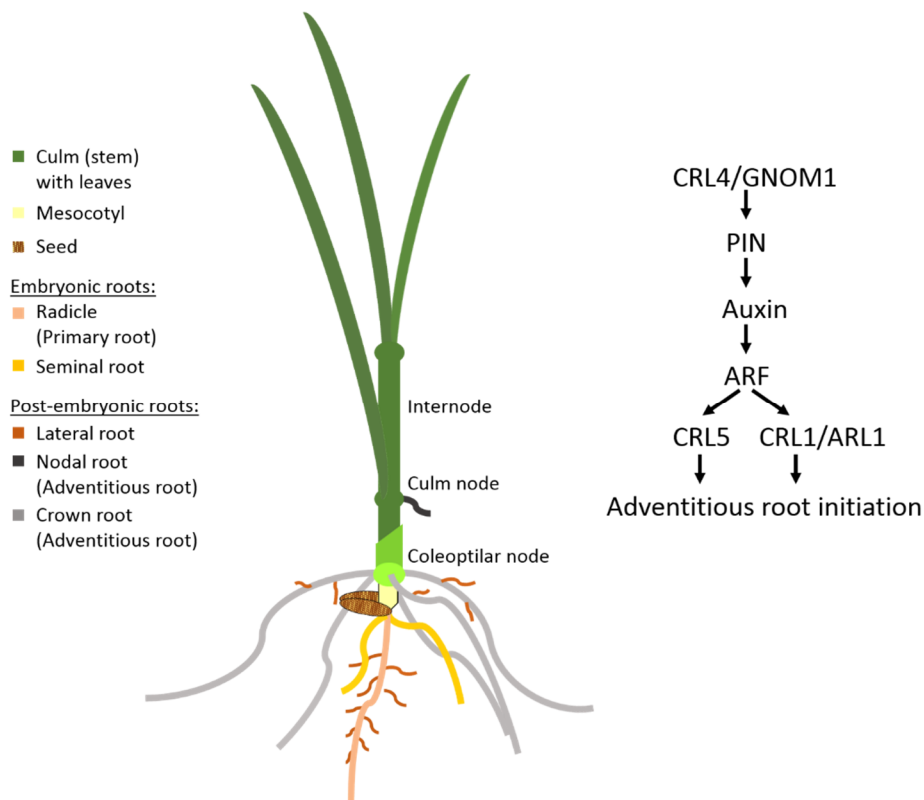


Figure 3: Schematic presentation of rice root system organisation (middle) and regulatory network acting in adventitious root formation (right). Plant structures and root types are colour-coded (left). Positive regulations are represented by arrows. CROWN ROOTLESS4/GNOM1 (CRL4/GNOM1) modulates expression of several PIN-FORMED (PIN) genes to cause auxin accumulation at the sites of adventitious root emergence (Kitomi et al., 2008; Liu et al., 2009). Auxin hinders repression of AUXIN RESPONSE FACTOR (ARF) genes (Chapman and Estelle, 2009). CRL1/ARF1 and CRL5 induce adventitious roots as downstream targets of the ARF-mediated auxin signalling pathway (Inukai et al., 2005; Kitomi et al., 2011).

4.2 Mechanical forces influence root growth and morphology

By altering auxin transport in the lateral root cap, gravitropic and mechanical stimuli can influence spacing of lateral roots (Lucas et al., 2008; Ditengou et al., 2008). Gravitropism forces the root to grow deeper into soil. Gravity, soil pressure or obstacles are first perceived by the root cap and transduced to the root that responds by altering root morphology, the rate or direction of growth and lateral root

formation (Monshausen and Gilroy, 2009; Arnaud et al., 2010). The columella at the very tip of the primary root harbours specialized starch-containing cells, the amyloplasts. In response to an altered gravitational vector the dense starch granules within these cells sediment towards gravity. This starch rearrangement causes relocation of auxin carriers. The resulting lateral auxin gradient in the root tip causes a temporal auxin maximum in the root elongation zone that, in turn, drives gravitropic bending and formation of lateral root primordia at the outside of the bend (Lucas et al., 2008; Sato et al., 2015). However, although the role of auxin in this differential growth response is well established, relatively little is known about receptors or signalling components that perceive and transmit the physical information. Indirect evidence propose starch sedimentation in amyloplasts to exert a tension on the plasma membrane or cytoskeleton that could cause opening of stretch-activated channels (Sato et al., 2015). Just as gravistimulated roots, mechanical impeded roots show an avoidance response that is accompanied with asymmetric growth and lateral root initiation at the emerging bend (Lucas et al., 2008; Ditengou et al., 2008; Richter et al., 2009; Monshausen and Gilroy, 2009; Sato et al., 2015). Similar to gravity sensing, force sensation was traced back to mechanosensitive channels that might be activated through deformation of the plasma membrane and associated cytoskeleton. Acceptance for this hypothesis was provided through the observation that transient elevations of cytosolic Ca^{2+} concentration coincides with touch, gravity and force stimulation. Downstream from Ca^{2+} signalling, proton fluxes and ROS production were suggested to play a role in direct modification of the cell wall or elicitation of transcriptional regulation (Monshausen and Gilroy, 2009; Monshausen and Haswell, 2013; Sato et al., 2015). However, taken together, signalling mechanism driving mechanosignalling are still poorly understood. Roots growing in hard soil or on impenetrable medium show a severe reduction in growth rate, an increase in root diameter and various other modifications of morphology, such as ectopic root hair formation (Atwell, 1993; Bengough et al., 2006; Okamoto et al., 2008). In maize, radial mechanical stress even causes rearrangement of the RAM from closed to opened organisation (Potocka et al., 2011). For this morphological alterations ethylene-mediated and

auxin-driven control of cell production and elongation were shown to be of central importance (Okamoto et al., 2008; Santisree et al., 2011)

In submerged plants reduced gas diffusion and enhanced biosynthesis causes ethylene accumulation (Jackson, 2008). Ethylene promotes adventitious root growth at rice stems via ROS signalling (Steffens et al., 2006, 2012). In epidermal cells overlaying root primordia ethylene induces PCD also via ROS signalling (Mergemann and Sauter, 2000; Steffens and Sauter, 2009). However, PCD is induced only when a force generated by the growing root acts as a second signal providing spatial resolution for cell fate change (Steffens et al., 2012). *OsULT1* and the *ALTERNATIVE NAD (P) H DEHYDROGENASE A1* (*OsNDA1*; LOC_Os07g37730) were upregulated by ROS and force in these epidermal cells and may thus be involved in cell fate acquisition in response to mechanical force. Epidermal cells that cover adventitious root primordia undergo programmed death to protect the meristem of the growing root and facilitate root penetration (Mergemann and Sauter, 2000; Steffens et al., 2012). In comparison to other non-dying nodal cells, cells covering adventitious root primordia share a different anatomical and molecular identity (Steffens and Sauter, 2009).

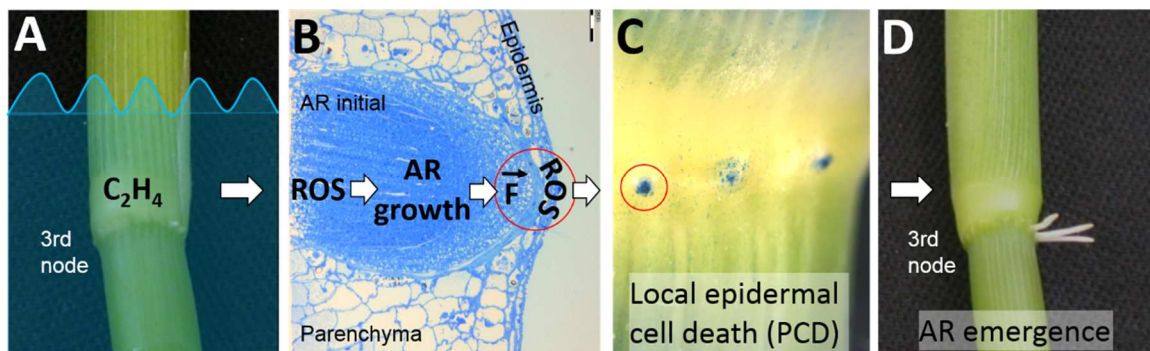


Figure 4: Signals driving adventitious root growth and emergence in rice.

A Ethylene (C₂H₄) accumulates in submerged tissue (Jackson, 2008). Shown is a 12- to 14-week-old rice stem, cultivar Pin Gaew 56, including the 3rd node.

B Ethylene-mediated reactive oxygen species (ROS) signalling induces growth of adventitious root (AR) initials at the rice node. Force (F) from the growing root acts together with ROS, which accumulate in response to ethylene in overlying epidermal cells, in inducing programmed cell death (Steffens et al., 2012). Presented is a semi-thin cross section through the 3rd node at the site of

adventitious root emergence from a 12- to 14-week-old rice plant, cultivar Pin Gaew 56.

C and **D** At the nodes, local death of epidermal cells facilitates adventitious root emergence (Steffens et al., 2012). Shown are 12- to 14-week-old rice stems of the cultivar Pin Gaew 56 after 24 hours (C) or 48 hours (D) treatment with 150 μ M ethephon, an ethylene-releasing compound. Epidermal cell death at the 3rd node was visualised by Evans blue staining.

4.3 ULTRAPETALA functions in reprogramming of cell fate in shoot and flower meristem of *Arabidopsis thaliana* L.

Plants preserve pluripotency of stem cells their life long. In contrast to animals, development of many organs proceeds after embryogenesis. The microenvironments harbouring pluripotent cells are called meristems. In plants two primary meristems, the RAM and the shoot apical meristem (SAM), exists. Both are responsible for longitudinal growth and establishment of the body plan. Stem cells of the SAM develop the aerial parts of the plant and RAM stem cells develop the above ground tissues. The SAM is organised as a dome-shaped structure that is flanked by lateral organ primordia (Weigel and Jürgens, 2001). In the vegetative phase of the plants life these primordia produce leaves and axillary meristems. During reproduction flanking cells of the SAM give rise to floral meristems and the central pool of pluripotent cells is maintained for further organogenesis (Poethig, 2003). Floral meristems produce flowers, which in *Arabidopsis* consists of four sepals on the outer whorl, four petals on the inner whorl, six stamens and a central carpel. In contrast to RAMs and SAMs, floral meristems are terminate structures whose activity ceases after inflorescences had formed (Sablowski, 2007). In most angiosperms the SAM is organised in three distinct zones functioning in coordination of cell proliferation and cell fate to define the anatomy of the SAM. The central zone lies at the summit of the meristematic dome and contains an extraordinarily constant number of slowly-dividing pluripotent stem cells. In the surrounding peripheral zone multipotent cells start to differentiate into lateral organs. Source of multipotent cells is the inward-situated rib zone (Laufs et al., 1998). Maintenance of the central zone is ensured by an organizing centre that expresses the homeodomain transcription

factor WUSCHEL (WUS; Laux et al., 1996). Unknown signals from these WUS-expressing cells preserves stem cell identity of overlying cells. Furthermore to keep the number of stem cells constant, a spatial regulatory feedback loop dynamically balances formation of new stem cells with loss of cells into differentiation (Carles and Fletcher, 2003).

In floral meristems stem cell maintenance is abolished when initiation of all floral organs is completed. Determinacy of the floral meristem requires the MADS domain transcription factor AGAMOUS (AG) for repression of *WUS* expression in the organising centre (Lenhard et al., 2001). The SAND-domain protein ULT1 and its paralog ULT2 were described to negatively regulate stem cell activity in shoot and floral meristems (Carles et al., 2005). Mutations in ULT1 caused delay in floral meristem termination and in consequence production of supernumerous flower organs. Furthermore induction of AG expression was hampered in *ult1* floral meristems (Fletcher, 2001). Constitutive *ULT1* expression, in turn, resembled the phenotype of AG gain-of-function mutants in such that stamen and carpels were converted to perianth organs (Mizukami and Ma, 1992; Carles and Fletcher, 2009). Taken together, the findings suggested that ULT1 restricts WUS expression in the organising centre via AG. And indeed, activation of AG expression through direct association with the AG locus and deposition of epigenetic marks was verified for ULT1 during flower development (Carles and Fletcher, 2009). Thus although homology to animal trithorax group (TrxG) components is absent, ULT1 was identified to be a plant-specific TrxG factor (Carles and Fletcher, 2009). TrxG factors control gene expression by shifting the histone methylation pattern of target loci to an activated stage. Furthermore TrxG factors counteract the deposition of repressive histone methylation marks by Polycomb group (PcG) factors. As epigenetic repressors and activators, TrxG and PcG factors play key roles in specification of cell fates and maintenance of cell differentiation states at all phases of the plants life cycle. Both, TrxG and PcG factors, act as multifactorial protein complexes in regulating developmental gene expression (Paz Sanchez et al., 2015). For floral meristem termination ULT1 acts antagonistically to PcG complexes involving CURLY LEAF1 (Carles and Fletcher, 2009). Furthermore, ULT1 was also described to function in patterning of the gynoecium and establishment of adaxial-

abaxial leaf polarity by countering the repressive activity of EMBRYONIC FLOWER1 and KANADI1, respectively (Pu et al., 2013; Pires et al., 2014). The ULT1 protein has a SAND domain that confers DNA binding capacity and a C-terminal located B-box-like motif that likely acts in interaction with proteins or ribonucleic acids (RNAs; Carles et al., 2005). However, ULT1 does not possess methyltransferase activity. Hence ULT1 rather functions in recruiting other TrxG factors on the deoxyribonucleic acid (DNA) of target loci (Carles and Fletcher, 2009). To date physical interaction with ULT2 and the histone H3K4 methyltransferase ARABIDOPSIS HOMOLOG OF TRITHORAX1 (ATX1) was shown (Carles and Fletcher, 2009; Monfared et al., 2013). Most likely, more target loci and association partners will be discovered in future.

4.4 The Arabidopsis ALTERNATIVE NAD (P) H dehydrogenase A1 may balance reactive oxygen species homeostasis

ROS, such as O_2^- and H_2O_2 , are produced as unavoidable consequence of aerobic respiration. However, ROS is not always an unwanted by-product, it also functions in growth control, pathogen defence and PCD. ROS can causes severe damage to proteins, lipids and DNA, that's why production and removal needs to be strictly controlled (Mittler, 2017). In plant cells the mitochondrial electron transport chain (ETC) and therein complex I and III are the major site of ROS production (Turrens, 2003). The mitochondrial ETC consists of 4 complexes that transport electrons to produce an electrochemical H^+ gradient which can be utilized for adenosine triphosphate (ATP) production. However, while transporting electrons only complex I, III and IV participate in proton translocation. Complex I is a trans-membrane dehydrogenase that reduces the mobile electron carrier ubiquinone with electrons from NAD (P) H oxidisation. Additional reduction of the ubiquinone pool is achieved though complex II that is a succinate dehydrogenase which also participates in the citric cycle. In a series of redox reactions one electron at a time is transferred from ubiquinone to complex III. Thereupon, electrons are passed to cytochrome c and afterwards to complex IV. At complex IV electrons and hydrogen ions are finally used to reduce molecular oxygen to water (Schertl and Braun, 2014). In contrast to mammals, plant mitochondria feature an alternative pathway consisting of type II

NAD (P) H dehydrogenases on each side of the inner mitochondrial membrane and a non-proton-pumping alternative oxidase that circumvents complex III and IV. Type II NAD (P) H dehydrogenases bypass complex I, since they modulate the redox state of ubiquinone without translocation of protons (Rasmusson et al., 2004; Schertl and Braun, 2014).

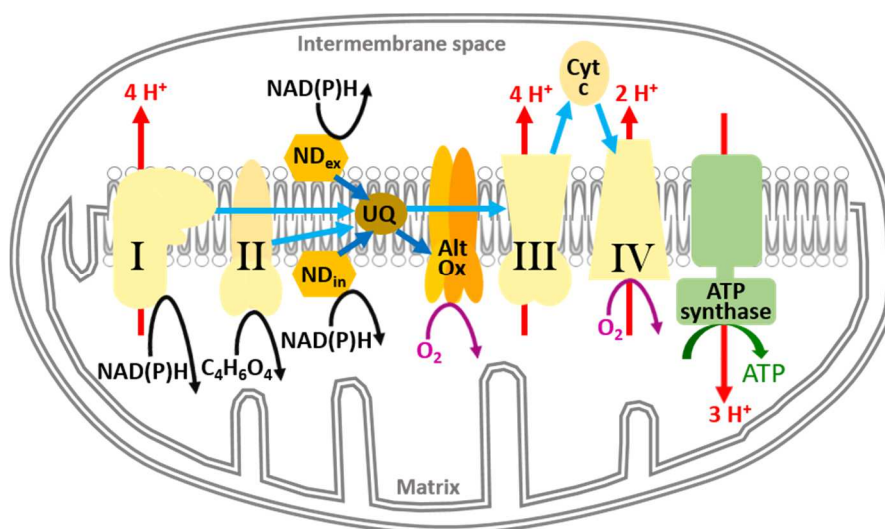


Figure 5: Schematic presentation of the electron transport chain in plant mitochondria. Red arrows indicate proton translocation. Electron flux is visualised by blue arrows. Oxidation reactions are shown with black and redox reactions with purple arrows. Roman numerals highlight complex I to IV. ND_{ex}, external type II NAD (P) H dehydrogenase; ND_{in}, internal type II NAD (P) H dehydrogenase; UQ, ubiquinone; Alt Ox, Alternative oxidase; Cyt c, Cytochrome c. For a detailed explanation see text above.

AtNDA1, together with its paralog AtNDA2 and a C-type alternative NAD (P) H dehydrogenase belongs to the matrix-facing bypass proteins (Elhafez et al., 2006). Theoretically these proteins, together with ubiquinone and the alternative oxidase, can form an independent ETC that is capable of limiting ROS production by keeping the ETC relatively oxidized (Rasmusson et al., 2004; Schertl and Braun, 2014). However, physiological roles and mechanism regulating type II NAD (P) H dehydrogenase activities remain to be elucidated. Even if in Arabidopsis a direct link is lacking, it exists references in yeast and rice that argue for an involvement of

internal type II NAD (P) H dehydrogenases in PCD. In rice, OsNDA1 was shown to be differential regulated upon force- and ROS-mediated PCD of epidermal cells overlying adventitious root primordia (Sauter et al., unpublished). In yeast (*Saccharomyces cerevisiae*), the internal NADH dehydrogenase ScNDi1 functions independently from its ubiquinone oxidoreductase activity also in execution of apoptosis. Under various stress, such as H₂O₂, the N-terminus of ScNDi1 is cleaved off and translocated to the cytoplasm where it provokes apoptosis (Cui et al., 2012).

5 MATERIALS AND METHODS

5.1 Plant material and growth conditions

For experiments involving *Arabidopsis thaliana* L., ecotype Columbia-0 was used as wildtype control and genetic background for transgenic modifications. Seed stock for *acr4-1* (GK-152C08), *acr4-2* (SAIL 240B04), *ult1-3* (SALK 074642), *ult2-1* (SAIL 748C04) and *nda1-1* (SALK 054530) insertion lines were obtained from Nottingham Arabidopsis Stock Centre (University of Nottingham, Loughborough, United Kingdom). Homozygosity for the T-DNA insertion and transcript absence were verified as described below.

For sterilization, seeds were immersed in a 2% (v/v) sodium hypochlorite solution with continuous shaking for 20 minutes, washed with autoclaved distilled water 4 times and planted on sterile 0.5 strength Murashige-Skoog (MS; Murashige and Skoog, 1962) medium (pH 5.8) containing 1.5% (w/v) sucrose (unless otherwise stated) solidified with 0.4% (w/v) Gelrite™ (Huang et al., 1995; Duchefa Biochemie, Haarlem, The Netherlands) or Bacto™ Agar (Difco Laboratories, Detroit, USA) at different concentrations as indicated in figure legends when applied. In some experiments 10 µM indole-3-acetic acid (IAA) or 10 µM 1-aminocyclopropane-1-carboxylic acid (ACC) were added to the medium from filter-sterilized stocks. For plants grown on soil a water-saturated sand/humus (1:1) mixture was used. Seeds placed on plates were stratified at 4°C for 2 days and induced to germinate by 6 hours illumination. Seedlings or plants were grown at 22°C, either at an average irradiance of 90 µmol photons × s⁻¹ × m⁻² for 16 hours (long-day) or in the dark.

5.2 Genotyping of T-DNA insertion lines

To test whether a transfer DNA (T-DNA) was inserted in both alleles of a gene, a polymerase chain reaction (PCR) with two gene-specific or a gene- and a T-DNA-specific oligonucleotide was performed (for primers see Table 2). For this purpose deoxyribonucleic acid (DNA) was isolated according to Weigel and Glazebrook (2002). Briefly, one leaf from a 2- to 3-week-old plant was ground in 400 µl extraction buffer (200 mM Tris-HCl (pH 7.5), 250 mM sodium chloride, 25 mM EDTA, 0.5%

(w/v) SDS) followed by 5 minutes centrifugation at $12000 \text{ g} \times \text{min}^{-1}$ and room temperature (RT). From the supernatant 300 μl were transferred to a clean tube and mixed with an equal volume of isopropanol. Thereafter the centrifugation step was repeated. The supernatant was drained, the pellet rinsed with 1 ml 70% (v/v) ethanol and dried. Subsequently, the DNA was dissolved in 100 μl water.

To test whether insertions results in a complete loss of transcript, seeds from individual plants were grown for 5 to 7 days. Ribonucleic acid (RNA) was isolated from 5 to 10 pooled seedlings and used for reverse transcription PCR (RT-PCR) analysis with primers listed in Table 2.

5.3 Isolation of total RNA

Depending on the quantity, plant material was harvested in 0.25 to 1 ml of TRI Reagent® in a reaction tube and either ground immediately with a micro pestle or frozen at -80°C to be processed later. After homogenisation samples were left for 3 minutes at RT before 0.2 volumes of chloroform were added. The solutions were mixed thoroughly by vortexing for 15 seconds and incubated for 5 minutes at RT. Then samples were centrifuged for 15 minutes at 4°C and $12000 \text{ g} \times \text{min}^{-1}$. The upper aqueous phase was transferred to a new tube where RNA was precipitated with 0.5 volume each of isopropanol and salt solution (1.2 M sodium chloride, 0.8 M sodium citrate) for 10 minutes at RT followed by 10 minutes centrifugation at 4°C and $12000 \text{ g} \times \text{min}^{-1}$. The supernatant was removed, the pellet washed with 1 ml 70% (v/v) ethanol, centrifuged for 10 minutes at 4°C and $12000 \text{ g} \times \text{min}^{-1}$ and dried at RT. RNA was dissolved at 60°C for 5 to 10 minutes in 20 μl water. Remaining DNA was digested with 1 Unit DNase I (Thermo Fisher Scientific, Darmstadt, Germany) and 0.1 volume of DNase I buffer (100 mM Tris-HCl (pH 7.5), 25 mM magnesium chloride, 1 mM calcium chloride) for 1 hour at 37°C . To purify RNA and to inactivate DNase I, samples were mixed with 1 volume phenol/chloroform (1:1) and centrifuged for 1 minute at $14000 \text{ g} \times \text{min}^{-1}$ at RT. The upper phase was transferred to a new tube and further purified by adding 1 volume chloroform. Phase separation was achieved through centrifugation as described above. From the upper phase, RNA was precipitated for 1 hour at -80°C or overnight at -20°C in 2.5 volume 100% (v/v) ethanol and 0.1 volume 3 M sodium acetate (pH 5). Subsequently RNA was

pelleted by 30 minutes of centrifugation at 4°C and 12000 g×min⁻¹, the supernatant was discarded and the pellet washed with 70% ethanol. Ethanol was drained, its residuals evaporated and the RNA dissolved in water for 5 to 10 minutes at 55°C. To determine the concentration and purity of the RNA absorbance at 230, 260 and 280 nm was measured with a Thermo Scientific NanoDrop™ 2000 spectrophotometer. RNA with a ratio greater than 2 for 260 nm/230 nm and greater than 1.8 for 260nm/280nm was considered to be pure. Nucleic acid concentrations were calculated by multiplying the absorbance at 260 nm with 40 ng/μl for RNA and 50 ng/μl for DNA.

To generate complementary DNA (cDNA), 0.5 to 1 μg RNA were reverse transcribed with 0.25 μg/μl of a deoxythymidine triphosphate 14-, 16- and 18-mer oligonucleotide mix and RevertAid Reverse Transcriptase (Thermo Fisher Scientific, Darmstadt, Germany) according to the manufactures' protocol.

5.4 Polymerase chain reaction (PCR) and gel electrophoresis

For amplification of gene-specific DNA fragments, PCRs were carried out with DreamTaq Green DNA Polymerase (Thermo Fisher Scientific, Darmstadt, Germany) according to the manufactures' instructions and run under the following conditions. One initial denaturation step at 94°C for 5 minutes, 25 to 35 cycles with 30 seconds at 94°C, 50 seconds at a temperature between 55 and 60°C, corresponding to the melting temperatures of the primers and 0.5 to 2 minutes depending on the expected length of the product at 72°C. The reaction was terminated with one elongation step at 72°C for 10 minutes. Primers and target sequences are listed in Table 2.

Depending on size, products were separated on 1 to 3% (w/v) agarose gels supplemented with ethidium bromide by electrophoresis in TAE-buffer (40 mM Tris (pH 7.6), 20 mM acetic acid, 1 mM EDTA). SmartLadder (Eurogentec, Seraing, Belgium), GeneRuler 100 bp or GeneRuler Ultra Low Range DNA Ladder (both Thermo Fisher Scientific, Darmstadt, Germany) served as markers for fragment size determination. Separated DNA was visualised by ultraviolet illumination and photographs were taken.

5.5 Quantitative real time PCR (qPCR)

National Center for Biotechnology Information (NCBI) PrimerBlast was used to pick primers that anneal at 60°C and yield gene-specific amplicons of 75 to 135 base pairs (bp). If applicable, primers were designed to either span an exon-exon junction or be separated by at least one intron of the gene of interest. In advance amplification of the desired PCR product was tested by RT-PCR and gel electrophoresis. Later on, specificity and identity were reviewed by melting curve analysis. Primer sequences can be found in Table 2. Quantification of transcript abundance was performed from 10 ng cDNA template with the Rotor-Gene Q real time PCR cyclor and the Rotor-Gene SYBR® Green PCR Kit (Qiagen, Hilden, Germany) following the manufactures' operating manual, except that the final reaction volume was scaled down to 15 µl. Cycling conditions of the reaction were as follows. First HotStarTaq Plus DNA Polymerase was activated by heating up to 95°C for 5 minutes, then 40 cycles of 5 seconds denaturation at 95°C and 10 seconds at 60°C were initiated.

Cycle thresholds (Ct) of samples were normalized by using *Arabidopsis thaliana* ACTIN2 (AtACT2; At3g18780) and *Arabidopsis thaliana* GLYCERALDEHYDE-3-PHOSPHATE DEHYDROGENASE C SUBUNIT (AtGAPC1; At3g04120) as reference genes (Ref). The relative expression ratio (R) of the gene of interest (GOI) was calculated with the following equation using the $2^{\Delta\Delta Ct}$ method (Livak and Schmittgen, 2001) including amplification efficiency (E) correction.

$$R = (E_{GOI})^{\Delta Ct_{GOI}(\text{wildtype} - \text{mutant})} / (E_{Ref})^{\Delta Ct_{Ref}(\text{wildtype} - \text{mutant})}$$

5.6 Cloning and transformations

Escherichia coli (*E. coli*) was grown at 37°C in lysogeny broth (LB; Bertani, 1951) medium and *Agrobacterium tumefaciens* (*A. tumefaciens*) was grown at 28°C in YEP medium (pH 7; 10 g/l yeast extract, 10 g/l peptone, 5 g/l sodium chloride) under continuous shaking at 300 or 200 rpm respectively. To obtain competent cells for transformation 100 ml growth medium was inoculated and bacteria were grown to 0.3 optical density at 600 nm (OD_{600nm}). All following steps were processed at 4°C. First, the bacterial culture was centrifuged for 5 minutes at 3500 g_xmin⁻¹ and the

supernatant rejected. The pellet was dissolved in 20 ml transformation buffer I (TFB; 30 mM potassium acetate, 50 mM manganese(II) chloride, 100 mM potassium chloride, 10 mM calcium chloride, 15% (v/v) glycerol) and incubated 5 minutes on ice. The cells were pelleted by 5 minutes of centrifugation at $5000 \text{ g} \times \text{min}^{-1}$ before they were dissolved in TFB II (10 mM MOPS, 75 mM calcium chloride, 10 mM potassium chloride, 15% (v/v) glycerol). Aliquots were immediately frozen in liquid nitrogen and stored at -80°C .

For transformation, 1 to 5 μl plasmid was added to competent cells and the mixture kept on ice for 30 minutes. *E. coli* cells were transferred to 42°C for 40 seconds, while *A. tumefaciens* cells were first frozen in liquid nitrogen for 1 minute and subsequently thawed at 37°C . After cells were kept for 3 minutes on ice, 900 μl lukewarm growth medium was added and cells were shaken for 1 hour at 28°C or 37°C . Transformed cells were plated on agar-solidified growth medium with kanamycin for entry clone selection or spectinomycin for destination and expression clone selection and grown for 1 day at 37°C (*E. coli*) or for 3 days at 28°C (*A. tumefaciens*).

Arabidopsis promoter regions were amplified from genomic DNA obtained by a Quick DNA Prep procedure (Weigel and Glazebrook, 2002). For coding sequences, RNA from 7-day-old seedlings was isolated with TRI Reagent® (Sigma Aldrich, St. Louis, USA) according to the manual. For rice transgenic lines 5-day-old *Oryza sativa* ssp. Japonica cv. Nipponbare seedlings were used to isolate RNA with the innuPREP Plant RNA Kit (Analytik Jena, Jena, Germany) and DNA with the DNAeasy Plant Mini Kit (Qiagen, Hilden, Germany) according the manufactures' instructions. For PCR amplification, *Pyrococcus furiosus* (Pfu) polymerase was applied for Arabidopsis samples and Phusion High-Fidelity PCR Master Mix with GC Buffer (Thermo Fisher Scientific, Darmstadt, Germany) for rice samples. For the primers used see Table 2.

All plasmids were generated by Gateway® cloning technology using pENTR™/D-Topo® (Thermo Fisher Scientific, Darmstadt, Germany) as entry vector. To this end promoter regions and coding sequences were amplified with a 5' CACC-overhang to perform a blunt-end directional ligation according to the manufactures' instructions. The entry clones were transformed in competent *E. coli* DH5 α cells.

Plasmids were isolated and insertions tested by PCR fragment size and restriction site analysis. Finally, the nucleotide sequences of putative correct entry plasmids were verified by *LIGHTrun*TM sequencing (GAPC Biotech AG, Köln, Germany). For sequencing, plasmids were isolated using the GeneJet Miniprep Kit (Thermo Fisher Scientific, Darmstadt, Germany) according to manufactures' instructions. To produce an expression clone the appropriate destination vector (see Table 1) was recombined with the entry plasmid using LR ClonaseTM II Enzyme Mix (Thermo Fisher Scientific, Darmstadt, Germany) following the instruction manual. *E. coli* DH5 α cells were transformed with the reaction product and insertion verified as described above, except that no sequencing was performed. A verified expression plasmid was used for transformation of the *A. tumefaciens* strain EHA105. Selected colonies were tested via PCR for plasmid incorporation and used to transform Arabidopsis plants according to Clough and Bent (1998).

In brief *A. tumefaciens* was grown to an OD_{600nm} between 0.5 and 1. 5% (w/v) sucrose and 5 \times 10⁻⁴% (v/v) Silwet® L-77 (Leu+Gygax AG, Birmenstorf, Schwitzerland) were added to the bacterial suspension and inflorescences of approximately 5-week-old plants were immersed in it for 15 seconds, covered with paper tissue and kept in the dark overnight. Plants were grown until mature seeds were harvested. Transgenic lines were selected through repeated spraying of 200 μ M glufosinate ammonium (Basta; AgrEvo, Berlin, Deutschland) on soil-grown seedlings one week after germination.

Destination vectors for the production of the rice transgenic plants, *OsULT1_{pro}:GUS* and *OsULT1ox*, were provided to Professor Mikio Nakazono (Nagoya University, Japan). Professor Mikio Nakazono and colleagues performed the transformation of Agrobacteria, subsequent transformation of rice calli, selection and propagation of transgenic rice plants.

Table 1: Destination vectors and applications.

Destination vector	Application
pBGWFS7,0	<i>AtNDA1_{pro}:GUS</i> , <i>AtULT1_{pro}:GUS</i> , <i>OsULT1_{pro}:GUS</i>
pHGWFS7,0	<i>OsULT1_{pro}:GUS</i>
pB7WG2,0	<i>ULT1ox (35S_{pro}:AtULT1)</i>
pH7WG2,0	<i>OsULT1ox (35S_{pro}:OsULT1)</i>

Table 2: Names, sequences, target sequences and applications of primers are shown together with accession numbers of the genes analysed. bp, base pairs; GUS, beta-glucuronidase; PCR, polymerase chain reaction; T-DNA, transfer deoxyribonucleic acid; TSS, transcription start site.

Target	Primer name	Sequence (5'→3')	Application
<i>AtACTIN2</i> (At3g18780)	ACT2 F1	CAAAGACCAGCTCTTCCATCG	Reverse transcription PCR and genotyping
	ACT2 R1	CTGTGAACGATTCTTGACCT	
<i>AtULT1</i> (At4g28190)	ULT1 F1	CTTCTCATTCTCCTCATACGC	
	ULT1 R1	ATGGACTGCCTTCTTCAAGC	
<i>AtULT2</i> (At2g20825)	ULT2 F1	TCGTGGTTTACTTGGTCC	
	ULT2 R1	GAGAAATGAAGTCAAATGGG	
<i>AtNDA1</i> (At1g07180)	NDA1 gDNA F2	TATGTGTGAATCATGCTCTTGG	
	NDA1 gDNA R2	GAGAAGAAGAAGCACGTGG	
<i>AtNDA1</i> (At1g07180)	NDA1 F3	CAGACCACTTCTTCGTCTGT	
	NDA1 R3	TGGCTTCAATGTGCTAGACC	
<i>AtACR4</i> (At3g59420)	ACR4 F1	GTTACCTTGCGGTCTGAGATCTG	
	ACR4 R1	CCAACATAGCACTCGCGATTCC	
<i>AtWOX5</i> (At3g11260)	WOX5 F2	CCAACCTCCAAGGTGGACAAA	
	WOX5 R2.2	TCGTGGTGGTCTCTCGAATA	
GK T-DNA	GK LB 08409	ATATTGACCATCATACTCATTGC	
SALK T-DNA	SALK LBb1	ACCGCTTGCTGCAACTCTC	
SAIL T-DNA	SAIL LB3	TAGCATCTGAATTTATAACCAATCTCGATACAC	
<i>AtULT1</i> (At4g28190)	ULT1 qF3	GTGGTTGTACCAGTCACCGAT	Quantitative real time PCR
	ULT1 qR3	GGTGTCAACTTGTCTTCATCGC	
<i>AtULT2</i> (At2g20825)	ULT2 qF4	TCGTGGTTTACTTGGTCCCG	
	ULT2 qR4	CGACGTAATCGTCTCCCACA	
<i>AtATX1</i> (At2g31650)	ATX1 qF1	CTGCCACATGGATGAGGAGT	
	ATX1 qR1	CCACAAAGCACCATCACAGG	
<i>AtWOX5</i> (At3g11260)	WOX5 F2	CCAACCTCCAAGGTGGACAAA	
	WOX5 R2.2	TCGTGGTGGTCTCTCGAATA	
<i>AtACR4</i> (At3g59420)	ACR4 qF2	ACTTGCGGAGTTCTCACAGG	
	ACR4 qR2	CTGGTGGACAAGGAGTGTC	
<i>AtCLV1</i> (At1g75820)	CLV1 qF1	GGATACATCGCCCCAGAGTATG	
	CLV1 qR1	ATTCACCAACAGGTTTCTTCCCA	
<i>AtSCR</i> (At3g54220)	SCR qF1	TGGAACTTGGACACTGAGAGAC	
	SCR qR1	AGGAGCTAATCTTTGGAGTAACCA	
<i>AtSHR</i>	SHR qF1	TCCTCCGTCCTTCGACTTCT	

(At4g37650)	SHR qR1	GAGCTCGTTGAGCGTCCATA	Quantitative real time PCR
<i>AtPLT1</i> (At3g20840)	PLT1 qF1	CTTCACCATCCGAGACCACC	
	PLT1 qR1	CTTCACCATCCGAGACCACC	
<i>AtPLT2</i> (At1g51190)	PLT2 qF1	GGAACATTCAGCACGGAGGA	
	PLT2 qR1	GTTGCTCTCCAGGATGGCTT	
<i>AtACT2</i> (At3g18780)	ACT2 qF1	ACATTCCAGCAGATGTGGATCTC	
	ACT2 qR1	GATCCCATTTCATAAAACCCAGC	
<i>AtGAPC1</i> (At3g04120)	GAPC qF1	GATTCTACAATGGCTGACAAGAAGA	
	GAPC qR1	ATGAAGGGGTCGTTGACAGC	
<i>AtULT1</i> (At4g28190)	ULT1ox F1	CACCATGGCGAACAATGAGGGAGA	<i>ULT1ox</i> (<i>35S_{pro}:AtULT1</i>)
	ULT1ox R1	TCAAGCTTTGACATTGCTGGT	
1052 bp upstream of <i>AtNDA1</i> TSS	NDA1gus F1	CACCCGTTGTGATCTCCTCTGTTC	<i>AtNDA1_{pro}:GUS</i>
	NDA1gus R1	GATTCTTTAGGTACTCTTCTTC	
1029 bp upstream of <i>AtULT1</i> TSS	ULT1gus F1	CACCACAACACTAGTATCCTCATCC	<i>AtULT1_{pro}:GUS</i>
	ULT1gus R1	CACTCTCTCTGAGATTTTC	
<i>OsULT1</i> (Os01g0780800, LOC_Os01g57240)	OsULT1ox F1	CACCATGGCTGCGGCGGCGAACG	<i>OsULT1ox</i> (<i>35S_{pro}:OsULT1</i>)
	OsULT1ox R1	CTACTCCTTGAGTTATGGTAG	
1961 bp upstream of <i>OsULT1</i> TSS	pOsULT1 F1	CACCTGAGGGAGCTCCATCA	<i>OsULT1_{pro}:GUS</i>
	pOsULT1 R1	GCCTCCAACCAAGAACAGCAAA	

5.7 Plasmid isolation

E. coli cells from one colony were grown overnight in LB medium at 37°C. All centrifugation steps were performed at 12000 $g \times \text{min}^{-1}$ and room temperature. Two to 4 ml of the culture were centrifuged for 2 minutes to collect cells as a pellet. The supernatant was removed and the pellet resuspended in 100 μl solution I (25 mM Tris-HCl (pH 8), 10 mM EDTA, 50 mM glucose, 300 mg/l RNase A). Subsequently 200 μl solution II (0.2 M sodium hydroxide, 1% (w/v) SDS) were added, the tube was inverted 5 times and cells were incubated at RT for 3 minutes. The samples were mixed with 150 μl of 3 M sodium acetate (pH 4.8), kept on ice for 10 minutes and centrifuged for 5 minutes. To the supernatant 1 ml of 100% (v/v) ethanol was added to trigger precipitation of DNA during a 10 minutes centrifugation step. The pellet was washed with 1 ml 70% (v/v) ethanol during 2 minutes of centrifugation and dried at RT before it was dissolved in 100 μl water to be used in PCR.

5.8 Crossing of plants

Anthers of approximately 5-week-old homozygous *ult1-3* plants were removed with a forceps to prevent self-pollination. Subsequently pollen from homozygous *ult2-1* were used to accomplish fertilization to obtain double heterozygous seeds (F1 generation). Seedlings of the next generation (F2) were grown for approximately 21 days on 0.5 strength MS including modified vitamins (pH 5.8; Murashige and Skoog, 1962) solidified with 0.4% Gelrite™ (Huang et al., 1995) and supplemented with 50 µM kanamycin and 50 µM Basta (AgrEvo, Berlin, Deutschland) for the selection of double heterozygous plants. Resistant plants were transferred to soil and tested for homozygosity of both insertions after 1 week of recovery.

5.9 Treatment with ethylene or 1-Methylcyclopropene (1-MCP)

Treatments were performed in transparent, gas-tight acrylic boxes with a volume of 7 litre. A maximum of three plates with lids ajar were placed in the box. For ethylene treatments 1% (v/v) ethylene in N₂ (AIR LIQUIDE, Düsseldorf, Germany) which equates to 10000 µl/l was diluted to 5 µl/l inside the box. The appropriate volume of ethylene was injected with a syringe through a septum. 1-Methylcyclopropene (1-MCP; AgroFresh, Frankfurt on the Main, Germany) at a concentration of 5 µl/l was released in the internal gas phase of the box by diluting 56 mg with 3 to 5 ml of water inside. Control seedlings were kept in the closed box without treatment.

5.10 Growth measurements

Hypocotyl length was measured directly with scale paper prior to counting of adventitious roots and adventitious root primordia with an Olympus BX41 microscope on the same seedling. The length of the primary root and the number of penetrated lateral roots was determined with an Olympus SZ61 binocular or Nikon SMZ18 stereomicroscope. Adventitious and lateral root number per millimetre was calculated. To measure root lengths, root curvature, waving frequency, waving amplitude and skewing angle, pictures were taken with a Canon PowerShot SX220 HS digital camera, Olympus SZ61 binocular or Nikon SMZ18 stereomicroscope. *ImageJ 1.48v* (Schneider et al., 2012) was used to analyse the parameters.

5.11 Histochemical Lugol's and GUS staining

To visualise starch granules in columella cells, roots were mounted in clearing solution containing 16.7% (v/v) Lugol's solution (4% (w/v) iodine, 6% (w/v) potassium iodine) and incubated for 1 minute prior to imaging. Beta-glucuronidase (GUS) staining modified according to Jefferson et al. (1987) was performed as follows. Plants, seedlings or stem sections were immersed in chilled 90% (v/v) acetone and incubated under gentle shaking for 20 minutes at RT. The plant material was washed two times in 50 mM sodium phosphate buffer (pH 7.2) to clear of acetone before it was placed in GUS staining solution (0.5 mM sodium phosphate buffer (pH 7.2), 0.2% (v/v) Triton® X 100, 2 mM potassium ferricyanide, 2 mM potassium ferrocyanide, 2 mM 5-Bromo-4-chloro-3-indolyl- β -D-glucuronic acid) for 15 to 18 hours at 37°C. After staining, Arabidopsis seedlings were transferred to 70% (v/v) ethanol and cleared in chloral hydrate solution (6 g chloral hydrate, 2 ml water, 1 ml glycerol) on the microscope slide before analysis. Rice samples were only cleared in 70% (v/v) ethanol for several days. To make cross sections Arabidopsis seedlings were embedded in Technovit 7100 (Heraeus Kulzer, Wehrheim, Germany) according to manufacturers' instructions and cut into 12 μ m thin sections with a Leica RM 2255 microtome. Sections were collected on a slide in water that was evaporated before samples were mounted in Leica CV Mount (Leica, Wetzlar, Germany). Sections from rice stems were carried out by hand using a razor blade. Staining was recorded by a camera-equipped Olympus BX4 microscope.

5.12 mPSPI (modified pseudo-Schiff propidium iodide) staining

Cell walls of embryonic roots were stained as described by Truernit et al. (2008) with slight modifications. Seeds were imbibed for 1 day in distilled water and for 1 day in 0.5 strength MS medium (pH 5.8) containing 1.5% sucrose at RT. Embryos were dissected from testa and aleurone layer under a binocular, collected in fixation solution (50% (v/v) methanol, 10% (v/v) acetic acid) and kept at 4°C overnight. After rinsing with water, embryos were incubated for 40 minutes in 1% (w/v) periodic acid at RT. Samples were washed with water and finally transferred to freshly prepared propidium iodide (PI) staining solution (1% (v/v) Schiff's reagent, 15 mM PI) for 30-

60 minutes until the tissue became reddish violet. The reaction was stopped with water and embryos mounted in clearing solution (6 g chloral hydrate, 2 ml water, 1 ml glycerol) on a slide for 2 days. Cellular organisation of root meristems was imaged with a Leica TCS SP5 confocal laser scanning microscope.

5.13 Statistical evaluation of the data

Statistical analysis was carried out using MINITAB Release 14.20 (Minitab Inc., Pennsylvania, USA). First, normal distribution and equal variances of single values were tested by Anderson-Darling or Barlett's test, respectively. If one or both conditions were not complied the probability of significance was set to $P \leq 0.001$. In all other cases statistical differences was achieved when $P \leq 0.05$. Statistical difference of means were rated by Students t-test and variances with an ANOVA (Tukey-test). *P* values and applied tests are specified in figure legends.

5.14 Databases for bioinformatics

The following databases and associated blast servers were used to find homologs, T-DNA insertion lines and to obtain sequence information.

- MSU Rice Genome Annotation Project
(RGAP, <http://rice.plantbiology.msu.edu/index.shtml>)
- National Center for Biotechnology Information
(NCBI, <http://www.ncbi.nlm.nih.gov/>)
- The Arabidopsis Information Resource
(TAIR, <https://www.arabidopsis.org/>)
- The Nottingham Arabidopsis Stock Centre
(NASC, <http://arabidopsis.info/>)
- Salk Institute Genomic Analysis Laboratory
(SIGNAL, <http://signal.salk.edu/>)

Alignments were performed using BioEdit version 7.2.5 and subcellular localisations were predicted with the TargetP 1.1 Server (<http://www.cbs.dtu.dk/services/SignalP/>) of the Centre for Biological Sequence Analysis.

6 RESULTS

6.1 Sequence and expression analysis of *ULTRAPETALA1* and *ALTERNATIVE NAD (P) H DEHYDROGENASE A1*

Deepwater rice shows enhanced internodal elongation and grows adventitious roots in response to partial submergence (Jackson 1985; Kende et al., 1998; Sauter 2013). To facilitate emergence of adventitious roots, overlying epidermal cells undergo programmed cell death (PCD; Mergemann and Sauter, 2000; Steffens and Sauter 2005; Steffens et al., 2006). Recently it was demonstrated that reprogramming of this epidermal cells is dependent on simultaneous mechano- and reactive oxygen species (ROS) signaling. More in detail, ROS accumulation, promoted by ethylene which concentrates in submerged tissues, acts together with force exerted by the growing adventitious root to trigger PCD of overlying epidermal cells (Steffens and Sauter 2009, Steffens et al., 2012). A microarray study identified 32 genes with altered expression in mechano-stimulated epidermal cells exposed to altered ROS levels (Table 3; Sauter et al., unpublished). Based on the observation that *OsNDA1* and *OsULT1* were upregulated in this study a possible role in cell fate regulation was suggested.

Moreover another microarray study investigating expressional changes in the intercalary meristem and elongation zone of the youngest rice internode upon hypoxia also revealed co-expression of *OsULT1* and *OsNDA1*. Enhanced 1-aminocyclopropane-1-carboxylate synthase activity upon anaerobiosis and hypoxia provokes ethylene accumulation even without occurrence of flooding that decreases gas diffusion (Zarembinski and Theologis, 1993). *OsULT1* and *OsNDA1* expression decreased in the intercalary meristem of the youngest internode (Table 3; Sauter et al., unpublished), where mitotic activity is induced (Sauter et al., 1995). Increased division activity in the youngest internode is the result of ethylene-mediated cyclin expression that promotes progression of cell cycle.

Table 3: Regulation of *OsULT1* and *OsNDA1* in response to different stress conditions. A 2-fold change (FCh ≥ 2 or ≤ 0.5) cutoff was applied to select differentially expressed genes between treatments. DPI, diphenyleneiodonium; FCh, fold change; 1-MCP, 1-methylcyclopropene; ns, not significant.

Tissue	Gene	<i>OsULT1</i>	<i>OsNDA1</i>
	Treatment	FCh	FCh
Epidermal cells at the third node covering adventitious root primordia. 12- to 18-weeks-old plants, cv. Pin Gaew56 Sauter et al., unpublished	Force (26.4 bar) vs. Control (1 h)	2.40	2.62
	Force vs. Force + DPI (1 h)	3.45	2.49
	Force + DPI vs. Control (1 h)	n.s.	n.s.
Intercalary meristem and elongation zone (1 cm) at the first internode. 12- to 18-weeks-old plants, cv. Pin Gaew56 Sauter et al., unpublished	21% O ₂ vs. 5% O ₂ (1 h)	0.19	0.03

To study a possible role of *OsULT1* and *OsNDA1* in ethylene-mediated cell state transitions, gene functions of Arabidopsis homologs were examined. To this end amino acid sequences of *OsULT1* (LOC_Os01g57240), *OsNDA1* (LOC_Os07g37730) and their family members *OsULT2* (LOC_Os05g42290) and *OsNDA2* (LOC_Os01g61410) were obtained from the MSU Rice Genome Annotation Project (RGAP) website and homologs in Arabidopsis identified through a blastp search in the National Center for Biotechnology Information (NCBI) and The Arabidopsis Information Resource (TAIR) database. In both species two *ULT* genes were found and with the exception of *OsULT2*, gene expression was verified through cDNA clones. Besides *OsULT2*, that lacks 3 cysteines for a complete B-box-like motif (Figure 6), all *ULT* proteins analysed have a SAND domain capable of binding DNA and a B box-like domain acting in protein interaction (Carles et al., 2005). Since functionality of SAND domains depends on secondary structure and association with other proteins, the AtULT1-intrinsic binding capacity to DNA or protein interaction partners might be hindered or not given in *OsULT2* proteins (Wojciak and Clubb, 2001). The SAND domains are 78 amino acids long and share 65% to 78%

identity. However an enlarged SAND domain may be produced through alternative splicing of *AtULT1*.

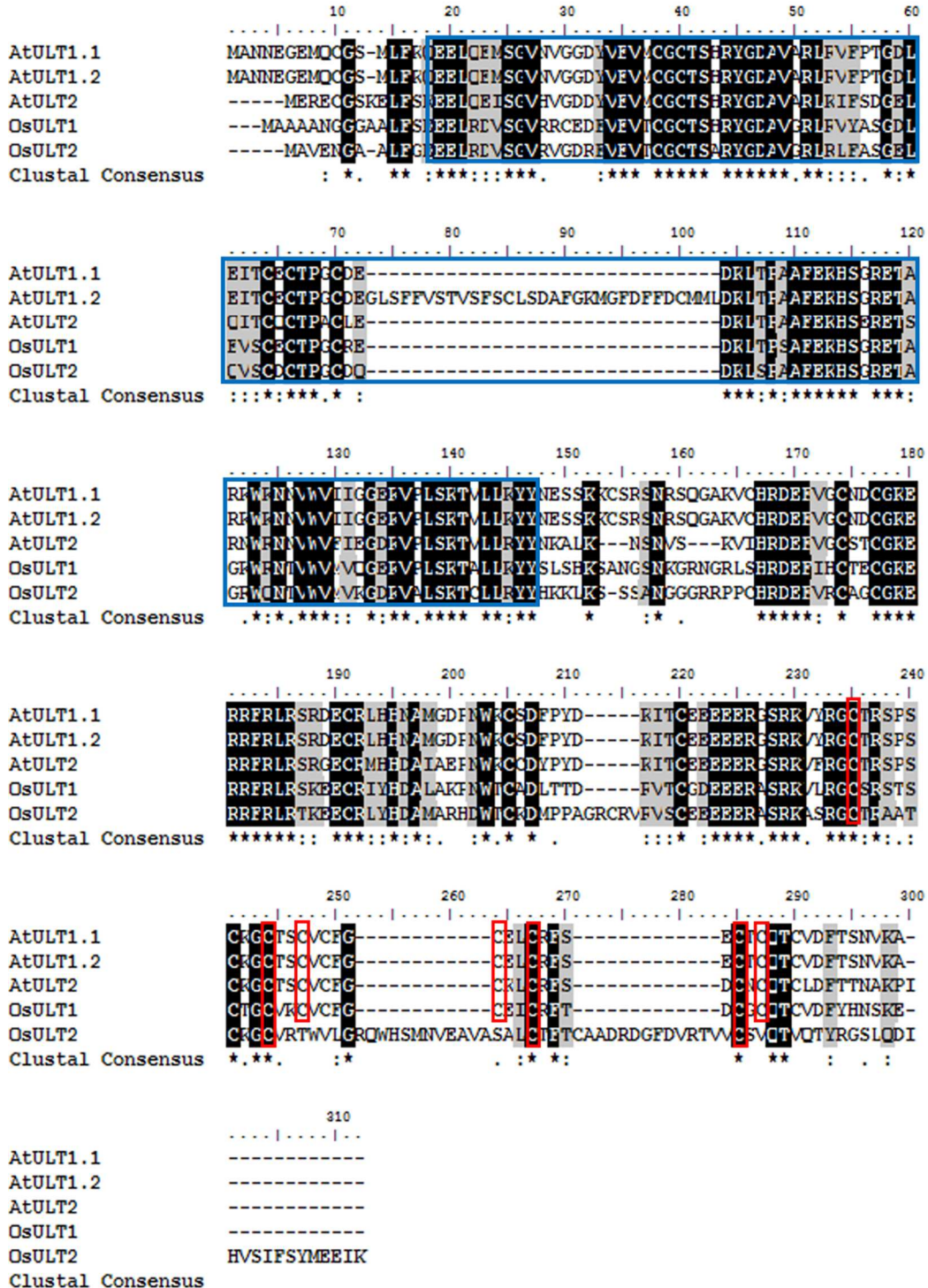
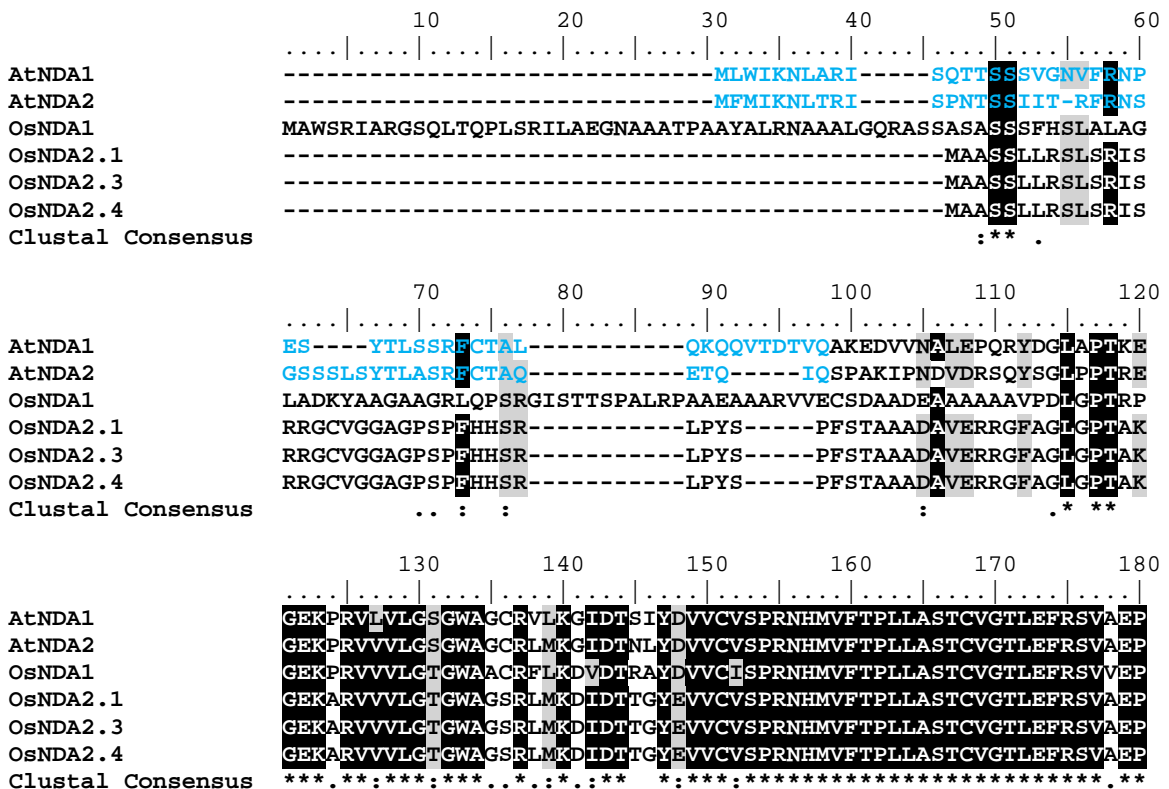


Figure 6: ULT1 and ULT2 are highly conserved in rice and Arabidopsis.

ClustalW Multiple Sequence Alignment was performed with ULTRAPETALA protein sequences from rice (OsULT1, OsULT2) and Arabidopsis (AtULT1, AtULT2). The blue

frame highlights SAND domains. Cysteines of B box-like motifs are boxed in red according to Carles et al. (2005). OsULT2 lacks cysteine residues in the B box-like motif. In the Clustal Consensus sequence * indicate identical amino acids, : amino acids with similar chemical features and . structurally identical.

Based on an OsNDA1 sequence blast, a second rice NDA, OsNDA2, and two NDAs in Arabidopsis, AtNDA1 and AtNDA2, were identified. For OsNDA2 three splice variants have been reported in the RGAP database. For Arabidopsis NDAs, mitochondrial presequences within the first 48 amino acids and C-terminal peroxisomal targeting signals (PTS) were deposited in the NCBI database (Figure 7). Furthermore dual targeting to mitochondria and peroxisome was verified by Carrie et al. (2008). The subcellular localisation of rice NDAs is predicted to be in mitochondria by TargetP 1.1 (Table 4). Translocation to peroxisomes appeared possible for the OsNDA2 splicing variant 1 as the protein sequence has a terminal PTS1 tripeptide (Figure 7). OsNDA2.1 and the Arabidopsis NDAs shared about 70% identical amino acids (Figure 8). OsNDA1 showed a rather low sequence similarity of 58% to OsNDA2, AtNDA1 and AtNDA2.




```

          190      200      210      220      230      240
AtNDA1      ISRIQPAISREPGSYFFLANCSKLDADNHEVHCETVTEG-SSTLKPWKFKIAYDKLVLAC
AtNDA2      ISRIQPAISREPGSFFFLANCSRLDADAHEVHCETLTDG-LNLTLPWKFKIAYDKLVIAS
OsNDA1      VSRIQSALATRPGSYFFLASCTGIDTGRHEVHCET-AADGDGLPANFYNFKVSYDKLVIAS
OsNDA2.1    LARIQPAVSKSPGSYFFLLARCTAVDPDAHTIDCETVTEGEKDTLKPWKFKVAYDKLVFAC
OsNDA2.3    LARIQPAVSKSPGSYFFLLARCTAVDPDAHTIDCETVTEGEKDTLKPWKFKVAYDKLVFAC
OsNDA2.4    LARIQPAVSKSPGSYFFLLARCTAVDPDAHTIDCETVTEGEKDTLKPWKFKVAYDKLVFAC
Clustal Consensus  ::***.*::  ***::** * : :.. * :.*  :.*  . :*::*:*****:*.

```

```

          250      260      270      280      290      300
AtNDA1      GAEASTFGINGVLENAIFLREVHHAQEIRRKLLLNLMLEVPGLGEDEKRRLLHCVVVGG
AtNDA2      GAEASTFGIHGVMENAIFLREVHHAQEIRRKLLLNLMLESDTPGLSKEEKRRLLHCVVVGG
OsNDA1      GSEPLTFGKGVNAENAIFLREVSHAQEIRRKLLLNLMLESENPLSSEEKRRLLHCVVVGG
OsNDA2.1    GAEASTFGIRGVTDHAIFLREVHHAQEIRRKLLLNLMLESDVPGISEEEKRRLLHCVVVGG
OsNDA2.3    GAEASTFGIRGVTDHAIFLREVHHAQEIRRKLLLNLMLESDVPGISEEEKRRLLHCVVVGG
OsNDA2.4    GAEASTFGIRGVTDHAIFLREVHHAQEIRRKLLLNLMLESDVPGMPQKHKT-----
Clustal Consensus  *:.  ****.* : :***** *****  ***** :* : :..*

```

```

          310      320      330      340      350      360
AtNDA1      GPTGVFESGELSDFIMKDVQRYSHVKDDIRVTLIARDILSSFDDRLRHYAIKQLNKSG
AtNDA2      GPTGVFESGELSDFIMKDVQRYSHVKDDIHVTLIARDILSSFDDRLRHYAIKQLNKSG
OsNDA1      GPTGVFESGELSDFITRDVREYAHVKDYVKVTLIANEILSSFVRLRQYATNQLTKSG
OsNDA2.1    GPTGVFESGELSDFIIRDVQRYSHVKDYIEVTLIANEILSSFVRLRQYATNQLTKSG
OsNDA2.3    GPTGVFESGELSDFIIRDVQRYSHVKDYIEVTLIANEILSSFVRLRQYATNQLTKSG
OsNDA2.4    -----TQIKIFVLLR-----
Clustal Consensus  ::*  : :

```

```

          370      380      390      400      410      420
AtNDA1      VKLVRGIVKVKPQKLILDDGTEVPYGPLVWSTGVGPSSFVRSILDFPKDPGGRIGVDEWM
AtNDA2      VRFVIRGIVKDVQSQKLILDDGTEVPYGLLVWSTGVGPSPFVRSILGLPKDPTGRIGVDEWM
OsNDA1      VNLVRGVVKEVKPREIELSDGSRVYGPLVWSTGVGPSEFVRSILPLPKSPGGRIGVDEWL
OsNDA2.1    VRLVRGIVKDVQPNKLILDNGEEVPYGLLVWSTGVGPSSFVRSILPFPKSPGGRIGVDEWL
OsNDA2.3    VRLVRGIVKDVQPNKLILDNGEEVPYGLLVWSTGVGPSSFVRSILPFPKSPGGRIGVDEWL
OsNDA2.4    -----
Clustal Consensus  -----

```

```

          430      440      450      460      470      480
AtNDA1      RVPSVQDVFAIGDCSGYLESTGKSTLPALAOVAEREGKYLANLNFVMGKAGGGRAN-SAK
AtNDA2      RVPSVQDVFAIGDCSGYLESTGKPTLPALAOVAEREGKYLANLNAIGKNGGGRAN-SAK
OsNDA1      RVPSVEDVFAIGDCAGFLEGTGRAVLPALAOVAEREGRYLARVMSRIAAQDGGRAVAVG
OsNDA2.1    RVPSARDVFAIGDCSGFLESTGKDVLPALAOVAERQCKYLAHLLNHVMKAGGGRAN-CEI
OsNDA2.3    RVPSARDVFAIGDCSGFLESTGKDVLPALAOVAERQCKYLAHLLNHVMKAGGGRAN-CEI
OsNDA2.4    -----
Clustal Consensus  -----

```

```

          490      500      510      520      530      540
AtNDA1      EMELGEPFVYKHLGSMATIGRYKALVDLRESKQKGGISMAGFLSWFIWRSAYLTRVVSQR
AtNDA2      EIELGVPFVYKHLGSMATIGRYKALVDLRESKDAKGISMGTGFVSWFIWRSAYLTRVISQR
OsNDA1      SAELGEPFVYKHLGSMASVGRYKALVDLRENKDAARGVSMAGFVSWLMWRSAYLTRVVSQR
OsNDA2.1    DVDLGPAPFVYKHLGSMATVGRYKALVDLRQSKESKGISLAGFVSWFIWRSAYLTRVVSQR
OsNDA2.3    DVDLGPAPFVYKHLGSMATVGRYKALVDLRQSKAGYCFCL-----
OsNDA2.4    -----
Clustal Consensus  -----

```

```

          550      560
AtNDA1      NRFYVAINWLTTFVFGRDISRI-
AtNDA2      NRFYVAINWLTTFVFGRDISRI-
OsNDA1      NRFYVAVNWATTLVFGRDNRIG
OsNDA2.1    NRFYVAINWLTLLFGRDISRI-

```

```

OsNDA2.3 -----
OsNDA2.4 -----
Clustal Consensus

```

Figure 7: NDA1 and NDA2 are highly conserved in rice and Arabidopsis.

ClustalW Multiple Sequence Alignment was performed with NDA protein sequences from rice (OsNDA1, OsNDA2) and Arabidopsis (AtNDA1, AtNDA2). Three alternative splice variants are annotated for OsNDA2 according to MSU Rice Genome Annotation Project (<http://rice.plantbiology.msu.edu>). Mitochondrial targeting sequences of AtNDA1 and AtNDA2 are shown in blue letters. Amino acids marked in yellow indicate peroxisomal targeting signal1 tripeptide motifs. In the Clustal Consensus sequence * show identical amino acids, : amino acids with similar chemical features and . the structurally identical.

Table 4: Localisation to mitochondria is predicted for rice NDAs.

Amino acid sequences of OsNDA1 and OsNDA2.1 were analysed for chloroplast transit peptide (cTP), mitochondrial targeting peptide (mTP), secretory pathway signal peptide (SP) or other signal sequences with TargetP 1.1 (Emanuelsson et al., 2000). Localisations (Loc) of OsNDA1 and OsNDA2.1 were assigned to mitochondria with a reliability class (RC) of 2 or 3, where 1 denotes the highest probability.

Name	Length	cTP	mTP	SP	other	Loc	RC
OsNDA1	562	0.116	0.782	0.002	0.051	M	2
OsNDA2	499	0.345	0.815	0.011	0.024	M	3

Sequence Identity Matrix

Sequence	AtNDA1	AtNDA2	OsNDA1	OsNDA2
AtNDA1	1	0,821	0,584	0,710
AtNDA2	0,821	1	0,584	0,705
OsNDA1	0,584	0,584	1	0,587
OsNDA2	0,710	0,705	0,587	1

Figure 8: OsNDA1 shows low similarity to OsNDA2 and Arabidopsis NDAs.

Identities of NDA protein sequences from rice and Arabidopsis were evaluated by a sequence identity matrix. The highest score 1 indicates 100% identity.

For Arabidopsis, a broad collection of T-DNA insertion lines exist, which can be used as a tool to study involvement of genes in developmental programs. For AtULT1,

AtULT2 and AtNDA1, insertion lines in the Columbia-0 ecotype were selected. The gene structures and locations of T-DNA insertions are shown in Figure 9 A. All insertions were located in exons to ensure gene disruption. Transgenic plants were tested for homozygosity of the T-DNA. If so, it was tested by RT-PCR whether insertions suppressed expression of the corresponding gene. From cDNA *AtACT2* was amplified as internal control for cDNA synthesis and to estimate RNA amount. In all lines transcripts were not detectable via RT-PCR (Figure 9 B). The *ult2-1* insertion was described as knockdown in the Landsberg erecta ecotype (Carles et al., 2005). Only homozygous lines were used for functional and phenotypical analysis. To study AtULT1 functions only *ult1-3* or *ult1-3 ult2-1* plants but not *ult2-1* plants were characterised.

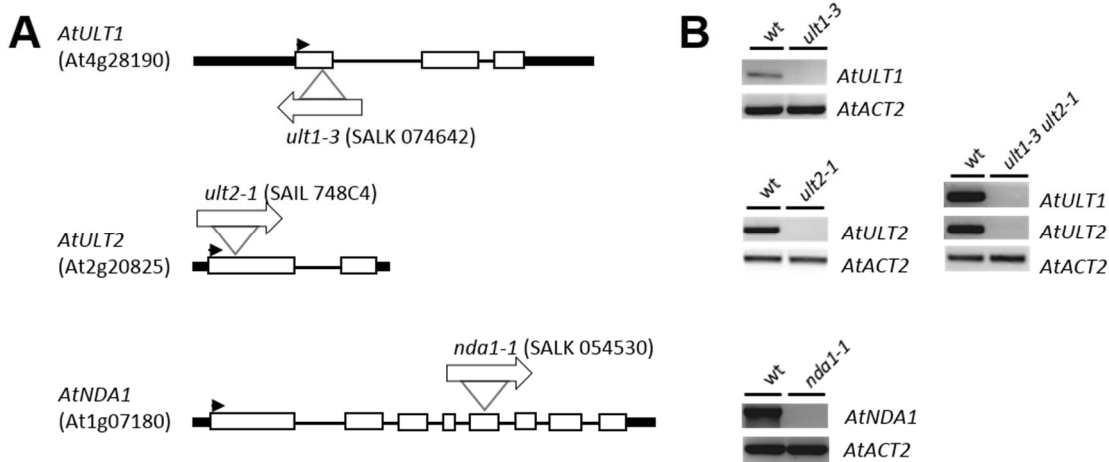


Figure 9: Position of T-DNA insertions in *AtULT1*, *AtULT2* and *AtNDA1* and analysis of gene expression.

A Gene structures with introns (thin black lines) exons (white boxes), 5-prime and 3-prime ends (thick black line) of the candidate genes and location of T-DNA insertions.

B In all T-DNA insertion lines transcripts of the corresponding genes were not detectable. *AtACT2* was used as control for cDNA synthesis. For *AtULT1* and *AtULT2* transgenic lines, transcripts from 7-day-old seedlings were analysed via RT-PCR. *AtNDA1* expression was tested in leaves of 3-week-old plants.

Promoter-GUS lines are widely used to obtain information whether, when and where genes are regulated during development. Promoter activity of *AtNDA1* was analysed after 3, 5 and 35 days of growth. Three days after seed imbibition (DAI) cotyledons

are expanded and the primary root has developed. Simultaneously biochemical as well as cellular changes are going to be completed to develop a fully photoautotrophic and actively growing seedling until day 5 (Mansfield and Briarty, 1996; Allen et al., 2010). In the early seedling stage, 3 DAI, *AtNDA1* promoter activity was detected only in cell files of the root apex (Figure 10 A, B). After 5 days of growth GUS expression also appeared in cotyledons (Figure 11 A, B and C).

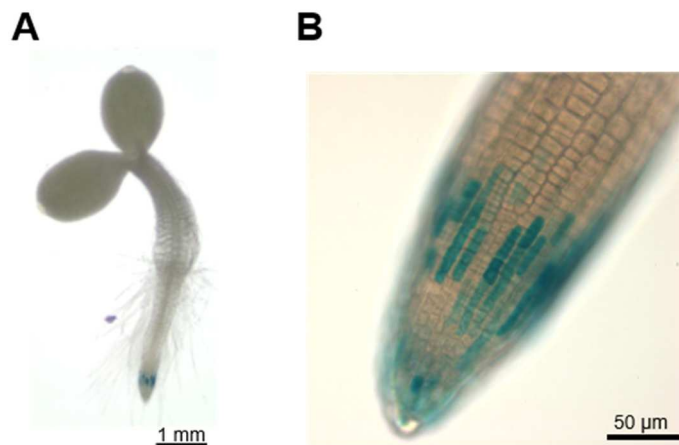


Figure 10: 3-day-old seedlings express *AtNDA1* at the primary root tip in distinct cell files. **A** *AtNDA1* promoter activity visualized in 3-day-old *AtNDA1_{pro}:GUS* seedlings. *AtNDA1* expression is present only at the root apex. **B** Magnified view of the primary root tip. Distinct cells of the lateral root cap express *AtNDA1_{pro}:GUS*.

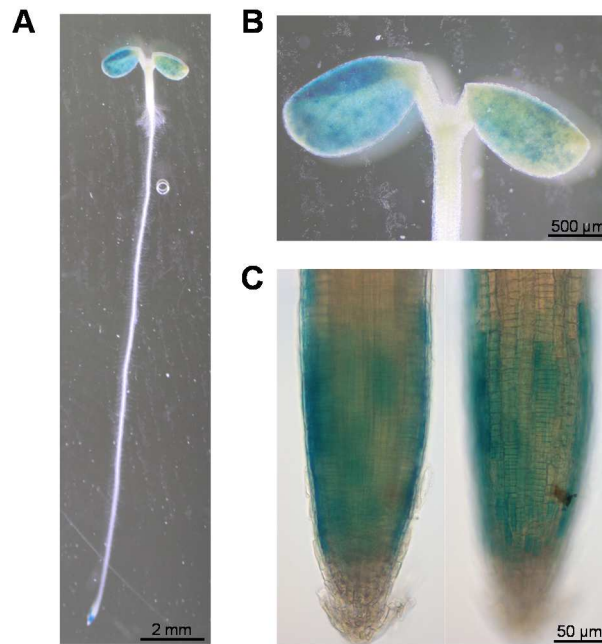


Figure 11: *AtNDA1* is expressed at the primary root tip and in cotyledons of 5-day-old seedlings.

A *AtNDA1* promoter activity was visualized in 5-day-old *AtNDA1_{pro}:GUS* seedlings.

B Magnified picture of cotyledons.

C Magnified pictures of root tips.

To analyse spatial expression of *AtNDA1* in roots in more detail GUS expressing areas were measured and correlated to distinct root zones with different cellular activities. Furthermore, cross sections were used to specify *AtNDA1* expression at the cellular level. In brief, the first 850 μm distal from the root cap junction (RCJ), which marks the transition from central root cap to the root apical meristem, can be divided in 3 zones. The meristematic zone (MZ) covers up to 200 μm and comprises cells of high mitotical activity. In the transition zone (TZ), about 200 to 520 μm away from the RCJ, cells undergo structural and metabolic changes for fast expansion in the adjacent elongation zone (EZ; Verbelen et al., 2006). In 5-day-old seedlings GUS expression covered 368 μm starting 21.6 μm from the root tip (Figure 12 A). Thus *AtNDA1* expression covered the MZ and about half of the TZ (Figure 12 B). Cross sections revealed *AtNDA1* expression to be specific to lateral root cap cells (Figure 12 C).

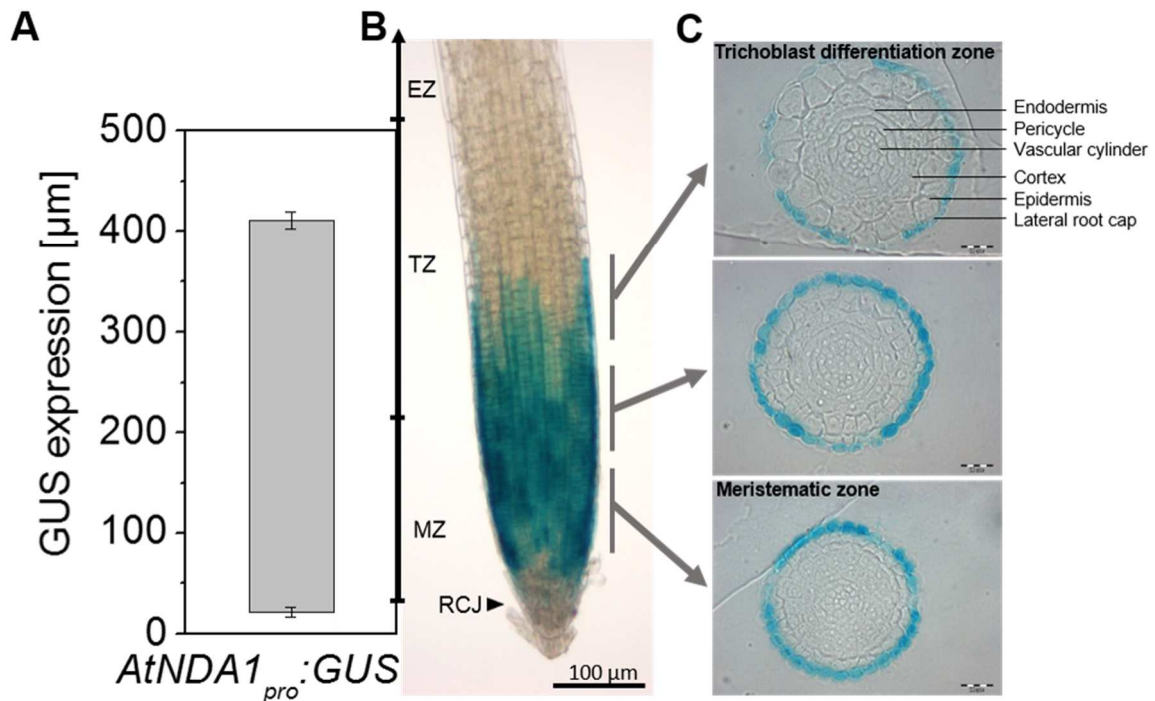


Figure 12: In the primary root *AtNDA1* is expressed in lateral root cap cells only.

A The mean length and position (\pm SE; $n=16$) of *AtNDA1*_{pro}:*GUS* activity on primary roots was measured after 5 days of growth.

B *AtNDA1*_{pro}:*GUS* expression starts at the root cap junction, covers the meristematic zone and ends within the transition zone. No expression was observed in the elongation zone. Root zones are shown to scale on a 5-day-old representative seedling root according to Verbelen et al. (2006). RCJ, root cap junction; MZ, meristematic zone; TZ, transition zone; EZ, elongation zone.

C Cross section through meristematic zone and trichoblast differentiation zone according to Dolan et al. (1993). The *AtNDA1* promoter is active only in lateral root cap cells. Bar, 20 μ m.

Germination and the change from the vegetative to the reproductive stage are the main phase transitions during plant development. As *Arabidopsis* is an annual weed with a short life cycle it enters the reproductive phase after approximately 26 days (Boyes et al., 2001). In this growth stage expression of *AtNDA*_{pro}:*GUS* is primarily observed in photosynthesizing tissues in young rosette leaves (Figure 13 I, J and K), cauline leaves (Figure 13 K), pedicels (Figure 13 F, G and H), sepals (Figure 13 A, C, E and F), and in immature anthers (Figure 13 B and D).

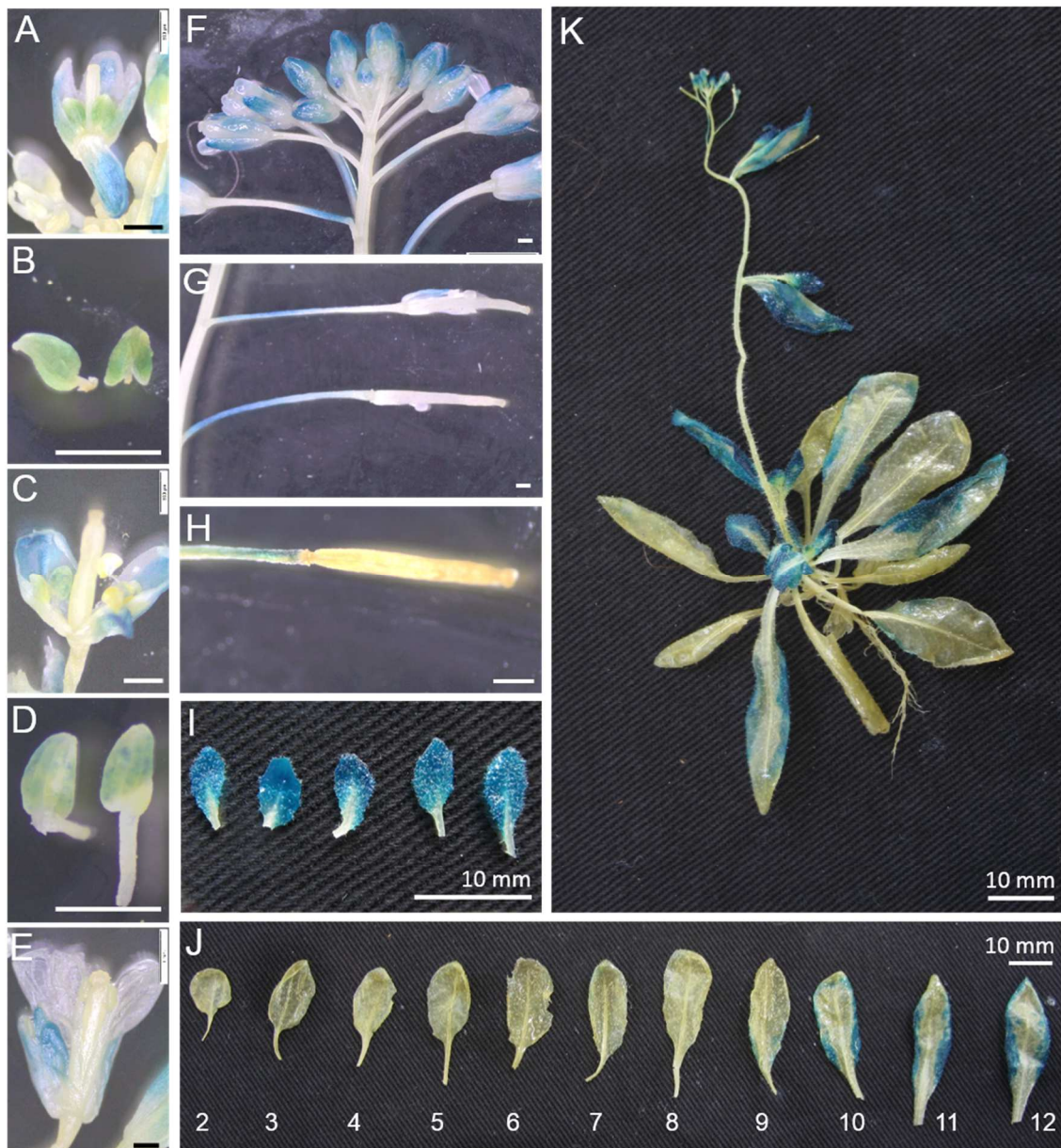


Figure 13: In 5-week-old plants *AtNDA1* is expressed in anthers, sepals and leaves.

A, C, E, G and **H** *AtNDA1_{pro}:GUS* expression was detected in stages 11 (A), 12 (C), 13 (E) of flower development and stage 16 (G), 18 (H) of fruit development according to Roeder and Yanofsky (2006).

B and **D** show a magnification of anthers from A (B) and C (D).

F and **K** presents an overview of an inflorescence (F) and plant (K) in the reproductive stage.

I The youngest rosette leaves exhibit strong *AtNDA1_{pro}:GUS* activity.

J *AtNDA1_{pro}:GUS* expression disappears in older leaves. Shown are leaves 2 to 12 in order of appearance.

Unless stated otherwise white or black bars represent 500 μ m.

AtULT1 expression was also studied in radicles 1 DAI prior germination, 2 DAI in emerged radicles with an active meristem and 3 DAI when seedlings were fully developed (Boyes et al., 2001; Nieuwland et al., 2016). *AtULT1* expression was first observed after 2 days of growth presumably in single columella cells. A spotty GUS expression at the columella and partly at the lateral root cap was visible after 3 days (Figure 14).

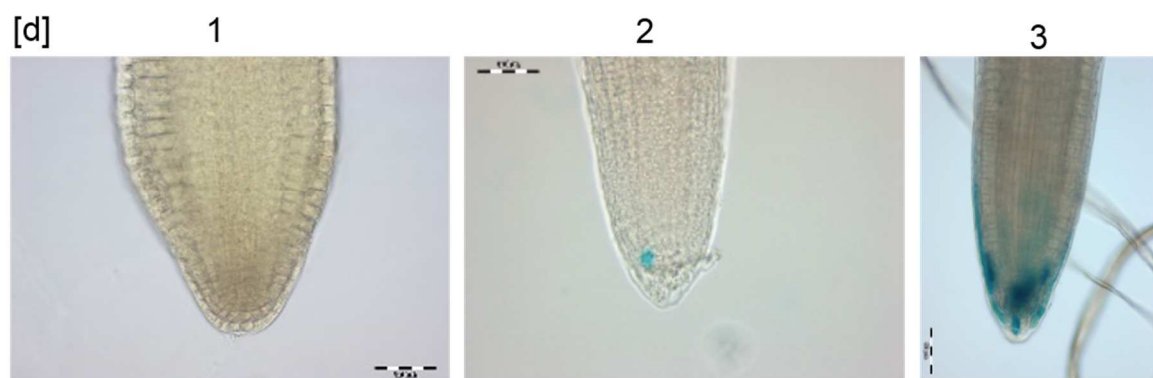


Figure 14: *AtULT1* expression in the primary root is first observed 2 days after imbibition and becomes stronger 3 days after imbibition.

Promoter activity of *AtULT1* was monitored after 1, 2 and 3 days [d] of growth following seed imbibition for 2 days at 4°C. After 1 day no expression was detected, while after 2 days weak staining was visible in a few cells close to the meristem. Three days after imbibition, expression expanded over the columella in a patchy pattern. Bars, 50 μm.

The root meristem reaches its full size and activity after 5 days of growth, when cell differentiation becomes balanced with cell production (Dello loio et al., 2007; Dello loio et al., 2008). At the same time, sloughing of border-like cells starts at the root cap (Vicré et al., 2005). At this particular time point *AtULT1* was expressed in the first 150 μm of the root tip (Figure 15 A) and in 53.6% of the seedlings in border-like cells. Thus expression spanned the columella and about half of the meristematic region in an inconsistent and patchy expression pattern (Figure 15 B). In cross sections expression was specified to single columella and lateral root cap cells (Figure 15 C).

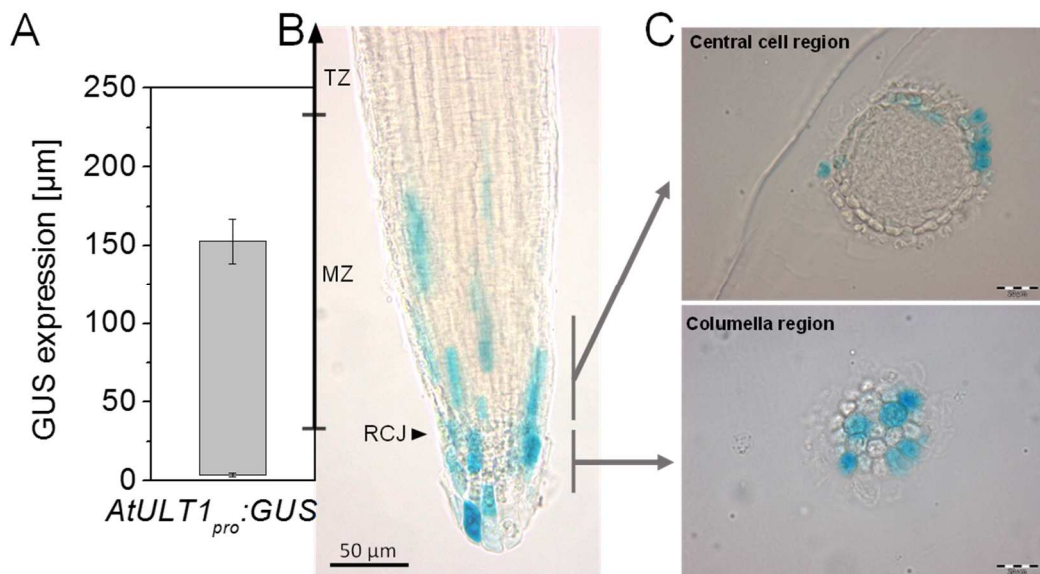


Figure 15: *AtULT1* exhibits a punctate expression pattern in the columella and the lateral root cap.

A Average length and area (\pm SE; $n=28$) of *AtULT1*_{pro}:*GUS* expression in primary root apices was determined after 5 days of growth.

B *AtULT1*_{pro}:*GUS* is expressed in border-like cells, central root cap cells and lateral root cap cells along the meristematic zone. No expression was observed in the transition zone. Root zones according to Verbelen et al. (2006) are presented to scale on a 5-day-old representative seedling. RCJ, root cap junction; MZ, meristematic zone; TZ, transition zone.

C Cross section through columella and central cell region according to Dolan et al. (1993). *AtULT1* promoter activity is present in single cells of the columella and the lateral root cap. Bar, 20 μ m.

In seedlings growing for 14 days, lateral roots developed at the primary root (Figure 16 D). The same patchy expression pattern found at root tips of 5-day-old *AtULT1*_{pro}:*GUS* seedlings was present in lateral roots (Figure 16 H and I). In lateral roots *AtULT1* expression rarely appeared in just emerged roots that were shorter than 1 mm, but was frequently observed in elongated roots longer than 1 mm (Figure 16 H and J). Lateral roots that exceeded a length of 4 mm were always expressing *AtULT1* at their tip. Expression was also observed at the base of lateral root primordia and persisted while lateral roots elongated (Figure 16 E, F, G and H). GUS expression was further observed in mature parts of the primary root with increasing strength proximal to the root shoot junction (Figure 16 D). Cross sections of the

primary root in regions more than 3 mm away from the apex suggested that *AtULT1* was expressed in the cortex, pericycle as well as xylem cells (Figure 16 B and C).

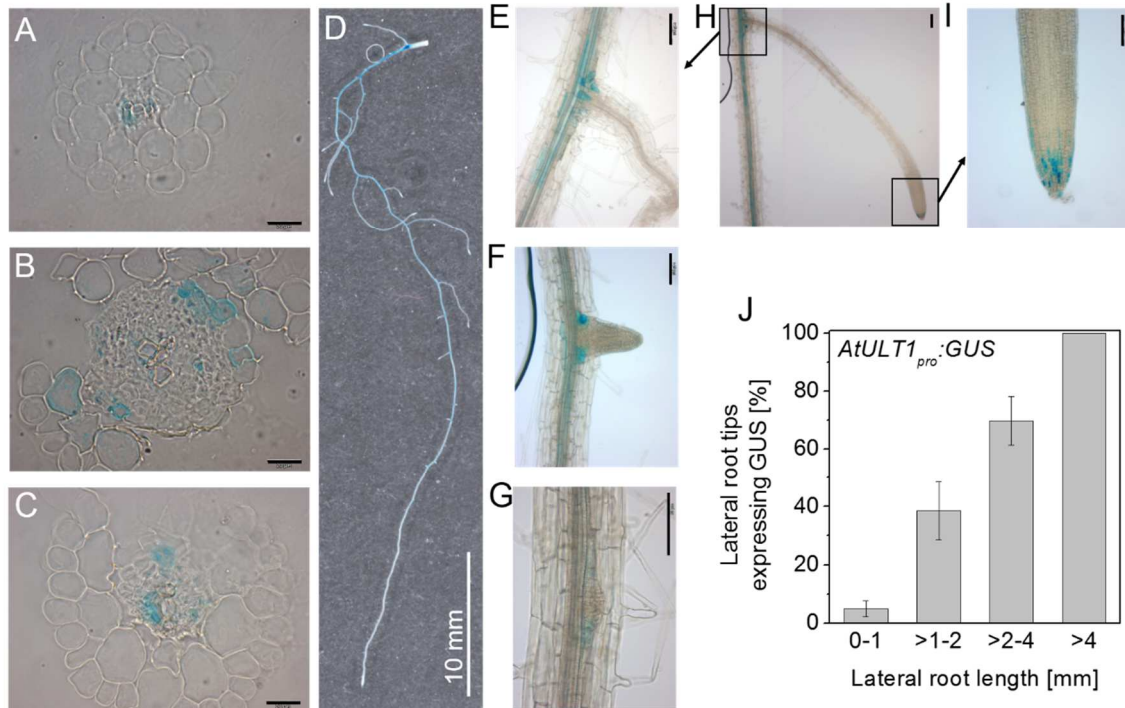


Figure 16: *AtULT1* expression appears at the base of lateral root primordia, in the primary root and in lateral root tips where expression increased with age.

A Cross section of a lateral root. *AtULT1_{pro}:GUS* is expressed in the vascular tissue. Bar, 20 μ m.

B, C Cross section of the primary root at a distance >50 mm (B) or >30 mm (C) from the tip. Cortex, pericycle and cells of the vascular tissue express GUS. Bar, 20 μ m.

D Primary root from an 11-day-old *AtULT1_{pro}:GUS* seedling. GUS expression is stronger in older parts of the root.

E, F, G, H, I Elongated (E, H), emerged (F) and initiated (G) lateral roots express *AtULT1* at their bases and during elongation at the lateral root tip (H, I). Bar, 100 μ m.

J GUS expression correlates with the length of lateral roots as measured in 11-day-old seedlings. Shown are averages (\pm SE; n=13) from 2 replicates.

During reproduction, *AtULT1_{pro}:GUS* expression was noted exclusively in the root system (Figure 17).



Figure 17: *AtULT1* is strongly expressed in roots of 35-day-old plants.

AtULT1pro:GUS plants grown on soil for 35 days were histochemically analysed. The root system was damaged during removal of soil.

In rice, the *OsULT1* expression pattern suggests a possible role in facilitating adventitious root penetration by promoting cell death of the overlying epidermis. In contrast to Arabidopsis, where postembryonic root formation at the stem is not a constitutive developmental program, cereals like rice develop an extensive stem-borne root system during their life-span (Bellini et al., 2014). In Arabidopsis adventitious roots are induced by environmental signals like wounding or prolonged darkness (Takahashi et al., 2003; Sorin et al., 2005; Steffens and Rasmussen, 2016), making it a suitable model to investigate fundamental molecular and physiological mechanism that control adventitious root emergence. For this reason *AtULT1* expression during adventitious root growth was analysed in hypocotyls of etiolated Arabidopsis seedlings (Figure 18 A). Promoter activity was observed at the base and flanks of young primordia before they were entering the inner cortical layer (Figure 18 B), but also later when primordia were fully developed and penetrated the second cortex layer of the hypocotyl (Figure 18 D). Expression was restricted to basal cells enclosing the primordium and was somewhat spread along the neighbouring vasculature of the hypocotyl (Figure 18 C). After adventitious root

emergence GUS staining was present at the basis of the root and spreading towards root vasculature (Figure 18 E).

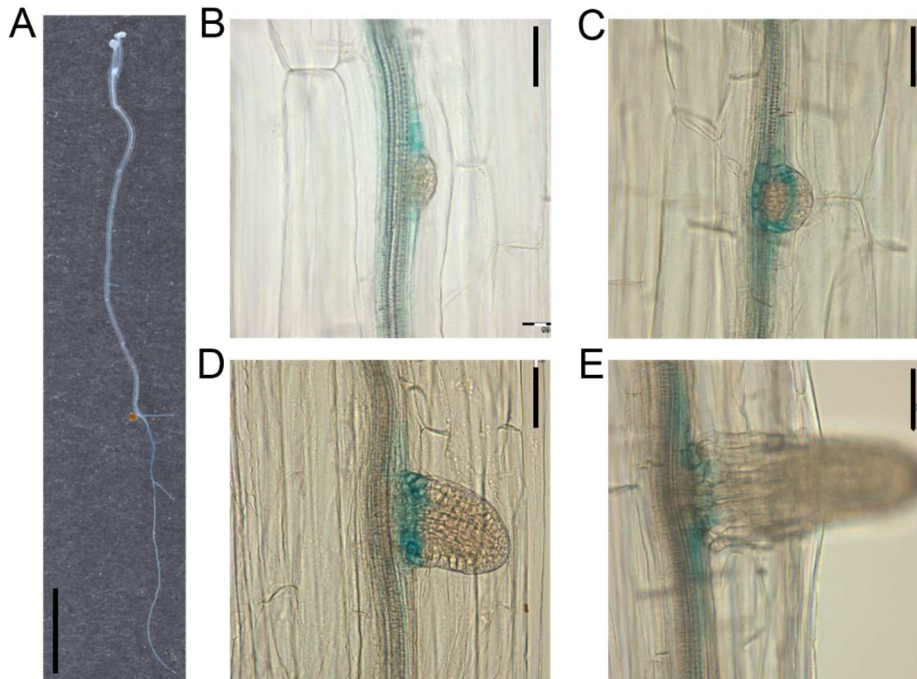


Figure 18: Circular *AtULT1*_{pro}:*GUS* expression was observed at the base of adventitious roots that develop at elongated hypocotyls of etiolated seedlings.

A *AtULT1*_{pro}:*GUS* seedlings were grown for 11 days in the dark prior to staining. Prolonged darkness induced hypocotyl extension and adventitious root formation. Bar, 5 mm.

B and **D** *AtULT1* is expressed at the base of early (B) and late (D) stage adventitious root primordia. Bar, 50 μ m.

C Ring-shaped GUS expression was visualised through a bottom view image. Bar, 50 μ m.

E After root penetration GUS staining at the base spreads towards roots vasculature. Bar, 50 μ m.

6.2 Root growth in response to mechanical stress and ethylene

Promoter-GUS studies showed that *AtULT1* as well as *AtNDA1* were expressed in the root cap or calyptra. This organ not only protects stem cells of the meristem from injury, it also receives and transmits environmental signals adjusting growth rate and direction of the root (Kumpf and Nowack, 2015).

Seedling root lengths were measured, as altered root growth may be expected if root cap maturation, maintenance or signal transduction is disturbed. After 7 days

of growth roots of *nda1-1* seedlings were shorter (Figure 19 B). Absence of *AtNDA1* reduced root length by 19.3% (Figure 19 A). In contrast, *AtULT1* had an inhibitory effect on root growth since *ult1-3* roots were significantly longer than roots of wild type (Figure 19 A, B).

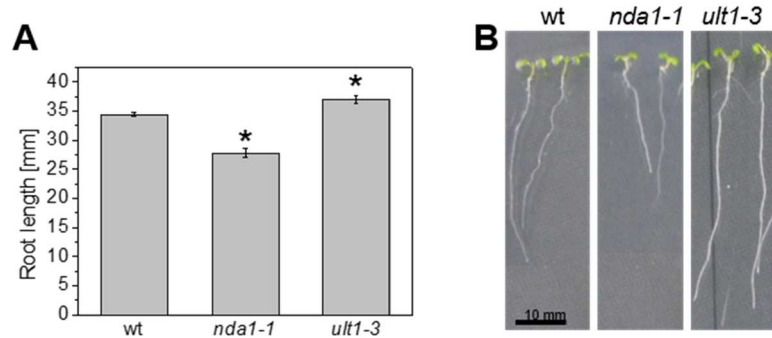


Figure 19: *AtNDA1* promotes and *AtULT1* inhibits root growth.

A Root lengths were analysed after 7 days of growth. Results are means (\pm SE; $n=78-242$) of three biological repeats. Asterisks show significant differences (Students t-Test, $P \leq 0.05$) to wildtype (wt).

B Representative seedlings of wildtype (wt), *ult1-3* and *nda1-1*.

In rice, force application induced expression of *OsULT1* and *OsNDA1* in epidermal cells covering AR primordia. To test in Arabidopsis whether root lengths in knockout lines of homologous genes are altered in response to mechanical stress, seedlings were grown on vertically or horizontally oriented plates with medium covered by a nylon membrane (Figure 20 A). When seedlings are placed upright they experience low mechanical resistance whereas resistance is high when plates are placed horizontally. Compared to wildtype *nda1-1* roots were shorter and *ult1-3* roots longer, when exposed to low mechanical resistance (Figure 20 B). On horizontally oriented plates, roots of the transgenic lines were as long as wildtype roots. Calculation of relative growth inhibition by mechanical resistance within genotypes uncovered 43.7% root length reduction in wildtype, a significantly decreased inhibition of 33.1% in *nda1-1* seedlings and increase of inhibition to 56.5% in *ult1-3* seedlings (Figure 20 B).

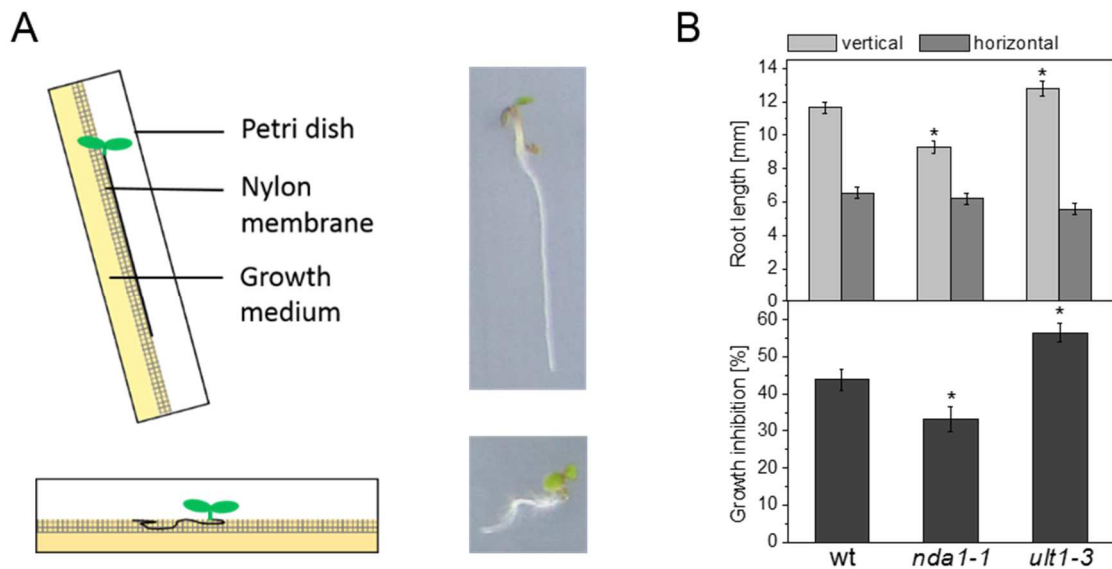


Figure 20: AtNDA1 and AtULT1 do not regulate root growth in response to mechanical impedance.

A To increase mechanical resistance, seedlings were grown on nylon membrane-covered media oriented in an upright or horizontal position for 4 days. The root phenotypes of wildtype are shown to the right. The experimental procedure was modified according to Okamoto et al. (2008).

B Root lengths were measured and growth inhibition by mechanical impedance was calculated. Results are means (\pm SE; $n=34-47$) of three independent experiments. Asterisks indicate a statistical difference (Students t-Test, $P \leq 0.05$) to the wildtype (wt). Root lengths on horizontal plates did not differ significantly.

Roots exposed to continuous mechanical resistance exhibit a characteristic ethylene phenotype as length is reduced to half, the diameter is enlarged and ectopic root hairs form (Figure 20 A; Okamoto et al., 2008). These changes result from enhanced ethylene signalling during mechanical stress. It was therefore tested whether the growth responses observed in *nda1-1* and *ult1-3* seedlings are ethylene-dependent. To that end, seedlings grown with or without mechanical impedance were either treated with 1-methylcyclopropene (1-MCP) to block ethylene perception (Sisler and Serek, 2003) or with 1-aminocyclopropane-1-carboxylic acid (ACC), an ethylene precursor, to increase ethylene biosynthesis (Adams and Yang, 1976; Kende, 1993). Due to constitutive ethylene signalling in *ctr1-1* (Kieber et al., 1993) and inhibited signal transduction in *ein3 eil1* (Chao et al.,

1997), corresponding seedlings fail to respond to these treatments (Figure 21). Since ethylene signalling regulates root growth and morphology during mechanical perturbation (Okamoto et al., 2008), *ctr1-1* mutants were used as controls for excessive mechanical stress perception and *ein3 eil1* seedlings for its disruption. Without mechanical resistance wildtype roots reached an average length of 3 mm. Mechanical impedance inhibited root growth in wildtype by 50%, as was also observed in *ult1-3* seedlings. *nda1-1* seedlings have shorter roots than wildtype at control conditions. Compared to wildtype growth inhibition by mechanical stress was minor in *nda1-1* seedlings and stronger in *ult1-3* roots. ACC application caused further decrease of root lengths in wildtype, *nda1-1* and *ult1-3* seedlings. Root lengths equal to those of *ctr1-1* seedlings were only observed when mechanical stress acted together with ACC. Without mechanical stress, 1-MCP treatment increased root lengths in all transgenic lines. Nonetheless roots of *nda1-1* seedlings still did not grow to the same length as wildtypes. Inhibition of ethylene perception combined with mechanical impedance resulted in root lengths coinciding with those of corresponding control seedlings that experienced low mechanical resistance.

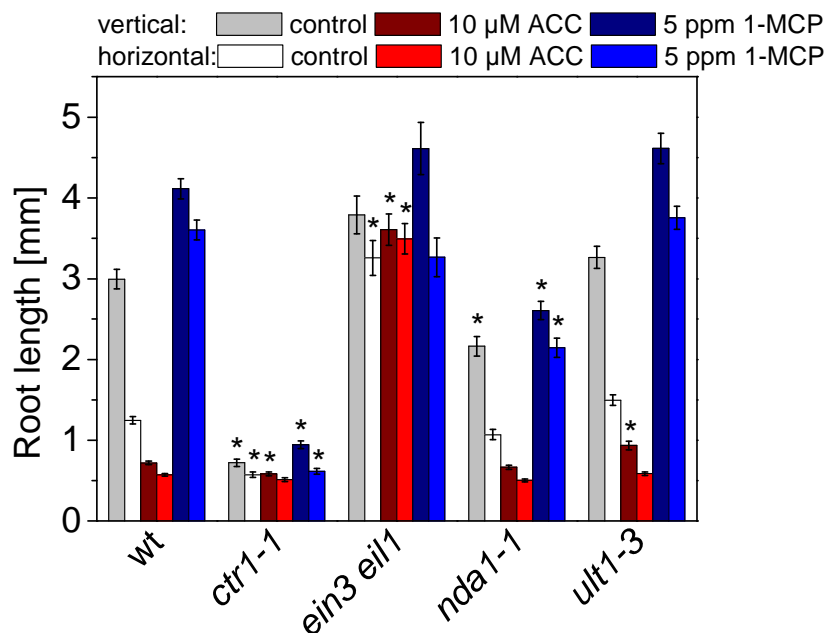


Figure 21: AtNDA1 supports root growth in response to continuous mechanical stress independently from ethylene.

Root lengths of 3-day-old seedlings grown on polyester membrane-covered media oriented in an upright or horizontal position were measured. The experimental procedure was modified according to Okamoto et al. (2008). Treatment with or without 1-methylcyclopropene (1-MCP) or 1-aminocyclopropane-1-carboxylic acid (ACC) was performed during the whole breeding. Results are means (\pm SE; n=46-116) of 3 independent experiments. * show significant differences to wildtype (wt) at a defined treatment (Students t-Test, $P \leq 0.001$).

In this study waving and skewing behaviour was analysed to test whether *AtNDA1* or *AtULT1* expression influences root perception of the underground or growth responses. The average distance between to sigmoidal curves or waving frequency was 1.67 mm in wildtype (Figure 22 A). Similar values were determined for *nda1-1* and *ult1-3*. The waving amplitude of 0.36 mm in wildtype was significantly increased by 80 μ m in *ult1-3* seedlings (Figure 22 B). In *nda1-1* seedlings no difference to wildtype was observed. An intermediate alteration of skewing angles, by 1.7° to 6.1° compared to wildtype, was observed for *nda1-1* and *ult1-3* seedlings (Figure 18 C). In conclusion, *AtNDA1* and *AtULT1* are likely not involved in thigmotropism, since waving frequency and skewing angle are unaffected. The increased waving amplitude in *ult1-3* seedlings may arise from reduced circumnutation or accelerated elongation growth.

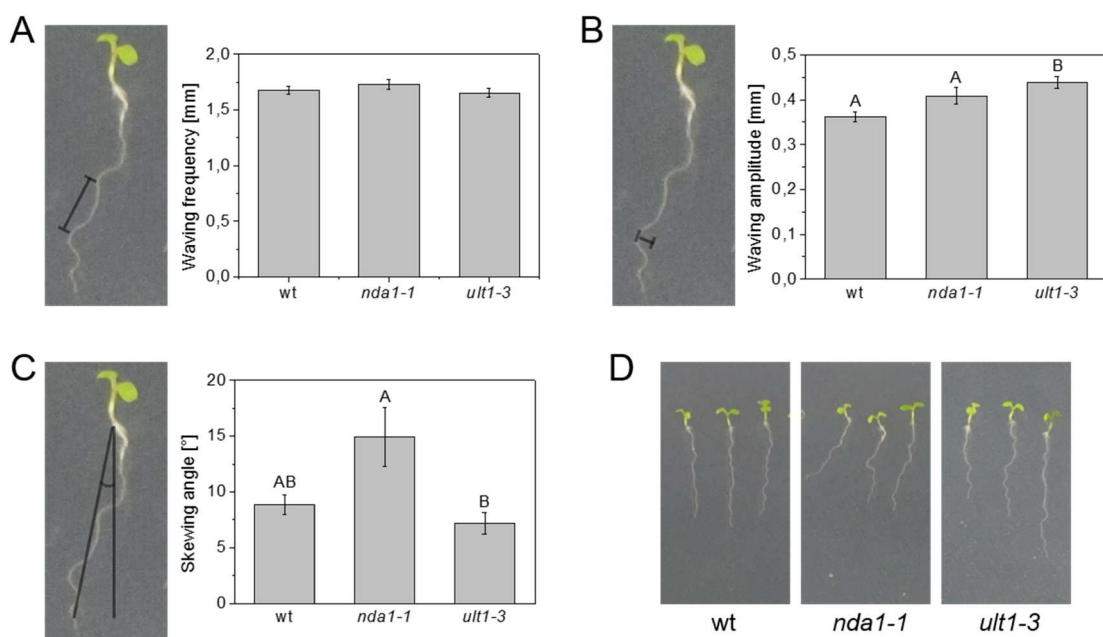


Figure 22: Root movement on hard agar is altered by AtULT1 and AtNDA1.

A, B, C Waving frequency (A), amplitude (B) and skewing angle (C) of wildtype (wt), *nda1-1* and *ult1-3* roots were determined according to Oliva and Dunand (2007). Means (\pm SE; n=38-55) and the measurements are shown. Seedlings were grown for 3 days on horizontally oriented and four more days on 45° tilted 1.2% (w/v) Bacto™Agar plates. Significant differences are shown by different letters (ANOVA, $P \leq 0.05$).

D Waving behaviour of wildtype (wt), *nda1-1* and *ult1-3* representative seedlings.

While exploring the underground, roots have two options to cope with dense soil layer or other barriers. Either they avoid obstacles by reorientation of growth direction or they penetrate through. In impeded roots release of border cells, radial thickening, as well as reduced elongation and cell production relieve stress in front of the root apex to facilitate growth (Bengough et al., 2006; Jin et al., 2013). The penetration ability of *ult1-3* and *nda1-1* seedling roots was assayed on agar medium of increasing strength. Penetration rates may provide an indication for involvement of AtULT1 or AtNDA1 in root elongation, meristem activity or cell wall remodelling. No significant difference to wildtype was observed (Figure 23).

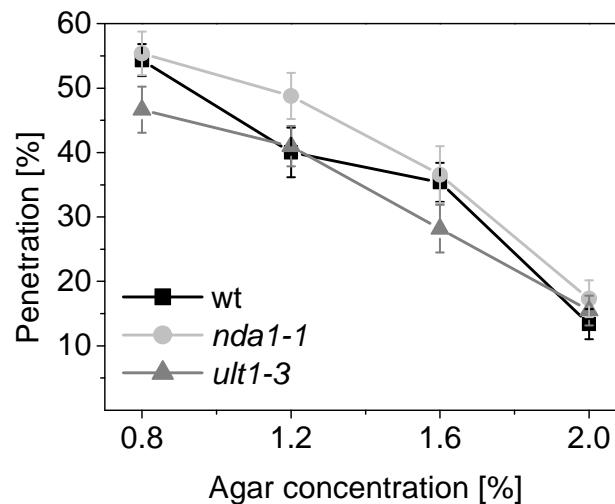


Figure 23: The ability of roots to penetrate growth medium is not influenced by AtULT1 or AtNDA1.

Root penetration into Bacto™Agar of increasing concentrations was measured for seedlings grown in the dark on horizontally oriented plates for 5 days. Results are means (\pm SE; n=27-

33) of five independent experiments. The analysed transgenic lines showed no difference to wildtype (wt).

To summarize, upregulation of *OsULT1* and *OsNDA1* during epidermal cell death in rice was suggestive for a role in ethylene-mediated mechanical signalling processes (Table 3). Experiments in *Arabidopsis* did not support this hypothesis for corresponding homologs. Neither force application (Figure 20, 22, 23) to root tips, where specific *AtNDA1* and *AtULT1* expression was found (Figure 12, 15), nor ethylene application (Figure 21) caused significant perturbations of growth or resistance perception. RT-PCR analysis additionally demonstrated no differential expression of *AtULT1* or *AtNDA1* in root tips exposed to mechanical resistance (Figure 24 A). Taking into account that root growth of *nda1-1* and *ult1-3* seedlings already alters without any trigger (Figure 19), involvement of *AtULT1* and *AtNDA1* in other cellular mechanisms needs to be considered. In rice, the consequence of force application to epidermal cells is induction of their PCD to facilitate root emergence (Steffens et al., 2012). Possibly upregulation of *OsNDA1* and *OsULT1* in these dying epidermal cells was rather a consequence of PCD execution than mechanical and ROS signal transduction. In general PCD results from changes in fate and differentiation programs of cells that are achieved by a comprehensive modification of chromatin organisation (Latrasse et al., 2016). A force-independent role is further supported through downregulation of *OsULT1* and *OsNDA1* in meristematic and elongation zone of the first internode upon hypoxia (Table 3). In deepwater rice, hypoxia causes rapid internodal elongation by promoting cell cycle entry (Sauter et al., 1995; Jackson, 2008). Differential regulation could indicate a possible role of *OsULT1* and *OsNDA1* in regulating growth or meristem activity.

Continuous root growth requires a meristem where cell production equals cell differentiation. Auxin, which accumulates in the root tip is known to coordinate cell division, expansion and meristem patterning in a dose-dependent manner (Blilou et al., 2005). Therefore, the effect of the synthetic auxin 1-naphthaleneacetic acid (NAA) on *AtULT1* and *AtNDA1* expression in root tips was tested. While *AtULT1* expression was not modified, *AtNDA1* expression strongly decreased in response to NAA (Figure 24 B). Aside from auxin, stem cell activity and differentiation is also determined through *Arabidopsis thaliana* *WUSCHEL RELATED HOMEODOMAIN 5*

(*AtWOX5*; At3g11260) in the quiescence centre of the root meristem (Sakar et al., 2007). To maintain stem cell identity *AtWOX5* expression is restricted by the receptor-like kinase *Arabidopsis thaliana* ARABIDOPSIS CRINKLY4 (*AtACR4*; At3g59420) in response to peptide signals received from differentiated columella cells (Stahl et al, 2009). Expression of *AtWOX5* or *AtACR4* was analysed in root tips of *nda1-1* and *ult1-3* seedlings by RT-PCR. In addition, mutual dependence of *AtULT1* and *AtNDA1* expression was tested, since co-expression of rice homologs was observed in epidermal cells and intercalary meristems (Table 3). Compared to wildtype no difference in *AtWOX5* or *AtACR4* transcript abundance was detected in *nda1-1* and *ult1-3* root tips (Figure 24 C). Weak expression of *AtNDA1* was found in root tips of wildtype. In *nda1-1* seedlings *AtNDA1* transcripts were not detectable. Increased *AtNDA1* expression was observed in root tips of *ult1-3* seedlings, which indicates downregulation of *AtNDA1* through *AtULT1* (Figure 24 C). *AtULT1* expression, in turn, seemed increased in *AtNDA1* deficient seedlings, when compared to wildtypes expression. Lack of *AtULT1* transcripts was evident in *ult1-3* transgenic seedlings.

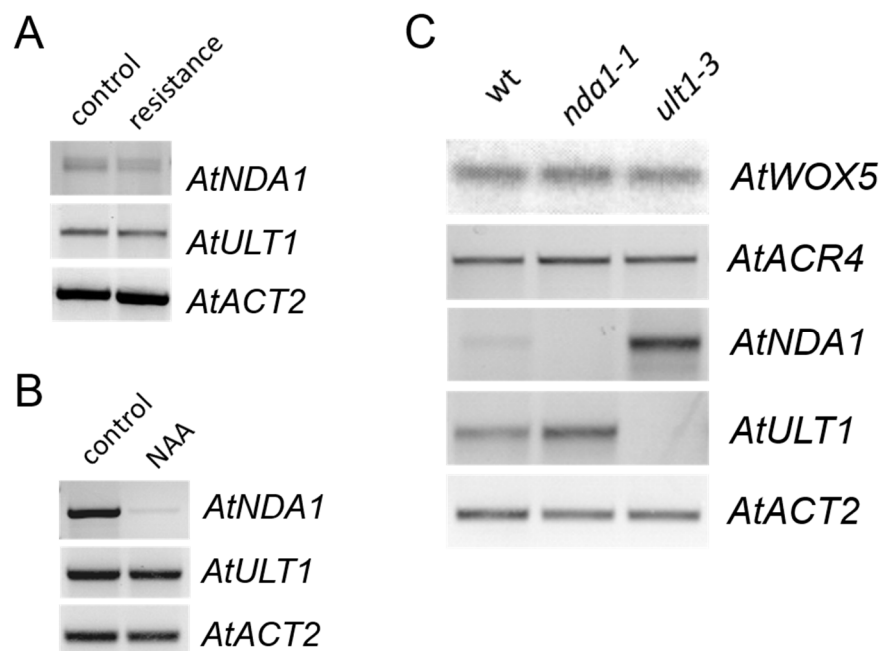


Figure 24: *AtNDA1* expression in root tips might be repressed by auxin and *AtULT1*.

A, B Mechanical resistance had no influence on *AtNDA1* and *AtULT1* expression. However, exogenous auxin downregulates *AtNDA1*. *AtNDA1* and *AtULT1* transcripts in root tips (0-3

mm) of 5-day-old seedlings exposed to no or continuous mechanical impedance (A) and of 7-day-old seedlings treated with or without 100 nM 1-naphthaleneacetic acid (NAA) for 18 hours (B) were quantified by RT-PCR. *AtACT2* was used as a control.

C *AtULT1* represses *AtNDA1*. Differential regulation of *AtWOX5*, *AtACR4*, *AtNDA1* and *AtULT1* in root tips (0-3 mm) of 5-day-old wildtype (wt), *nda1-1* and *ult1-3* seedlings was studied by RT-PCR. *AtACT2* was used as a reference.

Post-embryonic root development is a suitable model to study cell fate changes as cell cycle re-activation in already differentiated cells is required (De Smet, 2012; Lorbiecke and Sauter, 1999). Upon lateral root formation, initiation of cell cycle as well as establishment and maintenance of a *de novo* meristem requires auxin (Celenza et al., 1995). Auxin, the major regulator of lateral root formation mediates cell reprogramming during lateral root initiation as well as emergence. Founder cells of lateral root primordia become primed in the transition zone through oscillating auxin fluxes emitted from the root cap (De Smet et al., 2007). Later, auxin facilitates emergence by regulating gene expression of cell wall remodelling enzymes and aquaporins. (Swarup et al., 2008; Péret et al., 2012). However, lateral root initiation is also controlled by external stimuli like gravity (Lucas et al., 2008). In this study, lateral root initiation was synchronised through 90° gravistimulation (Figure 25 A). In wildtype, *nda1-1* and *ult1-3* seedlings, lateral root primordia always developed at the concave side of the primary root bend. In all genotypes tested root curvature of over 60° (Figure 25 B) and initiation of lateral root primordia upon gravistimulation was observed (Figure 25 C). These data suggest that neither proper gravity perception through columella cells, nor signal transduction by the lateral root cap was impaired (Swarup et al., 2005). Also initiation of lateral roots seemed to be unaffected. Lateral root emergence requires cell relaxation and separation of overlying tissues (Swarup et al., 2008; Péret et al., 2012). Failure in one or both requirements will cause a delay in time it takes the root to emerge and develop. Developmental stages of lateral root primordia at the root bend were determined to analyse root emergence (Figure 25 C). Two days after gravistimulation 69% of wildtype lateral root primordia were in stages IV to VI where they entered the cortex. At stage VII roots penetrate into the epidermal layer. In wildtype this was the case for 27.4% of the root primordia. Penetration through the primary root epidermis, that

equates to stage VIII, was observed for 3.6% of the lateral roots from wildtype. Compared to wildtype, 13% more lateral root primordia were in stages IV to VI in *nda1-1* seedlings. Percentage of stage VII primordia was reduced about 13%. Percentage of penetrated lateral roots was identical in wildtype and *nda1-1* seedlings. In *ult1-3* seedlings 54.7% of the primordia grew into the cortex. Penetration into and through the epidermis was achieved by 22.65% of the primordia. All in all the results indicate that neither gravitropic perception nor lateral root initiation were disturbed. However lateral root emergence in *ult1-3* seedlings might be faster than in wildtype or *nda1-1* seedlings.

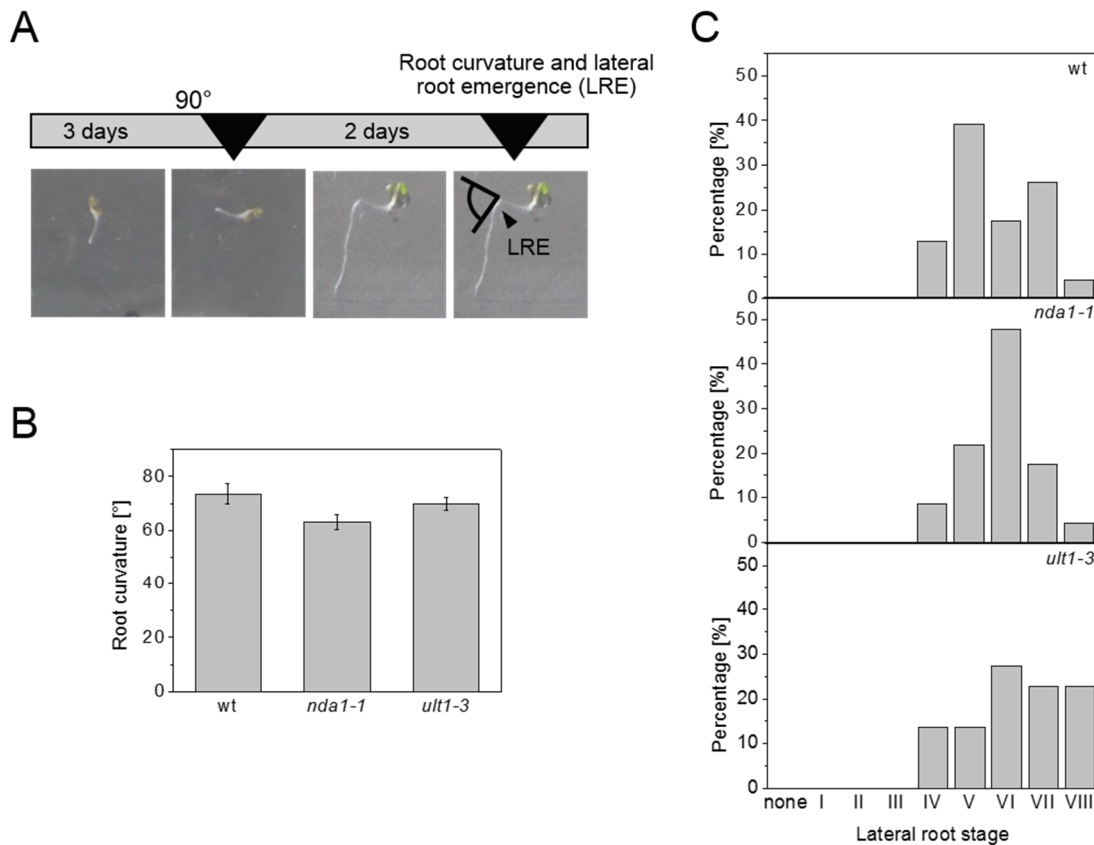


Figure 25: Lateral root emergence is not altered in *ult1-3* and *nda1-1* mutants.

A Seedlings were grown vertically for 3 days, rotated by 90° and grown for 2 more days. Subsequently the angle and developmental stages of the lateral root primordia formed at the root bend were quantified.

B Root curvature of wildtype (wt), *nda1-1* and *ult1-3* in response to 90° gravitropic stimulus. Shown are means (\pm SE; n=14) of 1 experiment.

C Primordia induction and distribution of lateral roots after gravistimulation is shown in percent (n=22-23) for 2 experiments. wt, wildtype.

In contrast to lateral roots, priming of founder cells is not described for adventitious roots. Although auxin plays a central role, environmental and molecular mechanism controlling lateral and adventitious root formation differ (Verstraeten et al., 2014). Initiation of adventitious roots is determined by environmental cues like wounding, flooding or prolonged darkness (Takahashi et al., 2003; Sorin et al., 2005; Steffens and Rasmussen, 2016). In this study prolonged darkness together with reduced sugar-availability was used to initiate adventitious roots at the Arabidopsis hypocotyl. During emergence, adventitious root primordia form in a similar manner as lateral roots but they need to traverse more cell layers to penetrate (Figure 26 B). For this reason, adventitious root primordia were classified according to the described anatomical and developmental stages of lateral roots (Casimiro et al., 2003). Adventitious root formation was analysed by determining the percentage distribution of early (Stages I-IV), late (Stages V-VII) and penetrated roots (Stage VIII). In wildtype, 56.8% of the adventitious root primordia were in the early, 25.9% in the late stage and 17.3% of the roots emerged (Figure 26 A). The distribution of adventitious root stages was comparable in *nda1-1* and wildtype. *AtULT1* knockout caused a 10% reduction of penetrated roots. Compared to wildtype, early stage primordia were increased by 17.3% in *ult1-3* seedlings.

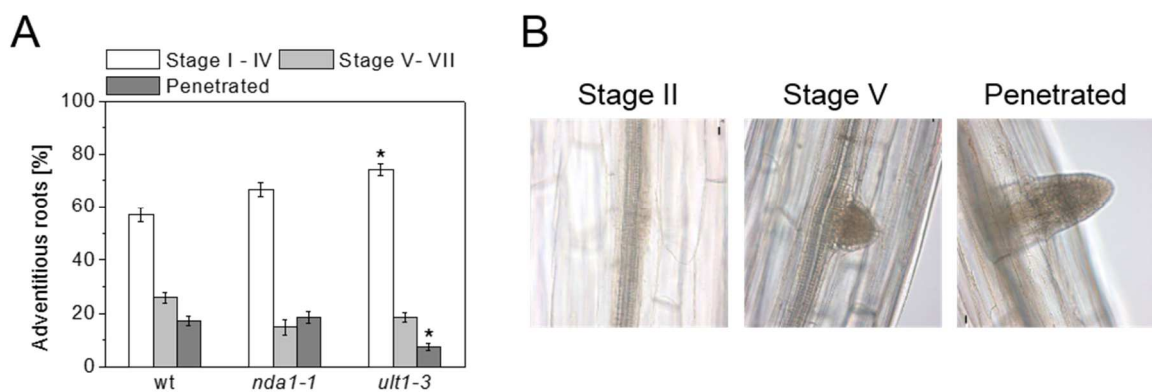


Figure 26: AtULT1 promotes adventitious root emergence.

A In *ult1-3* the percentage of early stage adventitious root primordia increased and the percentage of penetrated roots decreased. Percentage distribution of adventitious root stages at the hypocotyl was calculated for wildtype (*wt*), *nda1-1* and *ult1-3* seedlings after

11 days of growth in the dark. Shown are averages (\pm SE; n=32-41) of 3 independent experiments. Significant differences to wildtype are shown by * (Students t-Test, $P \leq 0.001$). **B** Examples of an early stage (Stage II), a late stage (Stage V) adventitious root primordia and a penetrated adventitious root.

In rice, OsNDA1 and OsULT1 may promote epidermal cell death in response to mechanical and ROS signalling (Table 3) and thereby facilitate adventitious root emergence (Mergemann and Sauter, 2000; Steffens et al., 2012). PCD of epidermal cells as well as the growth of the emerging adventitious root is induced by ethylene (Steffens et al., 2006). In Arabidopsis, ethylene inhibits adventitious root formation (Figure 27 A). To study a possible function of AtULT1 and AtNDA1 during adventitious root formation *ult1-3* and *nda1-1* seedlings were analysed. Wildtype had a density of 0.4 adventitious roots and adventitious root primordia per millimetre (Figure 27 B). Enhanced ethylene signalling in *ctr1-1* and ethylene application to wildtype lowered adventitious root density (Figure 23 A, B). Inhibition of ethylene perception with 1-MCP caused 2-fold increased adventitious root formation. A similar response was observed in *ein3 eil1* seedlings with impaired ethylene signal. Without treatment and upon ethylene application adventitious root density of *nda1-1* seedlings was similar to wildtype. Elevation of adventitious root density through 1-MCP was present in *nda1-1* seedlings, but not as strong as in wildtype (Figure 27 B). Compared to wildtype adventitious root density of *ult1-3* seedlings was elevated under control conditions. However upon ethylene or 1-MCP treatment adventitious root densities of *ult1-3* seedlings were equal to wildtypes. Thus an impact of *AtULT1* expression on ethylene perception can be excluded. In both cases, the responses of *nda1-1* and *ult1-3* seedlings argues for an ethylene-independent influence of *AtULT1* and *AtNDA1* on adventitious root formation in Arabidopsis hypocotyls. However, *AtNDA1* expression in hypocotyls was neither verified via RT-PCR nor through promoter-GUS analysis (not shown). *AtULT1* promoter activity appeared at the basis of secondary roots while growing across cortical tissue (Figure 18). Furthermore *AtULT1* expression favoured emergence, but inhibited initiation of adventitious roots (Figure 26). Taken together, results obtained for *AtULT1* provided indication for a role during *de novo* root organogenesis. So in the following *AtNDA1* was excluded from analysis and the focus set on ULTRAPETALA functions during

Arabidopsis cell fate reprogramming, meristem function and root organogenesis. To this end primary and secondary root development was analysed in *AtULT1* overexpressing and *ult1-3 ult2-1* seedlings.

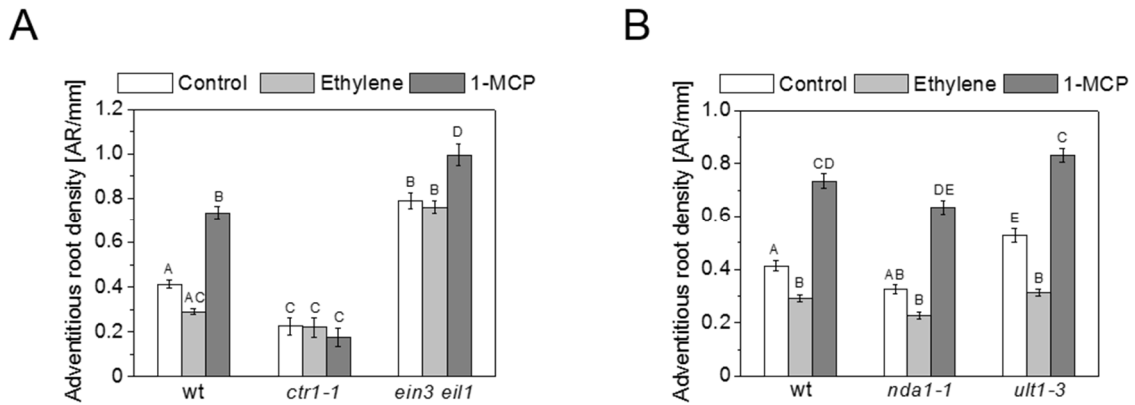


Figure 27: *AtULT1* inhibits and *AtNDA1* promotes adventitious root formation independent of ethylene.

A Ethylene inhibits adventitious root formation. The number of adventitious roots and primordia per mm of hypocotyl (AR density) was counted for 11-day-old etiolated seedlings treated with or without 5 ppm ethylene or 1-methylcyclopropene (1-MCP) for 5 days. Three independent experiments were performed and means (\pm SE; $n=27-41$) calculated. Significant differences are shown with letters (ANOVA, $P \leq 0.001$). wt, wildtype.

B *AtULT1* and *AtNDA1* knockout lines respond to ethylene and 1-methylcyclopropene (1-MCP) treatment. Adventitious root density per mm of hypocotyl was determined for 11-day-old dark grown seedlings treated with or without 5 ppm ethylene or 5ppm 1-MCP for 5 days. 3 independent biological replicates were performed and means (\pm SE; $n=32-41$) calculated. Different letters indicate significant differences (ANOVA, $P \leq 0.001$). wt, wildtype.

6.3 A role for *AtULT1* in root development

To investigate a possible role of *AtULT1* during early seedling development the germination rate, cell divisions in the RAM, as well as seedling root growth and differentiation were analysed in *AtULT1* transgenic lines. In addition, lateral and adventitious root formation was analysed.

Almost 100% of wildtype seeds germinated as indicated by radicle protrusion (Figure 28). Among *ult1-3* seeds none failed to germinate 2 days after stratification.

In *ult1-3 ult2-1* seeds visible germination of 87.6% was observed. Overexpression of *AtULT1* reduced the germination rate to 37-52.6%.

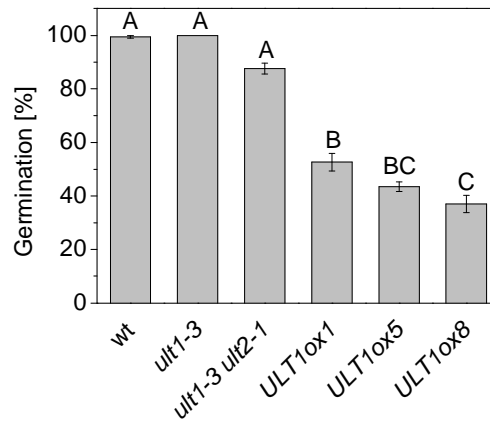


Figure 28: *AtULT1* overexpression inhibits germination.

Germination of wildtype (wt), *ult1-3*, *ult1-3 ult2-1* and *AtULT1* overexpressing lines (*ULT1ox*) were monitored after 2 days of stratification in 4°C and 2 day in long-day growth conditions. Seed coat rupture was defined as germination. Shown are means (\pm SE; n=124-150) from 4 independent analyses. Different letters indicate significant differences (ANOVA, $P \leq 0.001$).

Retarded germination may result from developmental disorder of the embryo that proceeds in disturbed seedling growth and development. Root differentiation of *AtULT1* mutant lines was monitored from 1 DAI at 4°C until 3 days of growth. Lugol's stained amyloplasts at the embryonic root apex of wildtype showed that the most proximal columella cells had already differentiated (Figure 29 A). In the following 2 days starch harbouring columella cells were present in 4 layers. No difference to wildtype was observed for *ult1-3* seedlings (Figure 29 A). In contrast, knockdown of both, *AtULT1* and *AtULT2* caused a severe root phenotype, which likely already established 1 DAI, in 22.1 % of the 3-day-old seedlings. One as well as 2 DAI, the root tips of *ult1-3 ult2-1* seedlings appeared denser and starch was detected throughout the root. In some cases no starch accumulated at the root apex and the cap appeared as a rigid structure, which was released by day 3. *AtULT1* overexpressing (*ULT1ox*) seedlings presumably failed to differentiate statocysts after 1 and 2 days of growth. No starch was detected at their root tips (Figure 29 C).

After 3 days of growth, 70% to 98.2% of the *ULT1ox* seedlings released a seemingly still embryonic root cap and revealed an unorganised batch of cells with starch grains at the root tip. According to quantitative RT-PCR analysis, *AtULT1* expression in root tips of *ULT1ox* seedlings was increased 20 to 35 times compared to wildtype (Figure 29 E). Highest *AtULT1* expression among the tested *AtULT1* overexpression lines was observed in *ULT1ox8* seedlings. Furthermore disturbed root cap formation was present in almost 100% of the *ULT1ox8* seedlings. Likely, appearance of a defective root cap phenotype correlates with strength of *AtULT1* overexpression. The developmental disorder observed in *ULT1ox* as well as *ult1-3 ult2-1* seedlings was also observed in 38.9% of *acr4-1* and 33.3% of *acr4-2* seedlings (Figure 29 B), which were tested by RT-PCR to be null mutants for *AtACR4*, a regulator of the apical root meristem (Figure 29 D).

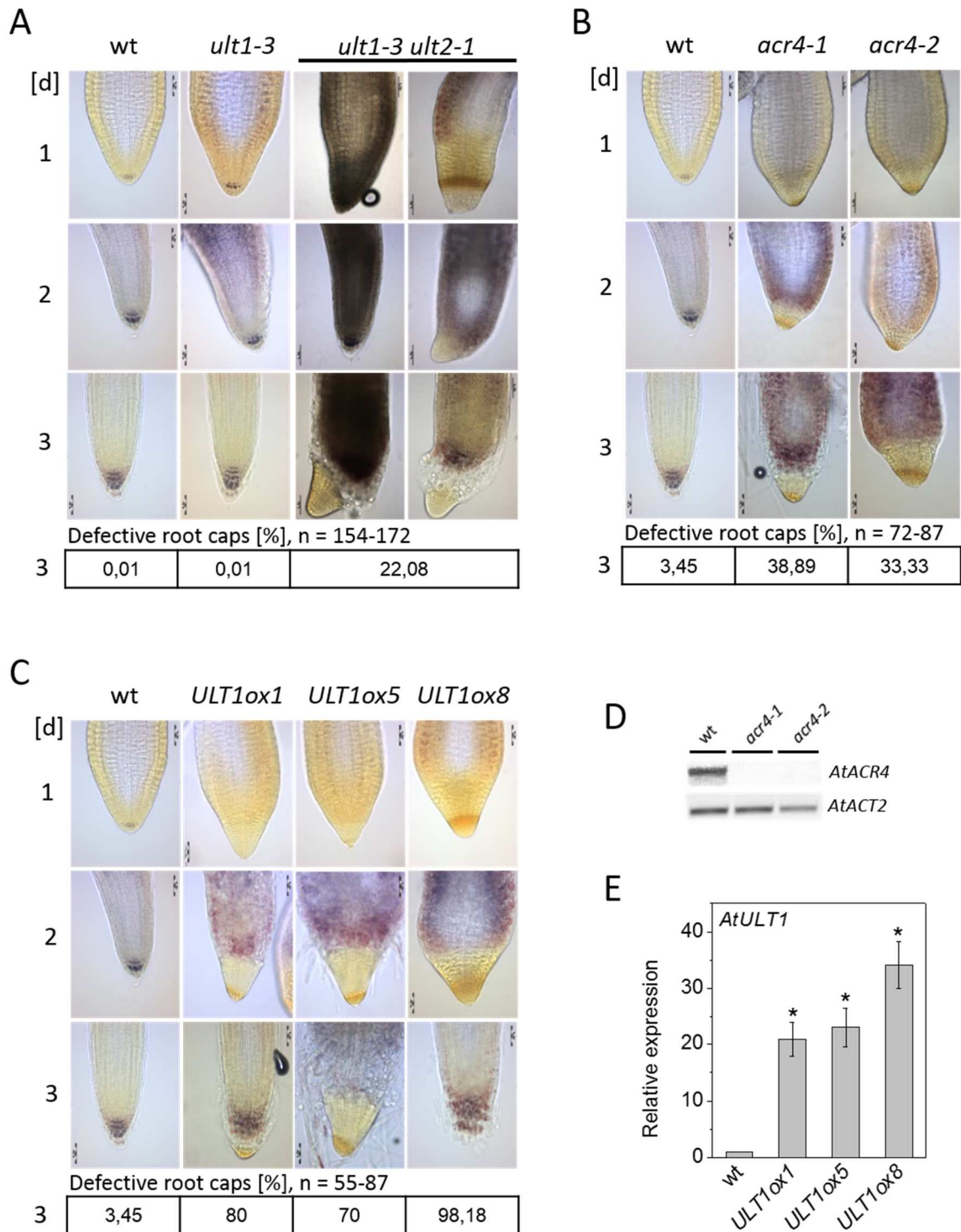


Figure 29: AtULT1 and AtACR4 may act in the same pathway to control proper root cap formation.

A, B, C Root cap development was analysed in wildtype (wt), *ult1-3*, *ult1-3 ult2-1* (A), *acr4-1*, *acr4-2* (B) and *ULT1ox1*, *ULT1ox5* and *ULT1ox8* (C) seedlings from day [d] 1 to 3 after

imbibition. The percentage of seedlings with a defective root cap was determined after starch staining with a mixture of Lugol's and chloral hydrate (1:5) solution.

D Transcripts for *AtACR4* were verified in 7-day-old wildtype (wt), *acr4-1* and *acr4-2* seedlings via RT-PCR. *AtACT2* was used as a control for cDNA synthesis.

E *AtULT1* expression was analysed by quantitative RT-PCR in root tips of 3-day-old seedlings. Relative expression in wildtype (wt) seedlings was set as 1. Asterisks indicate significant differences of average values from 3 to 4 biological replicates (Students t-Test, $P \leq 0.05$)

Root tips were analysed after 5 and 8 days of growth to observe whether and how calyptra organisation recovered. In *ult1-3* seedlings correct patterning of the root cap was observed after 5 and 8 days. As in wildtype, four clearly distinguishable columella layers with starch granules were present (Figure 30). In contrast, in *ULT1ox* and *ult1-3 ult2-1* lines misarrangement of distal columella cells occurred such that differentiation of single layers was difficult. Furthermore border-like cells that still attach to the distal columella layer in wildtype and *ult1-3* roots were detached. The root tips largely recovered after 8 days of growth. In the *AtACR4* knockout lines, *acr4-1* and *acr4-2*, a similar rearrangement of root tip organisation was detected, although impairment was stronger in *acr4-1* seedlings.

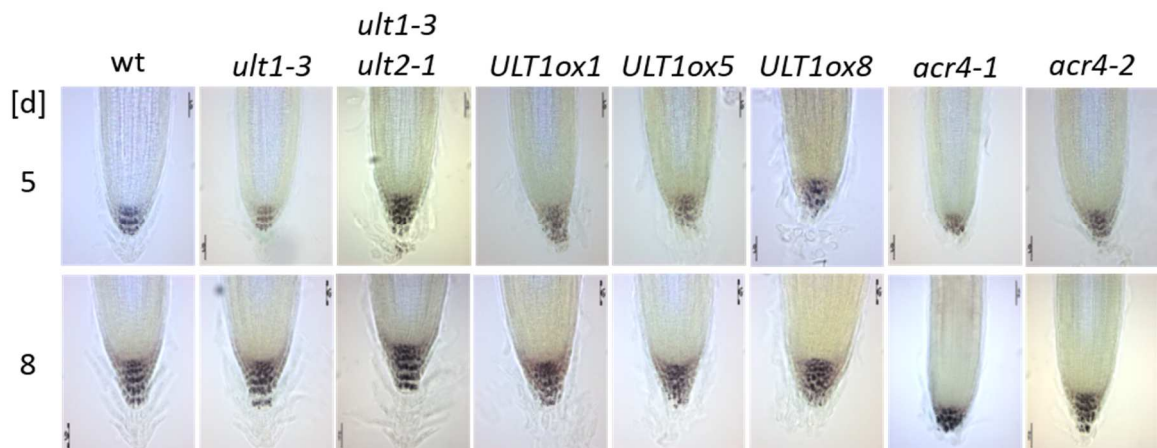


Figure 30: Recovery of disordered root cap organisation in *AtULT* and *AtACR4* transgenic lines likely starts after 8 days of growth.

Root cap organisations of wildtype (wt), *AtULT* single and double knockout (*ult1-3*, *ult1-3 ult2-1*), *AtULT1* overexpression (*ULT1ox*) and *AtACR4* knockout (*acr4-1*, *acr4-2*) lines were visualized after 5 and 8 days [d] of growth by Lugol's/chloralhydrate (1:5) staining.

To analyse the impact of disturbed root cap formation on root growth during seedling development, root lengths of *AtULT1* transgenic lines were monitored from the second to the fifth DAI and after 14 days of growth. One day after stratification when emergence of the radicle and establishment of the RAM is just completed (Boyes et al., 2001; Masubelele et al., 2005; Nieuwland et al., 2016) no significant root growth can be detected (Sliwinska et al., 2009). Therefore root growth was first measured 2 DAI and was assumed to be 0 right after germination at 1 DAI. *ULT1ox1* seedlings showed delayed root elongation after 2 days (Figure 31 A). One day later root growth retardation was also in evidence for *ULT1ox8* seedlings. Root growth in *ULT1ox1* and *ULT1ox8* seedlings was delayed up to the fifth DAI. In comparison to wildtype, *ULT1ox5* seedlings showed a minor but not significant reduction of root length 3 DAI and in the following days. *ult1-3* and *ult1-3 ult2-1* seedlings were undistinguishable from wildtype, except that *ult1-3 ult2-1* roots were slightly shorter after 5 days of growth. In 14-day-old seedlings a reduction of root length was neither detected for *ult1-3* nor *ULT1ox* plants (Figure 31 B). However, *ult1-3 ult2-1* seedlings grew about 16.4 mm shorter roots within this developmental stage (Figure 31 C).

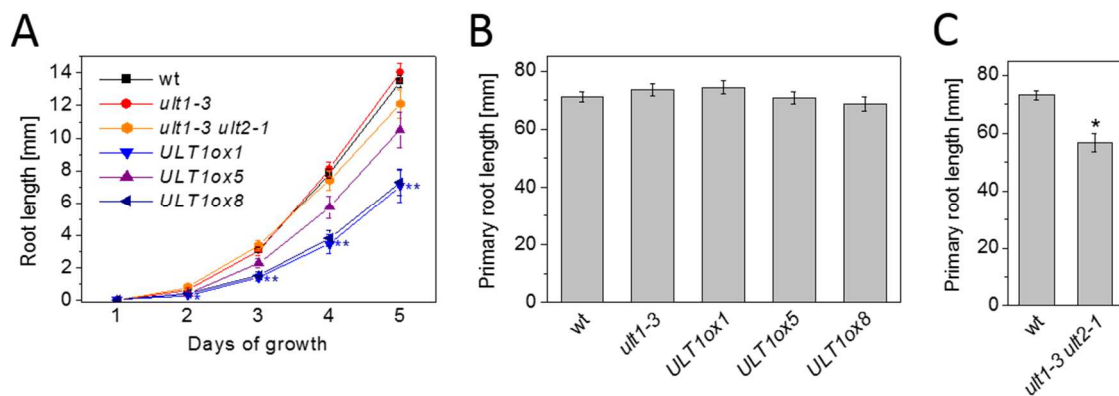


Figure 31: Arabidopsis *ULTRAPETALA* inhibits root growth during seedling establishment, but is required for root growth in fully developed seedlings.

A Root growth of *AtULT1* overexpressors (*ULT1ox*) and knockout lines (*ult1-3*, *ult1-3 ult2-1*) was monitored over a period of 4 days starting 2 day after seed imbibition and stratification. Root lengths after 1 day of growth were assumed to be 0. Depicted are means (\pm SE; n=26-74) from 3 independent analysis. Statistical difference to the corresponding wildtype (wt) value are highlighted by asterisks (Students t-Test, $P \leq 0.001$).

B and **C** After 14 days of growth on 0.8% (w/v) Bacto™ Agar solidified medium, root lengths of *AtULT1* knockout and overexpressing seedlings (**B**) or *ult1-3 ult2-1* seedlings (**C**) were measured and compared to the associated wildtype (wt). Shown are means (\pm SE; n=27-36 (**B**) or n=24-28 (**C**)) of 3 independent breeding. Asterisks mark significant differences (Students t-Test, $P \leq 0.001$).

Inhibition of germination at about half of the *ULT1ox* seeds (Figure 28), impaired root cap differentiation apparent 1 DAI in at least 70% of *ULT1ox* seedlings (Figure 29 C) and early retardation of root growth in *ULT1ox1* and *ULT1ox8* seedlings (Figure 31 A) led to the conclusion that *AtULT1* might function already in the embryo, possibly during RAM establishment prior to germination. To test this hypothesis, columella stem cell divisions in the post-embryonic meristem were analysed in wildtype, *ult1-3 ult2-1* and *ULT1ox8* embryos. By confocal imaging of a median longitudinal plane, 2 or 3 central QC cells with 4 columella stem cells at their periphery and three rows of 4 columella cells were visualised in 63.9% of the analysed wildtype radicles (Figure 32 A1, B). This regular pattern was also present in 48.5% to 59.6% of the *ult1-3 ult2-1* and *ULT1ox8* embryos (Figure 32 B). However, as divisions of columella stem cells are not exactly synchronised (Campilho et al., 2006) absence of one or two anticlinal divisions were detected in 21.3% of the wildtype and 14.9% of the *ULT1ox8* embryos, but with 4.5% rarely in *ult1-3 ult2-1* radicles (Figure 32 A2, B). In the *ult1-3 ult2-1* line additional transversal columella cell divisions were recognized (Figure 32 A4, B). Furthermore, missing periclinal separation between columella cells was observed 3 times more frequently in the transgenic lines than in wildtype (Figure 32 A3, B). For maintenance of the stem cell niche, mitosis of quiescence centre (QC) cells is strongly restricted. In consequence practically no QC cell division occurs until 3 days after germination (Forzani et al., 2014). In compliance with these findings, none of the wildtype and only 1.6% of the *ult1-3 ult2-1* embryos revealed divisions in the QC after 2 days imbibition (Figure 32 D). In contrast, divisions of QC cells were observed in 21.8% of the *ULT1ox8* embryos (Figure 32 C, D). Furthermore 12.7% of their post-embryonic meristems show an abnormal columella organisation (Figure 32 C, D).

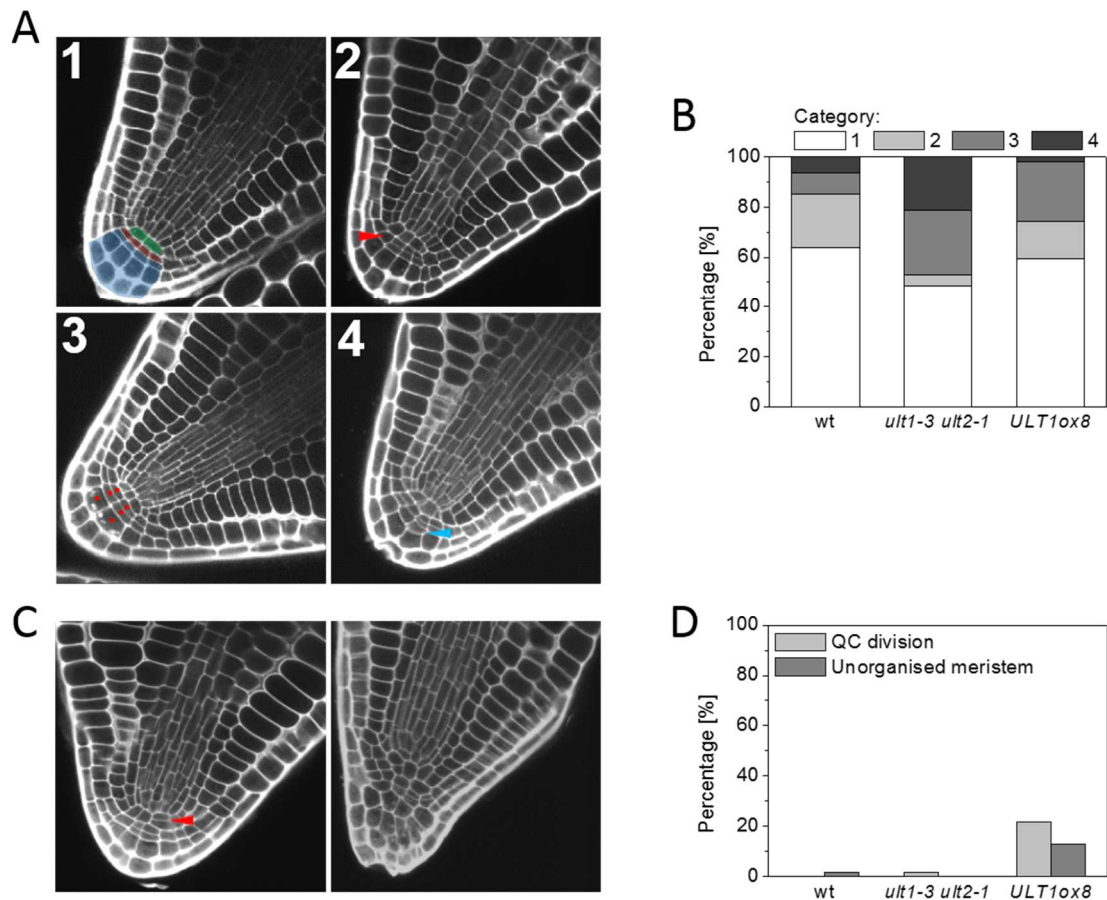


Figure 32: AtULT1 might balance cell divisions in the RAM.

A Radicles of 2 days imbibed wildtype (wt), *ult1-3 ult2-1* and *ULT1ox8* embryos were imaged after modified pseudo-Schiff propidium iodide (mPSPI) staining by confocal laser scanning microscopy. According to number and orientation of division planes in columella stem cells and columella cells, radicles were categorised into 4 groups. In category 1 simultaneous division of columella stem cells (red) resulted in 3 layers of columella cells (blue) distal from the quiescence centre (QC; green). In roots of category 2 Columella stem cells failed to perform one or two anticlinal divisions (red arrow). Missing periclinal divisions (red dots) in roots of category 3 yielded in fewer columella cells or columella stem cells in the corresponding layers. In category 4 additional anticlinal divisions (blue arrow) of single columella cells were observed. Categories were applied for B.

B Percentage of division patterns as described in A were calculated for embryos of wildtype (wt), *ult1-3 ult2-1* and *ULT1ox8* imbibed for 2 days (n=55-61).

C and **D** Percentage of embryos (D), that show division of QC cells (C, left) or complete rearrangement of the embryonic root meristem (C, right) was calculated for wildtype (wt), *ult1-3 ult2-1* and *ULT1ox8* genotypes (n=55-61).

Stem cell activity, root formation and growth largely rely on transcription factors in the root organising centre, the QC. One of the most important transcription factors regulating stem cell fate in roots is the homeodomain containing *AtWOX5*. *AtWOX5* is specifically expressed in the QC (Sarkar et al., 2007; Forzani et al., 2014). *AtWOX5* expression in the QC and asymmetric divisions in the stem cell niche are controlled by combinatorial activity of *Arabidopsis thaliana* SHORT ROOT (*AtSHR*) and *Arabidopsis thaliana* SCARECROW (*AtSCR*) proteins (Di Laurenzio et al., 1996; Sabatini et al., 2003; Welch et al., 2007). In parallel another pathway involving the APETALA2 class transcription factors *Arabidopsis thaliana* PLETHORA1 (*AtPLT1*) and *AtPLT2* is sufficient to specify QC identity and activity of the surrounding stem cells through stabilisation of an auxin maximum in the post-embryonic meristem (Aida et al., 2004; Blilou et al., 2005; Galinha et al., 2007). Similar to the phenotype observed in *ULT1ox* lines (Figure 29, 31 and 32), loss-of-function in *AtWOX5*, *AtSCR*, *AtSHR*, *AtPLT1* and *AtPLT2* alleles resulted in ectopic QC divisions, altered columella stem cell activity and premature termination of root growth (Benfey et al., 1993; Helariutta et al., 2000; Sabatini et al., 2003; Galinha et al., 2007; Forzani et al., 2014). *AtWOX5*, *AtSCR*, *AtSHR*, *AtPLT1* and *AtPLT2* could therefore be targets for regulation by *AtULT1*.

Particular in the columella cell lineage proliferation is controlled by a signalling module that includes the peptide ligand *Arabidopsis thaliana* CLAVATA3/ESR-RELATED40 (*AtCLE40*) and the receptor-like kinases *AtACR4* and *Arabidopsis thaliana* CLAVATA1 (*AtCLV1*). In a feedback mechanism, *AtCLE40* peptides secreted from columella stem cell daughters, are sequestered by homo- or heterodimers of *AtACR4* and *AtCLV1*. Thereby *AtWOX5* expression in the QC and columella stem cells differentiation becomes restricted (Sarkar et al., 2007; Stahl et al., 2009; Stahl et al., 2013). Besides the analogous root tip phenotype of *AtULT1* overexpression and *AtACR4* knockout lines (Figure 29), *AtACR4* together with *AtCLV1* also shows overlapping expression with *AtULT1* (Figure 14 and 15). Like *AtULT1*, *AtACR4* and *AtCLV1* are expressed in the distal root meristem (Stahl et al., 2013). Furthermore altered waving behaviour during root growth on hard agar was observed for *ult1-3* seedlings (Figure 22) and for *AtCLE40* loss-of-function mutants (Hobe et al., 2003). In consideration of these results *AtWOX5*, *AtSCR*,

AtSHR, *AtPLT1*, *AtPLT2*, *AtACR4* and *AtCLV1* expression was analysed in root tips of 3-day-old *ult1-3* and *ULT1ox* seedlings. In addition, a possible regulation of *AtULT2* or *Arabidopsis thaliana* ARABIDOPSIS HOMOLOG OF TRITHORAX1 (*AtATX1*) was analysed, since the resulting proteins were described to function together with *AtULT1* in a multifactorial complex on regulating target gene expression (Carles and Fletcher, 2009; Monfared et al., 2013).

AtACR4, *AtSCR* and *AtSHR* expression increased about half in the *ULT1ox1* transgenic line, but appeared rather unaffected in *ULT1ox8* seedlings (Figure 33). Upregulation in both *AtULT1* overexpression lines was only observed for *AtCLV1* transcripts. *AtULT1* knockout had only minor effects on candidate gene expression, with the exception of *AtWOX5*, where expression was reduced to almost half. *AtULT2* expression was reduced in *ULT1ox* lines, but not in *ult1-3*. Taken together, comparative analysis of gene expression in *ult1-3* and *ULT1ox* suggested that *AtULT1* might influence *AtWOX5*, *AtACR4* and *AtCLV1* expression.

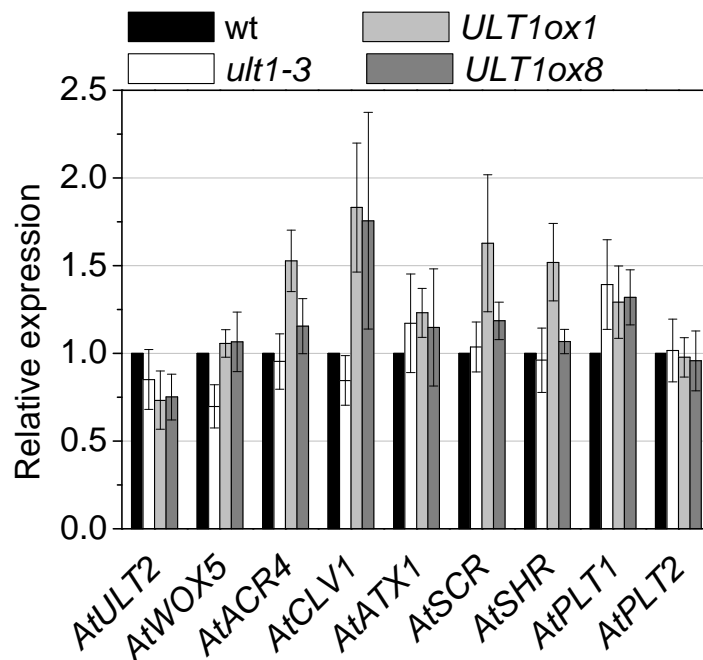


Figure 33: *AtWOX5*, *AtACR4* and *AtCLV1* expression might be regulated by *AtULT1*.

Expression of meristem marker genes (*AtWOX5*, *AtSCR*, *AtSHR*, *AtPLT1*, *AtPLT2*), genes controlling columella organisation (*AtACR4*, *AtCLV1*) and genes coding for *AtULT1* association partners (*AtATX1*, *AtULT2*) according to Carles and Fletcher (2009) and

Monfared et al. (2013) were analysed via qRT-PCR in root tips of 3-day-old wildtype (wt), *ult1-3* and two independent *AtULT1* overexpressors (*ULT1ox1*, *ULT1ox8*). Means (\pm SE) are shown for 4 biological replicates.

Expression analysis of root meristem marker genes only provided weak indications for a regulatory role of *AtULT1*. So in the following, due to the comprehensive role of auxin during root development, patterning and growth, it was tested for a down- or upstream function of *AtULT1* upon auxin signalling. To do so, *AtULT1* transgenic seedlings were grown in the presence of the naturally-occurring auxin indole-3-acetic acid (IAA) and phenotypically analysed after 5 and 11 days of growth (Figure 34). Exogenous auxin administration caused inhibition of root growth in all analysed genotypes (for reference see Figure 31 A). Although roots of wildtype and *ULT1ox* lines appeared stunted, root morphology was preserved and root hairs developed (Figure 34 A). Additionally the root cap phenotype of *ULT1ox* seedlings (Figure 29 C) was observed. In contrast, at least half of the *AtULT1* knockout seedlings showed an anomalous root anatomy in comparison to wildtype or *AtULT1* overexpression lines. Root elongation was inhibited stronger and *ult1-3* and *ult1-3 ult2-1* seedlings failed to develop root hairs. Moreover the root structure looked like a hypocotyl or leaf body and was coloured greenish yellow. After further growth for 6 days on IAA supplemented medium the majority of *AtULT1* knockout seedlings were not able to recover the abnormal root morphology that was observed after 5 days of growth (Figure 34 C). After 11 days of growth in the presence of IAA primary root elongation in wildtype and *ULT1ox* seedlings was still disturbed and secondary root growth was visible (Figure 34 B). In 66.7% to 92.3% of the *AtULT1* overexpressing seedlings roots grew from hydathodes of cotyledons (Figure 34 B and C). This rooting behaviour was also seen in 2.2% of *ult1-3* and in 26% of the *ult1-3 ult2-1* seedlings but not in wildtype (Figure 34 B).

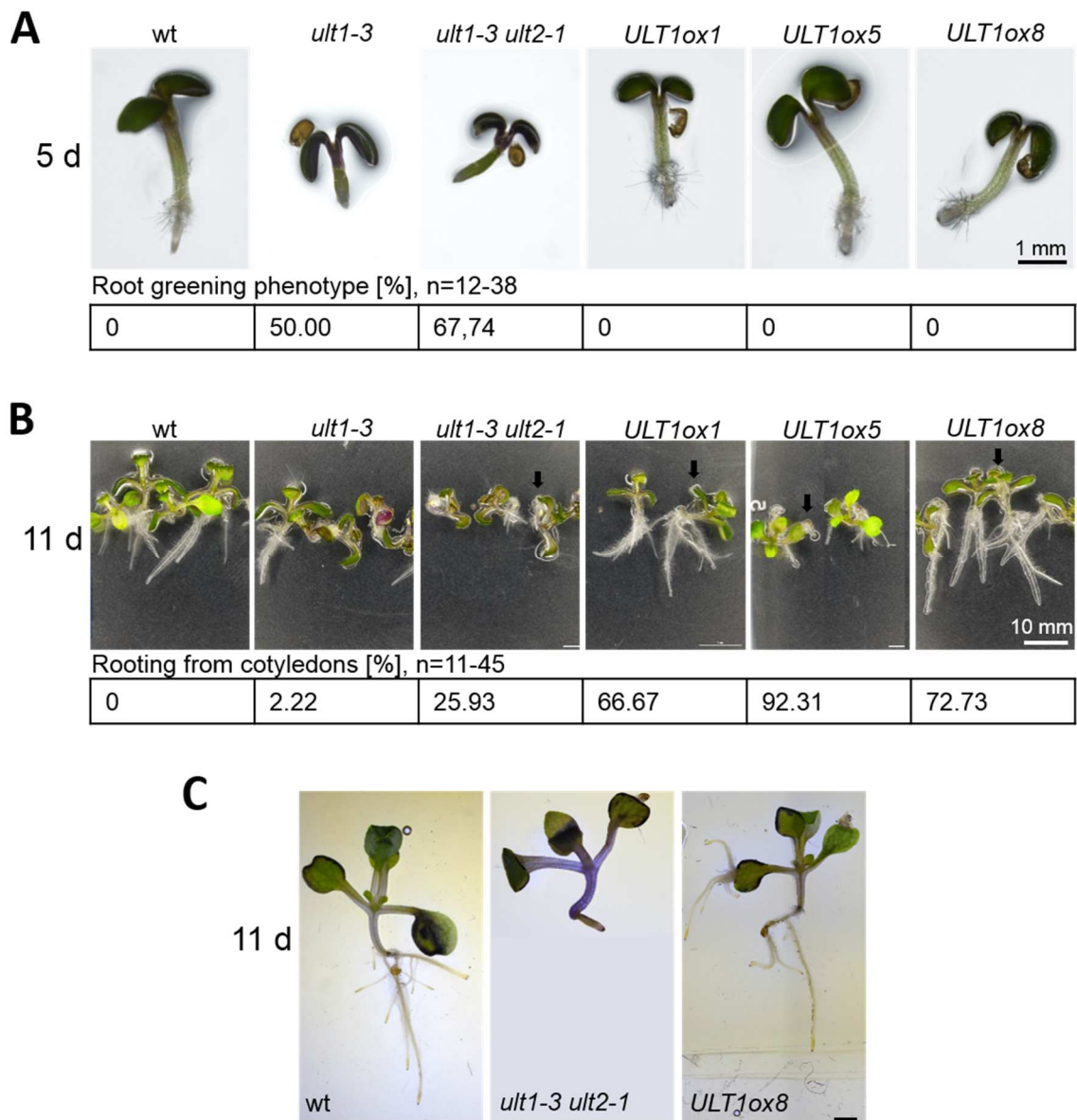


Figure 34: AtULT1 acts together with auxin to control root formation and differentiation.

A Wildtype (*wt*), *ult1-3*, *ult1-3 ult2-1* and *ULT1ox* seedlings were germinated and grown for 5 days on medium containing 10 μ M indole-3-acetic acid (IAA). Seedlings lacking *AtULT1* produced partially or fully greenish yellow roots.

B Phenotypes of *AtULT1* transgenic seedlings after 11 days of growth on medium supplemented with 10 μ M indole-3-acetic acid (IAA) are shown. IAA stimulated root growth from cotyledons in *ULT1ox* and *ult1-3 ult2-1* seedlings. Arrows point to roots growing from cotyledons. *wt*, wildtype.

The percentage of primary root greening and cotyledon rooting was determined in 2 independent experiments.

C Magnified pictures of wildtype (wt), *ult1-3 ult2-1* and *ULT1ox8* seedlings grown for 11 days on medium with 10 μ M indole-3-acetic acid (IAA) are shown. For better visualisation of roots Lugol's/chloralhydrate staining was performed. Bar, 1 mm.

In summary, auxin-induced phenotypes of *AtULT1* transgenic lines provided further insight into the role of *AtULT1* in root development. In the primary root *AtULT1* is required to suppress greening in response to auxin (Figure 34 A and C) Furthermore, ectopic *AtULT1* expression in the presence of auxin caused ectopic root formation at hydathodes. Taken together, *AtULT1* appears to control ectopic root formation, differentiation of the columella and of root hair cells possibly downstream from auxin. However, auxin is not only a key regulator of primary root growth and development, it is also involved in the control of lateral (Lavenus et al., 2013) and adventitious root formation (Pop et al., 2011). Mutants of the auxin signaling pathway show altered lateral and adventitious root formation. We therefore studied the role of *AtULT1* in secondary root formation.

Analysis of lateral roots after 14 days of growth revealed that lateral root density was significantly increased in *ULT1ox* lines compared to *ult1-3* seedlings (Figure 35 B). Compared to wildtype only *ULT1ox8* seedlings showed a significant elevation of lateral root density by 24.4%. In younger regions of *ULT1ox* primary roots excessive accumulation of lateral roots was recognized (Figure 35 A). Furthermore several seedlings showed strongly shortened lateral roots compared to wildtype. Examination of lateral root distribution along the primary root verified that lateral root number was significantly increased in the primary root region 4 to 5 cm away from the apex (Figure 35 D). Reduction in lateral root length was evident for *ULT1ox5* but not for *ULT1ox1* and *ULT1ox8* seedlings (Figure 35 C).

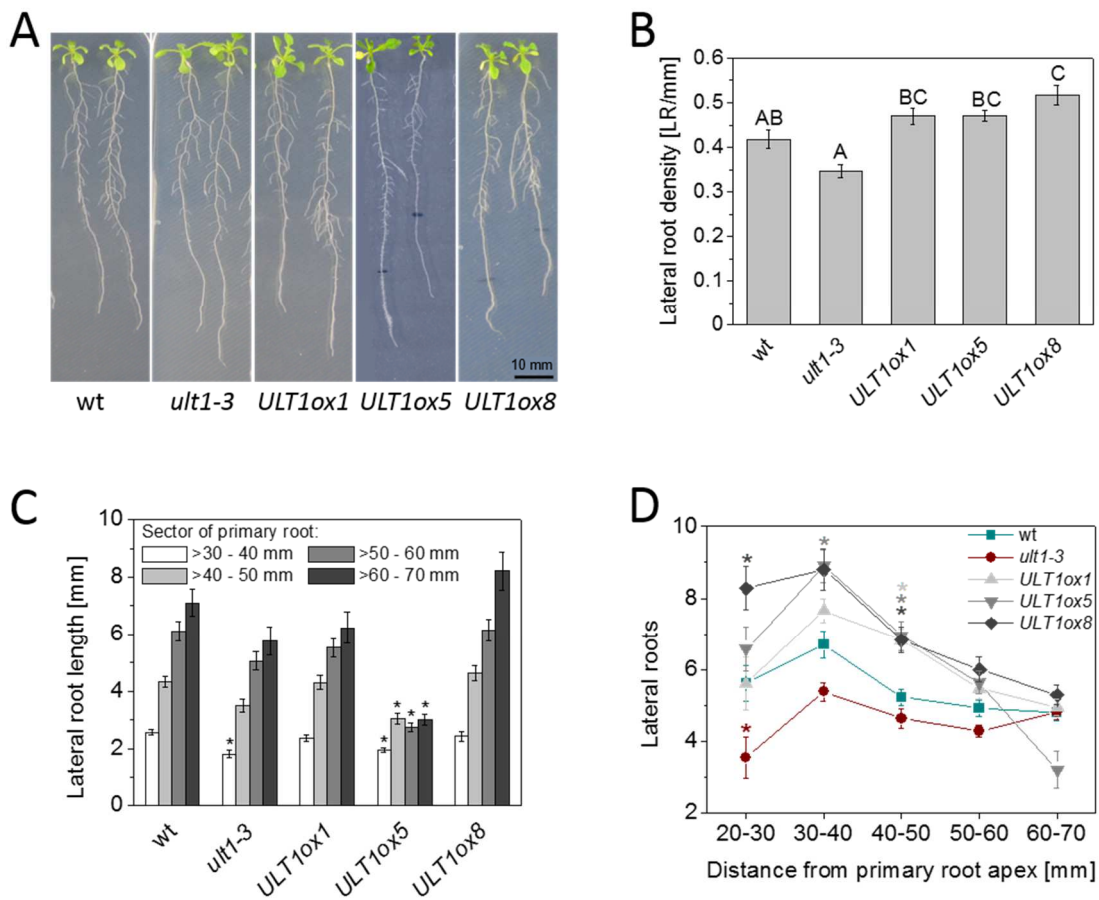


Figure 35: *AtULT1* promotes formation and changes spatial distribution of lateral roots.

A Phenotypes of wildtype (wt), *ult1-3* and three independent *AtULT1* overexpressing lines (*ULT1ox*) after growth on 0.8% (w/v) Bacto™ Agar-solidified medium for 14 days are shown. **B**, **C** and **D** Lateral root density (**B**), lateral root length (**C**) and lateral root distribution over the primary root (**D**) was determined for 14-day-old wildtype (wt), *ult1-3*, *ULT1ox1*, *ULT1ox5* and *ULT1ox8* seedlings grown on 0.8% (w/v) Bacto™ Agar medium. Lateral root density was calculated by dividing the number of penetrated lateral roots by the length of the primary root. Results in **B** are means (\pm SE, n=27-36) of 3 independent experiments. Means (\pm SE, n=19-36) in **C** and **D** were obtained from 3 to 4 independent experiments. Different letters (ANOVA, $P \leq 0.001$) and asterisks (Students t-Test, $P \leq 0.001$) indicate significant differences.

As in *ult1-3* seedlings (Figure 35 B), *ult1-3 ult2-1* seedlings with additional repression of *AtULT2* had significantly decreased lateral root numbers per millimeter primary root (Figure 36 B). Reduction of lateral root density in *ult1-3 ult2-1* seedlings was

equal to that of *ult1-3* seedlings, suggesting that *AtULT1* was primarily responsible for this phenotype (Figure 35 B, Figure 36 B).

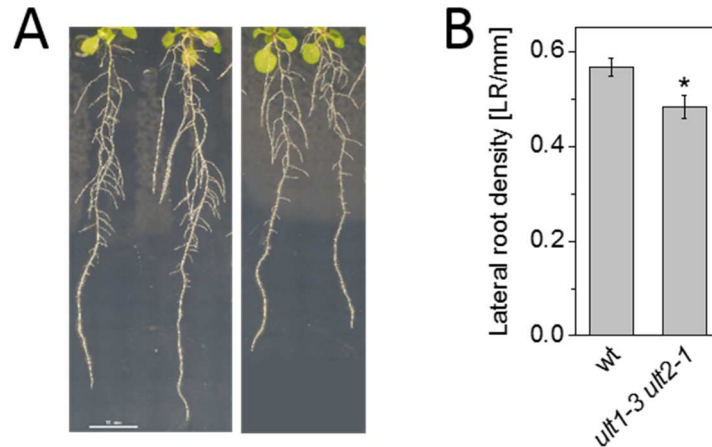


Figure 36: *ULTRAPETALA* promotes lateral root formation in Arabidopsis.

A Phenotypical appearance of 14-day-old wildtype (wt) and *ult1-3 ult2-1* seedlings was illustrated after 14 days of growth on 0.8% Bacto™Agar solidified medium.

B Lateral root density was determined for wildtype (wt) and *ult1-3 ult2-1* seedlings after 14 days breeding on medium solidified with 0.8% Bacto™Agar. Results are presented as averages (\pm SE, n=24-28) of 3 experiments with asterisks indicating statistical difference (Students t-Test, $P \leq 0.05$).

In contrast to monocots, the post-embryonic root system of Arabidopsis plants basically consists of lateral roots (Bellini et al., 2014). However, endogenous signals such as wounding or darkness can induce formation of adventitious roots (Takahashi et al., 2003; Sorin et al., 2005; Steffens and Rasmussen, 2016). A possible involvement of *AtULT1* in adventitious root formation at the hypocotyl was analyzed after 5, 7, 9 and 11 days of etiolation on medium with reduced sucrose concentration. Additionally, hypocotyl elongation was determined.

All *AtULT1* overexpressing lines had a significantly reduced adventitious root density after 11 days of growth (Figure 37 B). In *ULT1ox1* and *ULT1ox8* seedlings reduced adventitious root density was seen at earlier time points, while in *ULT1ox5* seedlings it was detected only after 11 days. In contrast, *ult1-3 ult2-1* seedlings showed a significant increase in adventitious root density after 7, 9 and 11 days of etiolation, whereas *AtULT1* single knockout seedlings were indistinguishable from

wildtype. Hypocotyl elongation was reduced in *ULT1ox* seedlings 7 days after onset of etiolation, which was two days earlier than in wildtype and *ult1-3 ult2-1* seedlings (Figure 37 A and C). Within the analyzed period no inhibition of growth was observed for *ult1-3* hypocotyls. Production of new adventitious roots in *ULT1ox* lines stopped after 7 days of growth. *ult1-3 ult2-1* seedlings showed increased formation of adventitious roots compared to wildtype (Figure 37 C). In conclusion, inhibition of adventitious root initiation in *ULT1ox* seedlings and continuous adventitious root production in *ult1-3 ult2-1* seedlings led to the hypothesis, that AtULT1 might reprograms adventitious root founder cell to initiate new adventitious root primordia.

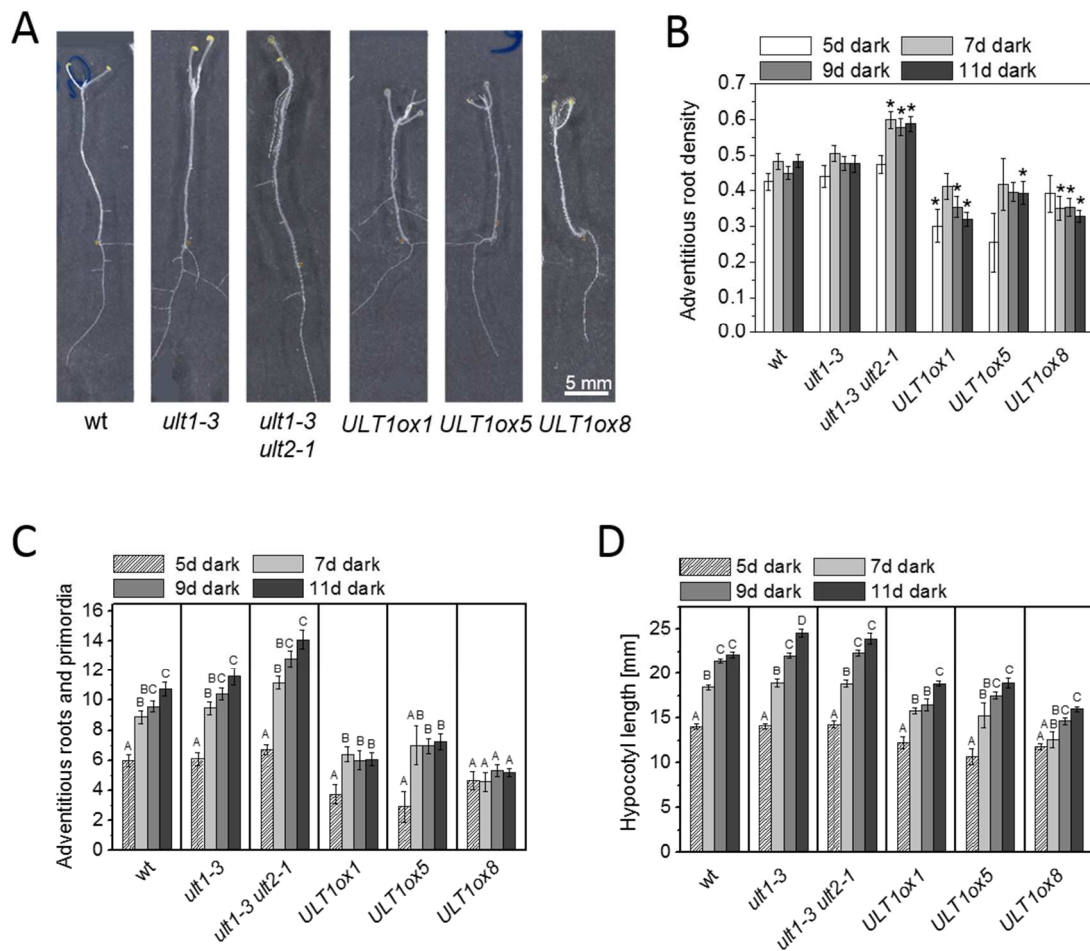


Figure 37: AtULT1 inhibits hypocotyl elongation and adventitious root formation in etiolated seedlings.

A Phenotype of wildtype (*wt*), *ult1-3*, *ult1-3 ult2-1*, *ULT1ox1*, *ULT1ox5* and *ULT1ox8* seedlings grown in the dark for 11 days are presented.

B, C and D To calculate adventitious root density (B) of wildtype (wt) *ult1-3*, *ult1-3 ult2-1*, *ULT1ox1*, *ULT1ox5* and *ULT1ox8* seedlings the number of adventitious roots and adventitious root primordia (C) and hypocotyl length (D) was determined for 5-, 7-, 9- or 11-day-old etiolated seedlings. *AtULT1* inhibited adventitious root formation and hypocotyl growth in prolonged darkness. Averages (\pm SE; n=9-58) from 3 to 4 biological replicates are shown. Asterisks indicate significant differences to respective wt (Students t-Test, $P \leq 0.001$). Letters point out statistical differences within genotypes (ANOVA, $P \leq 0.001$).

Spontaneous adventitious rooting of *Arabidopsis* hypocotyls in the dark is a consequence of *Arabidopsis thaliana* AUXIN RESPONSE FACTOR17 (*AtARF17*) degradation that is mediated by *Arabidopsis thaliana* ARGONAUTE1 (*AtAGO1*). The *ago1-3* mutant showed a defect in adventitious root formation, a reduced auxin level and hypersensitivity to light (Sorin et al., 2005). To analyse growth and secondary root formation in response to a changing light condition in *AtULT1* transgenic lines, seedlings were first grown for 7 days in the dark and then placed into light to grow for another 7 days. After transfer to light cotyledons and leaves of wildtype, *ult1-3* and *ult1-3 ult2-1* seedlings fully expanded and de-etiolated. Compared to wildtype, rosettes of *ult1-3 ult2-1* seedlings were bigger and leaves developed faster (Figure 38 A and S2). Greening of cotyledons in *ULT1ox* seedlings was retarded or completely inhibited. Furthermore rosette leaves were only slowly growing. *ult1-3* and *ult1-3 ult2-1* seedlings had an increased adventitious root density (Figure 38 B). Adventitious root density of *ULT1ox* seedlings was reduced. Lateral root density was not altered in *AtULT1* mutants. However, unlike to *ult1-3* and *ult1-3 ult2-1* seedlings, primary roots of *ULT1ox* seedlings were stunted and only half as long (Figure 38 A and C). When the absolute number of secondary roots was considered, *ULT1ox* seedlings developed 29.9% to 49.9% fewer lateral roots and 37% to 43.7% fewer adventitious roots compared to wildtype (Figure 38 A and D). Taken together the rosette and root system of *ULT1ox* seedlings was underdeveloped (Figure 38 A and S2). *ult1-3* and *ult1-3 ult2-1* seedlings, in contrast, grew 17.5% to 34.3% more adventitious roots. Compared with *ULT1ox* seedlings, the number of lateral roots was elevated in *ult1-3* seedlings (Figure 38 A, D and S2).

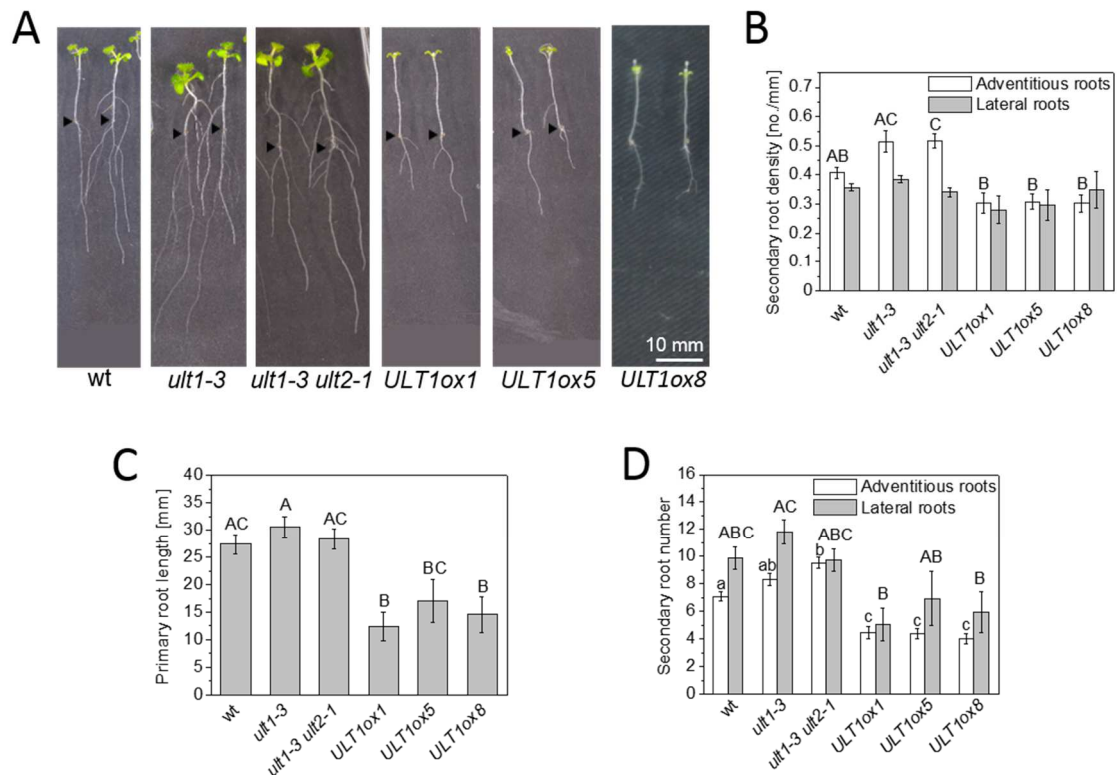


Figure 38: Switching from skotomorphogenesis to photomorphogenesis is impaired through elevated *AtULT1* expression.

A Representative wildtype (wt) and *AtULT1* transgenic seedlings grown for 7 days in darkness and 7 days in light. Increased *AtULT1* expression decelerates cotyledon and true leaf maturation (see also Figure S2).

B, C and **D** Root systems of *AtULT1* overexpressing (*ULT1ox*) seedlings are underdeveloped. Secondary root density (**B**), primary root length (**C**) and secondary root number (**D**) were analysed in 14-day-old seedlings grown in dark and light for 7 days respectively. Letters indicate statistical differences (ANOVA, $P \leq 0.001$) of means (\pm SE; $n=17-32$) from 3 experiments.

7 PERSPECTIVES

Analysis in *Arabidopsis* suggested a role of AtULT1 in primary, lateral and adventitious root development. Support for the idea that ULTRAPETALA might be involved in auxin-induced secondary root formation is provided through studies in rice. *Oryza sativa* *ULT1* (*OsULT1*) is upregulated by the auxin-responsive transcription factor *Oryza sativa* CROWN ROOTLESS1 (*OsCRL1*) during crown root formation (Coudert et al., 2015). Besides crown root formation *OsCRL1* was also shown to be required for adventitious and lateral root formation (Liu et al., 2005; Inukai et al., 2005).

To test for a conserved role of ULTRAPETALA in secondary root formation, rice plants overexpressing *OsULT1* were generated in corporation with professor Nakazono and colleagues from Nagoya university in japan. Preliminary tests supported a possible function of *OsULT1* in primary root development, emergence or elongation. Seeds of the wildtype cultivar Nipponbare germinated and developed a more than 15 mm long primary root after 5 days of growth at 27°C in the dark (Figure 39). In contrast, seed germination of *OsULT1* overexpressing plants (*OsULT1ox7*) was impaired. Of 15 imbibed *OsULT1ox7* seeds 4 germinated. *OsULT1ox7* seedlings developed a less than 10 mm long root after 11 days of growth at the same conditions.

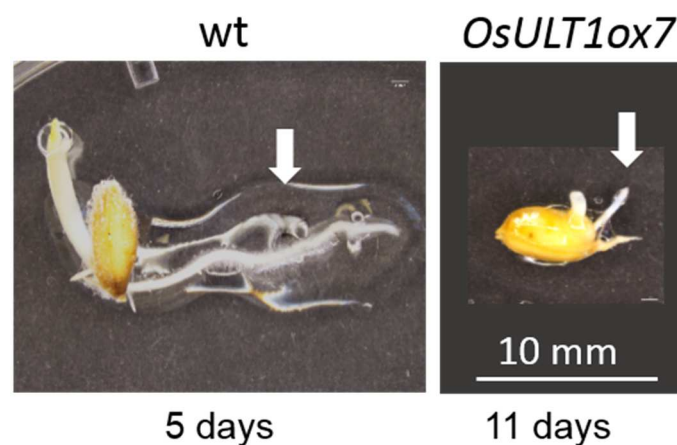


Figure 39: In rice *OsULT1* might repress primary root growth.

Seeds of *OsULT1ox7* and of the corresponding wildtype (wt) from the subspecies japonica cultivar Nipponbare were germinated and grown on wet filter paper at 27°C for 5 or 11 days in the dark. White arrows point to the radicles.

Observation of above ground growth in wildtype and *OsULT1ox7* plants showed that *OsULT1* slows down development. After 3 weeks of growth *OsULT1* overexpressing plants appeared stunted compared to wildtype (Figure 40 A). Furthermore *OsULT1ox7* plants had only formed a few leaves. Also after 4 months of growth a stunted stature which resulted from inhibited internode elongation was observed in *OsULT1ox7* plants (Figure 40 B). In comparison, wildtype plants grew twice as high.

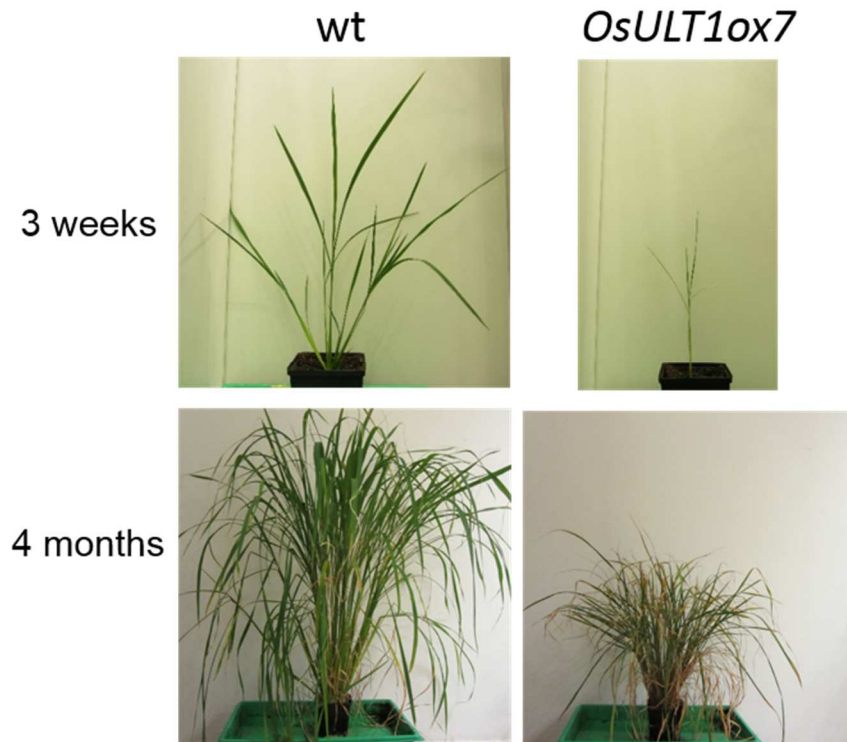


Figure 40: *OsULT1* overexpressing plants show inhibition of internodal elongation resulting in growth retardation.

Phenotypes of *OsULT1* overexpressing plants (*OsULT1ox7*) and wildtype (wt) plants of the cultivar Nipponbare are shown. Plants statures were documented after 3 weeks and 4 months of growth.

In rice height increment or rather internode elongation depends on cell division activity in the intercalary meristem and cell expansion in the adjacent elongation

zone. The intercalary meristem is located right above the nodes and covers approximately 2 mm of the stem (Kende et al., 1998). Stem elongation takes place from the lower to the upper internodes, successively. Thus mitotic activity is highest in the intercalary meristem at the base of the youngest internode. In *OsULT1_{pro}:GUS* plants it was tested whether *OsULT1* expresses in the growth zone of the first, second or third internode (Figure 41). At the first and second node weak *OsULT1* expression was observed at the base of the nodal septum and at the base of the leaf sheath. At the third node strong expression was visible in the same tissues.

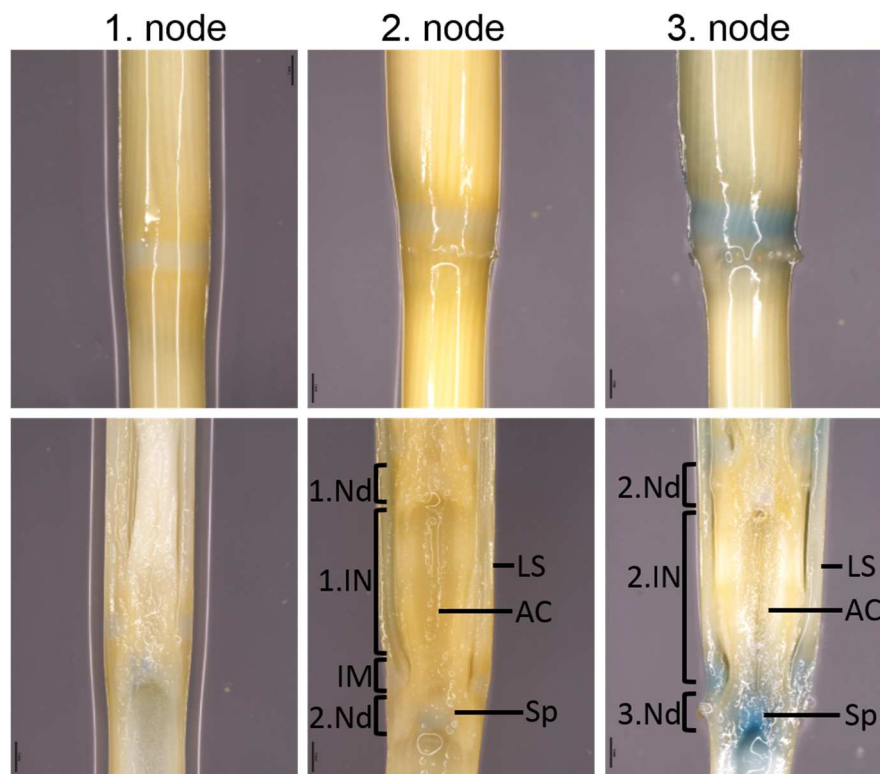


Figure 41: *OsULT1* expression at the node increased with age.

Histochemical GUS staining was performed at rice stems containing the first, second or third node of a 5-month-old *OsULT1_{pro}:GUS* plant. For more precisely localisation of GUS staining at the nodes longitudinal sections were carried out. AC, air channel; IM, intercalary meristem; IN, internode; LS, leaf sheath; Nd, node; Sp, septum. Bar, 1mm.

Cross section through root shoot junctions of 4-month-old *OsULT1_{pro}:GUS* plants revealed *OsULT1* to be expressed inside of the basal stem, where crown roots

initiated (Figure 42 C, D). In the third internode *OsULT1* expression was specific to phloem tissue of vascular bundles (Figure 42 A, B)

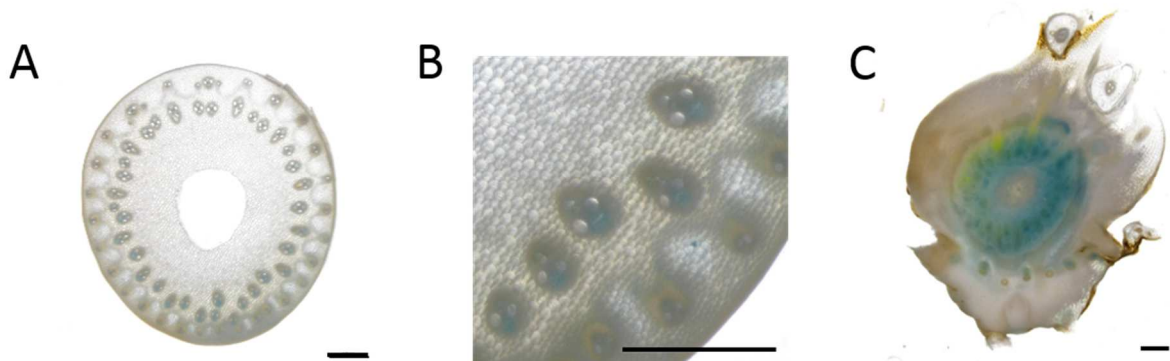


Figure 42: *OsULT1* is expressed at the root shoot junction and in vascular bundles of the third internode.

A After GUS staining of stem sections from 4-month-old *OsULT1* *pro*:*GUS* plants cross sections through the internode approximately 5 mm above the fourth node were performed. Bar, 500 μ m.

B Shown is a magnified view of A. Bar, 500 μ m.

C A cross section through the root shoot junction of a 4-month-old *OsULT1* *pro*:*GUS* rice plant is presented. Bar, 500 μ m.

8 DISCUSSION

8.1 Rice epidermal cells change cell fate in response to mechanical and ROS signalling

Deepwater rice faces waterlogging and partial submergence, which are the main reasons for oxygen deprivation in plants, with growth of adventitious roots (Jackson 1985; Sauter 2013). Adventitious root primordia constitutively develop at the nodes. Growth and emergence, however, require induction by ethylene (Lorbiecke and Sauter, 1999; Steffens et al., 2006). Ethylene accumulates in submerged tissues because of reduced gas diffusion and increased biosynthesis (Jackson, 2008). To protect the growing root from injury emergence is preceded by local programmed death of overlying epidermal cells (Mergemann and Sauter, 2000; Steffens et al., 2012). Reactive oxygen species (ROS), whose production and accumulation is promoted by ethylene, act as second messenger for both, growth of adventitious roots and programmed cell death (PCD; Steffens and Sauter, 2009; Steffen et al., 2012). However, PCD of epidermal cells is induced only when ROS act together with a force that is provided by the growing root (Steffens et al., 2012). *Oryza sativa* *ULTRAPETALA1* (*OsULT1*) and the *Oryza sativa* *ALTERNATIVE NAD (P) H DEHYDROGENASE A1* (*OsNDA1*) were upregulated by ROS and force in these epidermal cells and may thus be involved in cell fate decision in response to mechanical force (Table 3; Sauter et al., unpublished). Our study was aimed to test this hypothesis using a molecular genetic approach and physiological analyses.

8.1.1 In *Arabidopsis* mechanical signals have impacts on morphology and development of roots

ROS signaling and mechanical stress programmed rice epidermal cells overlying adventitious root primordia to die (Steffens et al., 2012). We used *Arabidopsis thaliana* to further study the function of *AtULT1* and *AtNDA1* and focused on the root response to mechanical stimulation. Promoter-GUS analysis revealed that both, *AtULT1* and *AtNDA1*, were expressed in the root cap in a highly cell-type specific manner. The root apex with its apical meristem is protected from abrasive damage in the soil by the root cap. The root cap releases mucilage and border cells or border-

like cells which eventually undergo cell death. Both act as lubricants to aid root penetration in compact soil (Arnaud et al., 2010). It is conceivable that penetration of rice adventitious roots through the epidermis and primary root growth in soil impose a similar mechanical stress on the root cap. However, in Arabidopsis no difference to wildtype was observed when *nda1-1* and *ult1-3* roots were forced to penetrate medium of increasing resistance. So root growth in response to mechanical stress was investigated in *AtNDA1* and *AtULT1* knockout seedlings. When *nda1-1* and *ult1-3* roots experienced low mechanical resistance a growth promoting role was discovered for *AtNDA1* and an inhibitory function for *AtULT1*. Upon mechanical stress the positive and negative effects on root growth through *AtULT1* and *AtNDA1*, respectively, were abolished. In *nda1-1* and *ult1-3* seedlings roots grown under resistance were as long as those of wildtype. Nevertheless relative inhibition of root growth was higher in *ult1-3* and lower in *nda1-1* seedlings. Possibly this phenotype is not a result of increased sensitivity to resistance but rather attributable to altered root lengths of corresponding control seedlings. Nonetheless, in *ult1-3* seedlings altered perception of the underground was indicated through increased root waving on tilted dense medium. Roots growing on an inclined and hard to penetrate underground, e.g. hard agar, exhibit a characteristic slanting and waving behaviour. These root movements are explained by two theories. Migliaccio and Piconese (2001) interpreted the phenotype as a result of gravitational growth intensifying a touch perception at the root apex together with inherent circumnutation of the root. Thompson and Holbrook (2004) assumed continued elongation of the root, while growth at the root tip periodically becomes obstructed through the slanted medium. Since *ult1-3* roots were longer when grown without interference, an inhibitory effect on root elongation might be suggested for *AtULT1*. Morphological and developmental changes of the root that occur in response to mechanical impedance result from enhanced ethylene signalling and an altered auxin response (Okamoto et al., 2008). In rice, transcriptional regulation of *OsNDA1* and *OsULT1* was identified during ethylene-mediated adaptations (Steffens et al., 2006, 2012; Table 3; Sauter et al., unpublished). However, in mechanically stressed root tips of Arabidopsis seedlings, where increased ethylene signalling is expected (Okamoto et al., 2008), expression

of *AtNDA1* and *AtULT1* was unaffected. A function of *AtNDA1* or *AtULT1* downstream from ethylene was also not verified from experiments analysing *Arabidopsis* primary root growth with or without mechanical influence and ethylene signalling. Neither loss of *AtNDA1*, nor loss of *AtULT1* expression resulted in an altered root response to 1-aminocyclopropane-1-carboxylic acid (ACC), an ethylene precursor (Adams and Yang, 1976; Kende, 1993), or 1-MCP, an ethylene antagonist (Sisler and Serek, 2003). Furthermore, inhibition of ethylene perception through 1-methylcyclopropene (1-MCP) in *nda1-1* seedlings did not abolish shortening of roots. From these results an involvement of *AtNDA1* and *AtULT1* in the regulation of root growth in response to mechanical stress or ethylene was excluded.

8.1.2 ALTERNATIVE NAD (P) H DEHYDROGENASE A might act in reactive oxygen species homeostasis

According to RT-PCR analysis, exogenously applied auxin decreased *AtNDA1*, but not *AtULT1* expression in root tips. Further RT-PCR analysis suggested that *AtULT1* might confer inhibition of *AtNDA1* expression. Auxin, together with abscisic acid regulates stem cell division and proliferation in *Arabidopsis* primary root meristems (Takatsuka and Umeda, 2014). In the root tip, abscisic acid promotes ROS production in mitochondria through alternative splicing of several complex I pre-messengerRNAs of the respiratory chain (He et al., 2012; Yang et al., 2014). By reducing stability, induction of catabolism, downregulation of metabolic genes and repression of polar transport, oxidative stress can have a negative impact on auxin response and homeostasis (Tognetti et al., 2012). A dramatically reduced auxin concentration or a shifted auxin maximum, in turn, decreases meristem activity and primary root growth (Blilou et al., 2005; Dello Iorio et al., 2007). ROS can be produced by fatty acid β -oxidation and glycolate oxidases in peroxisomes and by electron transport in chloroplasts and mitochondria (Karuppanapandian et al., 2011). In the mitochondrial ETC, the major sites for ROS production are complex I and complex III (Turrens, 2003). *AtNDA1*, together with its paralog *AtNDA2*, is located on the inside of the mitochondrial inner membrane and functions in by-passing of complex I (Rasmusson et al., 2004; Elhafez et al., 2006). Complex I and the alternative NAD (P) H dehydrogenases A1 and A2, both, pass electrons from matrix NAD (P) H to

the mobile lipophilic electron carrier ubiquinone. However, in contrast to complex I, AtNDA1 and AtNDA2 do not translocate protons from the matrix to the intermembrane space of the mitochondrion. Together with an alternative oxidase which transfers electrons from ubiquinone to the final electron acceptor oxygen, AtNDA1 and AtNDA2 can form an independent ETC that omits complex I and complex III. This implicates that AtNDA1 may protect against oxidative stress by avoiding electron leakage from excessively reduced respiratory chain components (Rasmusson et al., 2004; Schertl and Braun, 2014). Thus, it could be speculated that AtNDA1 influences the accumulation of auxin in root tips by controlling ROS production in mitochondria. *AtNDA1* was expressed in the entire lateral root cap. In a way, specific expression of *AtNDA1* in the lateral root cap also is compatible with the previously reported hypothesis. Perception of environmental changes primarily occurs at the root cap (Arnaud et al., 2010). For the control of root growth, tropic responses and organ initiation, root tip-derived auxin is transported through the lateral root cap to the elongation zone (Blilou et al., 2005; Swarup et al., 2005; Dubrovsky et al., 2008). It is conceivable that AtNDA1 in the lateral root cap mediates fine-tuning or fast adjustment of auxin levels in response to a changing environment. Besides a mitochondrial localisation, additional targeting of AtNDA1 to peroxisomes was shown (Carrie et al., 2008). According to metabolic roles, morphology and location at least three different types of peroxisomes can be distinguished in higher plants. Leaf peroxisomes in photosynthetic tissue and glyoxysomes in oil-rich tissue of germinating seeds play major roles in β -oxidation, glyoxylate cycle and photorespiration. In roots and all other plant tissues existence of unspecialised peroxisomes with unknown physiological function have been reported (Beevers, 1979; Olsen, 1998). In the root it was just recently shown that peroxisomes accumulate in lateral root cap cells, where also specific expression of *AtNDA1* was observed. Moreover, since abundance of these peroxisomes was strongly reduced in *Arabidopsis thaliana* *SOMBRERO* (AtSMB) loss-of-function mutants, a role in root cap-specific PCD was assumed, which likely associates with the organelles-intrinsic role in ROS homeostasis (Fahy et al., 2017). In the lateral root cap, activation of PCD-associated genes by AtSMB balances cellular turnover and with that root growth and meristem size (Fendrych et al., 2014). In common to

all classes of peroxisomes is inclusion of ROS-metabolising enzymes like catalase and peroxisomal targeting signal1- (PTS1) or PTS2-directed protein import (Beevers, 1979; Olsen, 1998; Mano et al., 2002). A PTS1 tripeptide was also identified at the C-terminus of AtNDA1 and AtNDA2. For unspecialised peroxisomes additionally it was demonstrated that they house enzymes necessary for fatty acid β -oxidation and are capable of importing key enzymes of the glyoxylate cycle (Gerhardt, 1983; Gerbling and Gerhardt, 1987, Olsen et al., 1993). In summary, root-specific, as well as metabolic functions similar to those of leaf peroxisomes and glyoxysomes can be assumed for unspecialised peroxisomes in the lateral root cap. Moreover, AtNDA1 and AtNDA2 possibly belong to the set of enzymes that are present in these peroxisomes. Besides the involvement in several pathways of the cells energy metabolism, peroxisomes are also organelles that function in production and scavenging of ROS (Corpas et al., 2001). In peroxisomes, AtNDA1 might balance the ratio of NADH/NAD⁺ and NADPH/NADP⁺ for β -oxidation in the matrix or ROS generating enzymes that utilize NADH and NADPH in short membrane-associated electron transport chains (ETCs; Hicks and Donaldson, 1982; Fang et al., 1987; López-Huertas et al., 1999; Wallström et al., 2014). Particularly H₂O₂, can diffuse to the cytosol where it, depending on the cellular concentration, can promote growth and development or even cell death (Bienert et al., 2006; Singh et al., 2016). In addition, peroxisomes are a source of auxins, such as indole-3-acetic acid (IAA). IAA is the most important auxin that is naturally produced in plants (Enders and Strader, 2015). In peroxisomes IAA is produced through β -oxidation of the auxin precursor indole-3-butyric acid (IBA) (Strader and Bartel, 2011). Maintenance of root auxin and ROS levels strongly contributes to meristem activity and primary root growth (Tognetti et al., 2012). Possibly growth promotion through AtNDA1 is attributable to NADH oxidation in mitochondria or peroxisomes that influences ROS or auxin concentrations in the root apex. However, so far the drawn conclusions are largely speculative. First of all, it remains to be proven whether AtNDA1 influences ROS accumulation in root tips. For this purpose ROS dyes, like diaminobenzidine tetrahydrochloride, nitroblue tetrazolium or 2', 7'-dichlorofluorescein diacetate could be helpful tools (Jambunathan, 2010). In addition, the quantification of IAA or the IAA precursor indole-3-butyric acid in root

tips of wildtype and *AtNDA1* transgenic lines could offer valuable clues about a possible influence of *AtNDA1* on auxin accumulation. For this approach, prevalent techniques allowing good sensitivity and low detection limits are gas or liquid chromatography combined with mass spectrometry (Du et al., 2012). A spatial and temporal resolution of auxin distribution could be provided by auxin signalling sensors, such as *DR5:GUS/GFP* or *DII-Venus* (Ulmasov et al., 1997; Brunoud et al., 2012). Furthermore there is the question whether the intracellular localisation of *AtNDA1* confers different physiological roles. An answer to this question could likely be achieved through directed targeting of transgenic *AtNDA1* to either mitochondria or peroxisomes in *AtNDA1* null mutants. Unfortunately, so far none of these approaches were pursued, since in the course of the study our focus became more set on *AtULT1*'s role in root growth and development. Nonetheless, a functional link between *AtULT1* and *AtNDA1* was suggested by upregulation of *AtNDA1* in the *ult1-3* T-DNA insertion line. An inverse relationship between *AtULT1* and *AtNDA1* activities was further supported by the observation that *ult1-3* seedlings had longer roots whereas *nda1-1* seedlings had shorter roots. However, unlike to *ult1-3* seedlings, auxin dependent processes like secondary root initiation and emergence were not disturbed in *nda1-1* seedlings. This observation together with specific expression of *AtNDA1* in the lateral root cap indicates that *AtNDA1* function might be restricted to the primary root. In rice, the *NDA* gene family is comprised of two members, *OsNDA1* (LOC_Os07g37730) and *OsNDA2* (LOC_Os01g61410). For *OsNDA2* three possible splice variants exist which differ in their C-terminal end. By bioinformatic analysis using the TargetP 1.1 software (Emanuelsson et al., 2000), a mitochondrial presequence was predicted at the N-terminus of *OsNDA1* and *OsNDA2*. A peroxisome targeting signal at the C-terminus was only identified in the sequence of *OsNDA2* splice variant 1 (*OsNDA2.1*). In contrast to their Arabidopsis homologs where dual localisation to mitochondria and peroxisomes was verified (Carrie et al., 2008), subcellular localisations of *OsNDA1* and *OsNDA2* was not proven experimentally yet. In summary, Arabidopsis NDAs showed high sequence similarity of 82.1%, identical subcellular location and a redundant genetic function in growth and metabolism (Wallström et al., 2014). Intracellular location of *OsNDA1* and *OsNDA2*, however, might differ and sequence similarity between *OsNDA1* and

OsNDA2 is rather low with 58.7%. Moreover, cDNA-supported annotation of three OsNDA2 splice isoforms in the MSU Rice Genome Annotation Project database might suggest a specific spatial and temporal regulation across tissues or development for OsNDA2. With more than 70% identical amino acids, OsNDA2.1 was highly similar to the Arabidopsis homologs AtNDA1 and AtNDA2. Possibly OsNDA1 acquired a novel function in epidermal cell death and elongation growth which is unique to rice, while OsNDA2, AtNDA1 and AtNDA2 functions are more convergent.

8.2 Root organogenesis

8.2.1 Cell cycle regulation and meristem maintenance

Analysis of lateral and adventitious root formation in *ult1-3* seedlings suggested a possible role of *AtULT1* in secondary root emergence. Primary roots are of embryonic origin, ground tissues and meristematic cells become predestined during embryogenesis (Dolan et al., 1993). Secondary root formation, however, requires reprogramming of already differentiated cells and cell-cycle entry of these G1-arrested cells (Beeckman et al., 2001). In the cell cycle 4 distinct phases can be distinguished. In order of progression this is G1-, S-, G2- and M-phase, whereupon M abbreviates mitosis, the actual phase of chromosome segregation and cytokinesis. S describes the phase of DNA replication. In the two gap phases, G1 and G2, cells increase in size and prepare to progress into the next phase (Morgan, 2007). Cell cycle progression among others is controlled by multiple cyclin-dependent kinases (CDKs) that complex with a cyclin subunit to become activated. Interaction between different classes of CDK and cyclin proteins can determine cell cycle transition at specific points of development. Beside cyclins, activity of CDKs is also influenced through association of CDK inhibitors and phosphorylation status (Morgan, 2007). However cell cycle regulators not only participate in activation of meristematic activity, they also can be involved in PCD execution (Sabelli et al., 2013; Zebell and Dong, 2015). For development of an organism not only progression of the cell cycle, but also its arrest is an important factor. Studies on BY2-tobacco cells indicated that initiation of apoptotic-like cell death is dependent

on the specific phase of the cells cycle (Herbert et al., 2001; Kuthanova et al., 2008). Especially stress factors occurring during the S-phase and G2/M transition provoked cells to exit into apoptotic-like PCD. A role of *OsULT1* in coordination of cell phase progression would be conceivable, since upregulation of *OsULT1* and *OsNDA1* was identified in epidermal cells that undergo cell death (Table 3; Sauter et al., unpublished). Moreover, Coudert et al. (2015) uncovered initiation of *OsULT1* transcription through *OsCRL1* which indicates a possible involvement of *OsULT1* in postembryonic root development such as crown root formation. Crown root growth and emergence, in turn, is accompanied by induction of G2/M transition (Sauter et al., 1995; Wang et al., 2011). Additionally co-regulation of *OsULT1* and *OsNDA1*, albeit reverse, was observed in internodes that were triggered to grow by hypoxia (Table 3; Sauter et al., unpublished). Growth of the stem occurs in the intercalary meristem at the base of the youngest internode (Kende et al., 1998). In the rice internode oxygen depletion causes enhanced activity of the key enzyme in the ethylene biosynthetic pathway, the ACC synthase (Zarembinski and Theologis, 1993). The accumulating ethylene induces cell division and elongation in the intercalary meristem via gibberellin (Sauter and Kende, 1992). Gibberellin, in turn, promotes expression of cyclin genes and enhances activity of the p34^{cdc2}-like histone H1 kinase (Sauter et al., 1995). In the intercalary meristem the resulting progression of cell cycle from G2 to M phase increases mitotic activity of cells and thus cell-production rate.

In this study, *AtULT1* was shown to inhibit germination, as well as primary root differentiation and growth. Primary root morphology and development becomes determined through cell fate decisions and patterning during embryogenesis. In this stage the basic tissues and first stem cells are formed (Barton and Poethig, 1993; Dolan et al., 1993). During subsequent germination growth from embryo to seedling is primarily driven by water uptake and elongation of the embryonic axis (Sliwiska et al., 2009). However, completion of germination, future seedling development and growth is dependent on cell cycle activity of apical meristems (Masubelele et al., 2005). Incorrect cellular organisation or failure to activate e.g. the root apical meristem (RAM) often results in disturbed primary (Benfrey et al., 1993; Hamann et al., 2002, Sabatini et al., 2003; Aida et al., 2004), but also secondary root growth or

formation (De Smet et al., 2008; Lucas et al., 2011; Della Rovere et al., 2015), since underlying mechanism are re-initiated later in plant development (Tian et al., 2014). Prior to germination expression of *Arabidopsis thaliana* D-type cyclins (AtCYCDs) is required for induction of meristematic activity. Repression of D-type cyclins inhibits activation of the RAM and in consequence subsequent germination fails (Masubelele et al., 2005). This was the case in 47.4% to 63% of the *ULT1ox* seedlings.

In the root meristem of a mature embryo 4 almost mitotically inactive cells form the quiescence centre (QC; Dolan et al., 1993). In the QC the transcription factor AtWOX5 represses AtCYCD3;3 to re-establish quiescence that is necessary for stem cell maintenance. In the root cap the D-type cyclins AtCYCD1;1 and AtCYCD3;3 maintain division activity of columella and epidermis/lateral root cap initials (Forzani et al., 2014). For *AtULT1* spotty expression in the columella and the lateral root cap covering the meristematic zone was observed. Hence *AtULT1* expression might overlaps with those of *AtCYCD1;1* and *AtCYCD3;3*. Ectopic expression of *AtCYCD3;3* and *AtCYCD1;1* induced transversal cell divisions of QC cells. *AtCYCD3;3* expression resulted in 100% QC divisions, *AtCYCD1;1* expression had a minor influence that triggered 9% QC divisions (Forzani et al., 2014). Divisions of QC cells were also observed in 21.8% of the *ULT1ox8* seedlings. Moreover, also in the columella abnormal cell division activity that was comparable to those of *AtCYCD1;1* and *AtCYCD3;3* transgenic embryos was present in *ULT1ox8* and *ult1-3 ult2-1* embryos. *AtULT1* expression starts 2 days after imbibition in single cells of the columella. In *ULTox* seedlings, however, expression of *AtULT1* that precedes germination can be expected. Hence, repression of D-type cyclins through premature *AtULT1* expression might explain inhibition of germination and inaccurate columella divisions. Post-germination, activity of AtCYCD3;3 and AtCYCD1;1 in the columella stimulates formative divisions and prevents differentiation of columella stem cells (Forzani et al., 2014). Thus the arrest of root cap development that was visible in 3-day-old *ULT1ox* seedlings could also be attributable to reduced cyclin expression. Furthermore, specific binding of cyclins to CDKs controls progression of cell cycle to adjust growth in response to environmental conditions (Doerner et al., 1996). Correspondingly, lack of *AtULT1*

promoted root growth, while overexpression hindered growth of roots up to one week after germination. However, not in conformity with the hypothesis is induction of quiescence centre (QC) cell divisions in *ULT1ox8* embryos, since this would rather result from an increased *AtCYCD* expression in the QC. Upstream from *AtCYCD3;3* and *AtCYCD1;1*, *AtWOX5* expression controls QC quiescence and stem cell differentiation. Thus ectopic QC cell divisions also can be a consequence of decreased *AtWOX5* expression in the QC, which causes *AtCYCD* accumulation (Forzani et al., 2014). An influence on *AtWOX5* expression was not detected in root tips of 3-day-old *ULT1ox* seedlings, but suggested for *ult1-3* seedlings. The observed downregulation of *AtWOX5* in *ult1-3* seedlings may imply positive control of *AtWOX5* expression through *AtULT1*. Furthermore growth of *ULT1ox* seedlings was only diminished but not arrested. Correspondingly stem cell activity and QC functionality was still given, which makes a root cap-specific deregulation or radial patterning defect more probable. Columella layers originate from coordinated anticlinal divisions of columella stem cells, which attach as mono-layered disc distal to the QC (Dolan et al., 1993; Campilho et al., 2006). The peptide ligand *AtCLE40* influences stem cell homeostasis and differentiation of columella cells in a dose-dependent manner. In the most distal columella cells *AtCLE40* concentration is high and promotes differentiation. In proximal columella cells sequestration of *AtCLE40* by the receptor-like kinases *AtACR4* and *AtCLV1* avoids stem cell proliferation. *AtACR4* and *AtCLV1*, in turn, downregulate *AtWOX5* expression in the QC dependent on *AtCLE40* abundance. In consequence columella stem cells are induced to divide as long as the population of differentiated cells is predominant (De Smet et al., 2008; Stahl et al., 2009, Stahl et al., 2013). Timing and plane of cell divisions in epidermal/lateral root cap stem cells are controlled by alternating oscillation of the NAC-domain transcription factors *AtFEZ* and *AtSMB* (Willemsen et al., 2008). In the cortex/endodermis initials the GRAS transcription factors *AtSCR* and *AtSHR* are required to control cell divisions and asymmetric fate specification (Di Laurenzio et al., 1996; Helariutta et al., 2000; Nakajima et al., 2001; Heidstra et al., 2004; Cui et al., 2007). In parallel, *AtPLT1* and *AtPLT2* control mitotic activity of stem cells and their transit amplifying cells in a concentration-dependent manner. In this study, transcriptional regulation of *AtACR4*, *AtCLV1*, *AtSCR*, *AtSHR*, *AtPLT1*

and *AtPLT2* in *AtULT1* transgenic lines was tested via qRT-PCR. Taken together, the results indicated that *AtULT1* overexpression might be beneficial for *AtCLV1* expression. Physiological analysis of root cap development in *AtULT1* and *AtACR4* transgenic lines, however, suggested *AtULT1* to act via down regulation of *AtACR4*. *AtACR4* acts together with *AtCLV1* as homo- or heterodimers in controlling columella differentiation (Stahl et al., 2013). Thus compensation of *AtACR4* function through *AtCLV1* might be possible. On the other hand, qRT-PCR analysis in *ULT1ox* seedlings did not provide any support for this hypothesis. Indeed, ectopic *AtULT1* expression may cause deregulation of gene expression in the same genetic network and in some cases this might result in phenotypical similarities. For a direct influence of *AtULT1* on *AtACR4* or *AtCLV1* expression, however, the obtained results were not convincing. For technical and temporal reasons *AtCLE40*, *AtFEZ* and *AtSOMBRERO* expression was not analysed, yet. This, however, could still be done.

From analysis of flower development in single and double knockout lines, it was assumed that *AtULT1* and its paralog *AtULT2* regulate a common set of genes (Carles et al., 2005; Monfared et al., 2013). *AtULT2*, however, contributed minor to target gene regulation. In inflorescences *AtULT1* knockout caused an abnormal flower phenotype that was enhanced through an additional *AtULT2* deficit (Monfared et al., 2013). In roots, null mutation of *AtULT1* alleles had no obvious phenotype. Seemingly, loss-of-function in just one *AtULT* homolog could easily be compensated through the one remaining. A deficit of both homologs, in *ult1-3 ult2-1* seedlings, however, caused severe defects in root differentiation in 22.1% of the analysed seedlings. Hence, it can be assumed that *AtULT1* and *AtULT2* are partially or fully redundant in roots, whereas genetically redundancy in flowers is unequal. Accordingly, future analysis that aim to identify *AtULT1* targets in roots should be performed with plants carrying a combination of *AtULT1* and *AtULT2* loss-of-function alleles.

8.2.2 ULTRAPETALA1 and auxin may act in converging regulatory networks

Congruent with transcription factor and peptide signalling pathways, the phytohormone auxin is a major regulator of root patterning and growth (Sabatini et al., 1999; Fu and Harberd, 2003; Blilou et al., 2005). In the distal stem cell region an auxin gradient is created through the combinatory operation of PIN-mediated polar auxin transport and local biosynthesis (Blilou et al., 2005; Ljung et al., 2005). The resulting auxin response maximum stabilizes the stem cell region and controls cell division and differentiation in an AtPLT-dependent manner (Aida et al., 2004; Galinha et al., 2007). Thus it appears that failure to establish a local auxin gradient results in inhibition of distal stem cell differentiation, while an increased auxin level in the root tip triggers accumulation of differentiated starch-containing columella cells. During the seed-to-seedling transition, the majority of *ULT1ox* seedlings developed an apparently quiescent and undifferentiated root cap. Root tips of *ult1-3* seedlings, indeed, were undistinguishable from wildtypes. 22.08% of the *ult1-3 ult2-1* seedlings, however, developed a root in which excessive starch accumulation was observed. Elicitor of the described phenotypes could be a modified auxin signalling or an altered local concentration. Promotion of hypocotyl growth and adventitious root formation in *AtULT1* knockout seedlings might also correlate with increased auxin sensitivity or auxin accumulation (Boerjan et al., 1995, Sorin et al., 2005). Supportive to this hypothesis, *ULT1ox* seedlings showed the opposite phenotype in such that hypocotyl elongation and adventitious root initiation were stagnating after 7 days of growth in the dark. An auxin-associated function of AtULT1 was also indicated by the observation that 50% to 67.74% of *AtULT1* knockout seedlings exhibited a root cap differentiation defect when exposed to IAA. Roots of *ult1-3* and *ult1-3 ult2-1* seedlings excessively accumulated starch in the central and lateral root cap, failed to grow and develop root hairs. Thus IAA application induced abnormal root cap development in *ult1-3* and enhanced formation of the phenotype in *ult1-3 ult2-1* seedlings. Root cap development of *ULT1ox* seedlings was not further impaired when exposed to IAA. Long-term IAA administration, however, induced ectopic adventitious root formation at the hydathodes of *ULT1ox* leaves. Specific types of ARFs regulate the sensitivity to

auxin and in that play a central role during different events of primary root differentiation, secondary root organogenesis and hypocotyl growth (Chapman and Estelle, 2009; Enders and Strader, 2015). For root cap development, it was more recently shown that auxin acts in parallel to *AtWOX5* through the auxin response factors (ARF), *AtARF10* and *AtARF16* (Bennett et al., 2014). In the distal region of the root meristem *AtARF10* and *AtARF16* expression is required for root cap differentiation. In consequence, seedlings defective in *AtARF10* and *AtARF16* lack starch accumulation in the columella (Wang et al., 2005; Bennett et al., 2014). Accumulation of *AtARF10* and *AtARF16* transcripts is post-transcriptionally controlled by tissue-specific expression of the *Arabidopsis thaliana microRNA160* (*AtMIR160*) (Rhoades et al., 2002; Wang et al., 2005). MicroRNAs are about 22 nucleotides long, non-coding RNAs that regulate gene expression through RNA silencing or translational repression (Voinnet, 2009). However, RNA silencing through *AtMIR160* is not only restricted to *AtARF10* and *AtARF16* transcripts, also *AtARF17* was identified to be a target of *AtMIR160* (Rhoades et al., 2002; Mallory et al., 2005). Repression of *AtARF17* expression, in turn, was shown to be beneficial for lateral root production, adventitious rooting and hypocotyl elongation (Mallory et al., 2005; Sorin et al., 2005). In more detail, adventitious root formation and hypocotyl growth are controlled by a regulatory network that involves feedback circuits between *AtARF17*, *AtARF6*, *AtARF8* and their repressive microRNAs. In contrast to *AtARF17*, *AtARF6* and *AtARF8* are positive regulators of adventitious rooting and hypocotyl elongation (Sorin et al., 2005, Gutierrez et al., 2009). Accumulation of *AtARF6* and *AtARF8* transcripts is post-transcriptional controlled by *AtMIR167*-mediated degradation (Rhoades et al., 2002; Gutierrez et al., 2009). *AtMIR167* production, in turn, can be adjusted through *AtMIR160* abundance (Gutierrez et al., 2009). Hence, on the one hand, inhibition of adventitious root formation and hypocotyl growth that was observed in etiolated *ULT1ox* seedlings could be caused through a direct influence of *AtULT1* on *AtMIR167* expression or a function downstream of *AtARF17*. On the other hand, *AtMIR167* induction could also be the consequence of an *AtULT1*-mediated *AtMIR160* overproduction. If so, production of adventitious roots and hypocotyl elongation of *ULT1ox* seedlings in the first 7 days of etiolation could be explained through primary *AtMIR160*

expression, which resulted in *AtARF17* elimination. Additionally to microRNAs, *AtARF6* and *AtARF17* expression can be modified through light availability (Gutierrez et al., 2009). Moreover, seedlings that over-accumulated *AtARF17* were suggested to be hypersensitive to light (Sorin et al., 2005). A comprehensive analysis of light signalling in *AtULT1* transgenic seedlings is not provided, yet. Phenotypes of etiolated seedlings that were transferred to light, however, indicated that repression of *AtULT1* is also important for adaptive responses to light. A role of *AtULT1* downstream from *AtARFs* or in inducing miRNA expression might also be assumed for another number of reasons. Missing starch accumulation and differentiation in *ULT1ox* root caps is highly similar to phenotypes published for *arf10 arf16* mutants. Moreover, *AtARF16* expression at the primary root apex, lateral root apex and base of emerging lateral roots reflects those of *AtULT1_{pro}:GUS* seedlings (Wang et al., 2005). In the vasculature, where further *AtULT1* expression was observed, elimination of *AtARF16* transcripts through *AtMIR160* ensures proper lateral root formation (Wang et al., 2005). Correspondingly, *ult1-3* and *ult1-3 ult2-1* seedlings, but not *ULT1ox* seedlings produced fewer lateral roots. In addition, strongly reduced lateral root elongation in at least one *ULT1ox* line could also be a consequence of altered microRNA or *AtARF* abundance. Accumulation of *AtMIR390* determines lateral root elongation and is adjusted by an auto-regulatory network that involves *AtARF4*. Just as *AtULT1* expression, *AtMIR390* expression is restricted to the basal region and flanks of lateral root primordia (Marin et al., 2010). However, the observed lateral root phenotype in *ULT1ox* transgenic seedlings could possibly also be an indirect consequence of the phenotype that was observed on their primary root tips. Analysis of lateral root distribution over the primary root displayed that increased production of lateral roots in *ULT1ox* seedlings was only temporary. It is conceivable that failure in root cap differentiation and the subsequent release of the non-functional structure caused unsteadiness of auxin flux to the elongation zone. Thus, initially auxin transport might have been discontinuous or decreased. Upon release of the root cap, however, removal of possibly accumulated auxin would be capable to induce a multitude of founder cell priming events. Enhanced lateral root induction, that was visible when the primary root length of *ULT1ox* seedlings exceeded 20 mm, could be the consequence. Additionally,

coincides the area of lateral root accumulation at the primary root with the average primary root length of *ULT1ox* seedlings after 3 days of growth, which, in turn, designates the time point of root cap release. Notwithstanding to this theory, existing knowledge about adventitious root initiation in rice supports the idea that ULT1 might act downstream of ARFs. In rice, as well as in Arabidopsis, ARFs act as regulators of auxin signalling (Chapman and Estelle, 2009). The promoter of the *OsCRL1* gene has been identified to be a direct target of rice ARFs (Inukai et al., 2005). The transcription factor OsCRL1, in turn, is required to induce secondary root organogenesis at primary roots, the basis of unelongated internodes and nodes of the stem in response to auxin (Inukai et al., 2005; Liu et al., 2005). In recent studies, transcriptional control of *OsULT1* through OsCRL1 was indicated (Coudert et al., 2015). Taken together, it might be assumed that *OsULT1* is auxin-inducible, a downstream target of OsARFs and involved in postembryonic root formation. In some instances, the drawn conclusions for OsULT1 coincided with the interpretation of results obtained for AtULT1 in Arabidopsis. However, due to developmental and anatomical differences between monocots and dicots, especially in terms of root formation and architecture, a complete congruence in ULT1 regulation and function in rice and Arabidopsis can most likely not be expected (Bellini et al., 2014). Anyway, at least the high sequence similarity of OsULT1 and Arabidopsis ULTRAPETALA homologs supports a functional redundancy within these species. In AtULT1 a SAND domain and a B box-like motif confers specificity for interaction with target DNA and recruitment of chromatin-remodelling proteins (Carles et al., 2005). AtULT2, OsULT1 and OsULT2 also comprise a SAND domain and B box-like motif. The B box-like motif in the OsULT2 sequence, however, is fragmentary. Taken together, DNA-binding capacity can only be assumed for AtULT1, AtULT2 and OsULT1 since functionality of SAND domains not only depends on their secondary structure but also on interaction with other proteins that most likely bind to the B-box-like motif (Wojciak and Clubb, 2001).

In future studies, the effect of auxin on ULT1 expression and root formation in rice and Arabidopsis should be further investigated. In Arabidopsis division patterns and number of columella stem cell tiers in response to auxin could possibly also deliver some interesting insights. Auxin induces differentiation of columella stem cells

upstream from AtARF10 and AtARF16 in a dose-dependent manner (Ding and Friml, 2010). Due to the observed root tip phenotypes in *AtULT1* mutants it is conceivable that *AtULT1* knockout seedlings are more sensitive to elevated auxin levels while *ULT1ox* seedlings respond with delay of columella stem cell differentiation. Such findings would support the hypothesis that AtULT1 acts downstream of auxin, possibly through ARF transcription factors. To analyse a possible function of AtULT1 downstream of microRNAs or ARFs a complementation test with appropriate mutant lines could be helpful. Since indications concerning cell cycle regulation through AtULT1 were rather conflicting, introduction of *AtCYCD* reporters in *AtULT1* transgenic plants could provide clarification. The suggested regulation of *AtULT1* through auxin or illumination, could be tested by using the *AtULT1_{pro}:GUS* line or qRT-PCR. However, for a more efficient identification of ULT1 targets novel methods, such as RNA sequencing (RNAseq) or chromatin immunoprecipitation followed by high-throughput sequencing (ChIPseq) should be considered. Because AtULT1 on the one hand mediates transcriptional activation and on the other hand directly associates with target gene loci, particularly the integration of both methods could unravel reliable indications for regulation of gene expression (Angelini and Costa, 2014). The RNAseq technique would provide a precise and high resolution quantification of transcript abundance and their isoforms. Moreover, also small and non-coding RNA species, such as microRNAs could be detected (Wang et al., 2009). ChIPseq, in turn, could identify genome-wide AtULT1 binding sites. Thus, the ChIPseq and vice versa the RNAseq approach could provide proof for candidate gene regulation (Angelini and Costa, 2014).

9 REFERENCES

- Adams DO and Yang SF (1979) Ethylene biosynthesis: Identification of 1-aminocyclopropane-1-carboxylic acid as an intermediate in the conversion of methionine to ethylene. *Proceedings of the National Academy of Sciences* 76(1): 170-174
- Aida M, Beis D, Heidstra R, Willemsen V, Blilou I, Galinha C, Nussaume L, Noh Y, Amasino R, Scheres B (2004) The PLETHORA genes mediate patterning of the Arabidopsis root stem cell niche. *Cell* 119(1): 109-120
- Alatzas A (2013) Histones and plant hormones: New evidence for an interesting interplay. *The Botanical Review* 79(3): 317-341
- Allen E, Moing A, Ebbels TMD, Maucourt M, Tomos AD, Rolin D, Hooks MA (2010) Correlation Network Analysis reveals a sequential reorganization of metabolic and transcriptional states during germination and gene-metabolite relationships in developing seedlings of Arabidopsis. *BMC Systems Biology* 4(1): 1-16
- Angelini C and Costa V (2014) Understanding gene regulatory mechanisms by integrating ChIP-seq and RNA-seq data: Statistical solutions to biological problems. *Frontiers in Cell and Developmental Biology* 2: 51
- Arnaud C, Bonnot C, Desnos T, Nussaume L (2010) The root cap at the forefront. *Comptes rendus biologies* 333(4): 335-343
- Atwell BJ (1993) Response of roots to mechanical impedance. *Environmental and Experimental Botany* 33(1): 27-40
- Barton MK and Poethig RS (1993) Formation of the shoot apical meristem in *Arabidopsis thaliana*: An analysis of development in the wild type and in the shoot meristemless mutant. *Development* 119(3): 823-831
- Beeckman T, Burssens S, Inzé D (2001) The peri-cell-cycle in Arabidopsis. *Journal of Experimental Botany* 52(Special Issue): 403-411
- Beevers H (1979) Microbodies in higher plants. *Annual Review of Plant Physiology* 30(1): 159-193
- Bellini C, Pacurar DI, Perrone I (2014) Adventitious roots and lateral roots: similarities and differences. *Annual Review of Plant Biology* 65: 639-666
- Benfey PN, Linstead PJ, Roberts K, Schiefelbein JW, Hauser MT, Aeschbacher RA (1993) Root development in Arabidopsis: Four mutants with dramatically altered root morphogenesis. *Development* 119(1): 57-70

- Bengough AG, Bransby MF, Hans J, McKenna SJ, Roberts TJ, Valentine TA (2006) Root responses to soil physical conditions; growth dynamics from field to cell. *Journal of Experimental Botany* 57(2): 437-447
- Bennett T, van den Toorn A, Willemsen V, Scheres B (2014) Precise control of plant stem cell activity through parallel regulatory inputs. *Development* 141(21): 4055-4064
- Bertani G (1951) Studies on lysogenesis I. The mode of phage liberation by lysogenic *Escherichia coli*. *Journal of Bacteriology* 62(3):293-300
- Bhalerao RP, Eklöf J, Ljung K, Marchant A, Bennett M, Sandberg G (2002) Shoot-derived auxin is essential for early lateral root emergence in *Arabidopsis* seedlings. *The Plant Journal* 29(3): 325-332
- Blilou I, Xu J, Wildwater M, Willemsen V, Paponov I, Friml J, Heidstra R, Aida M, Palme K, Scheres B (2005) The PIN auxin efflux facilitator network controls growth and patterning in *Arabidopsis* roots. *Nature* 433(7021): 39-44
- Boerjan W, Cervera MT, Delarue M, Beeckman T, Dewitte W, Bellini C, Caboche M, Van Onckelen H, Van Montagu M, Inzé D (1995) Superroot, a recessive mutation in *Arabidopsis*, confers auxin overproduction. *The Plant Cell* 7(9): 1405-1419
- Boyes DC, Zayed AM, Ascenzi R, McCaskill AJ, Hoffman NE, Davis KR, Görlach J (2001) Growth stage-based phenotypic analysis of *Arabidopsis*: A model for high throughput functional genomics in plants. *The Plant Cell* 13(7): 1499-1510
- Brunoud G, Wells DM, Oliva M, Larrieu A, Mirabet V, Burrow AH, Beeckman T, Kepinski S, Traas J, Bennett MJ, Vernoux T (2012) A novel sensor to map auxin response and distribution at high spatio-temporal resolution. *Nature* 482(7383): 103-106
- Campilho A, Garcia B, Toorn H, Wijk H, Campilho A, Scheres B (2006) Time-lapse analysis of stem-cell divisions in the *Arabidopsis thaliana* root meristem. *The Plant Journal* 48(4):619-627
- Carles CC and Fletcher JC (2003) Shoot apical meristem maintenance: The art of a dynamic balance. *Trends in Plant Science* 8(8): 394-401
- Carles CC, Lertpiriyapong K, Reville K, Fletcher JC (2004) The ULTRAPETALA1 gene functions early in *Arabidopsis* development to restrict shoot apical meristem activity and acts through WUSCHEL to regulate floral meristem determinacy. *Genetics* 167(4): 1893-1903
- Carles CC, Choffnes-Inada D, Reville K, Lertpiriyapong, Fletcher JC (2005) ULTRAPETALA1 encodes a SAND domain putative transcriptional regulator that controls shoot and floral meristem activity in *Arabidopsis*. *Development* 132(5): 897-911

- Carles CC and Fletcher JC (2009) The SAND domain protein ULTRAPETALA1 acts as a trithorax group factor to regulate cell fate in plants. *Genes & Development* 23(23): 2723-2728
- Carrie C, Murcha MW, Kuehn K, Duncan O, Barthelet M, Smith PM, Eubel H, Meyer E, Day DA, Millar AH, Whelan J (2008) Type II NAD(P)H dehydrogenases are targeted to mitochondria and chloroplasts or peroxisomes in *Arabidopsis thaliana*. *FEBS Letters* 582(20): 3073-3079
- Casimiro I, Beeckman T, Graham N, Bhalerao R, Zhang H, Casero P, Sandberg G, Bennett MJ (2003) Dissecting Arabidopsis lateral root development. *Trends in Plant Science* 8(4): 165-171
- Celenza JL, Grisafi PL, Fink GR (1995) A pathway for lateral root formation in *Arabidopsis thaliana*. *Genes & Development* 9(17): 2131-2142
- Chao Q, Rothenberg M, Solano R, Roman G, Terzaghi W, Ecker JR (1997) Activation of the ethylene gas response pathway in Arabidopsis by the nuclear protein ETHYLENE-INSENSITIVE3 and related proteins. *Cell* 89(7):1133-44
- Chapman EJ and Estelle M (2009) Mechanism of auxin-regulated gene expression in plants. *Annual Review of Genetics* 43: 265-285
- Clough SJ and Bent AF (1998) Floral dip: A simplified method for Agrobacterium-mediated transformation of *Arabidopsis thaliana*. *The Plant Journal* 16(6): 735–743
- Corpas FJ, Barroso JB, del Río LA (2001) Peroxisomes as a source of reactive oxygen species and nitric oxide signal molecules in plant cells. *Trends in Plant Science* 6(4): 145-150
- Coudert Y, Le VAT, Adam H, Bés M, Vignols F, Jouannic S, Guiderdoni E, Gantet P (2015) Identification of CROWN ROOTLESS1-regulated genes in rice reveals specific and conserved elements of postembryonic root formation. *New Phytologist* 206(1): 243–254
- Cui H, Levesque MP, Vernoux T, Jung JW, Paquette AJ, Gallagher KL, Wang JY, Blilou I, Scheres B, Benfey PN (2007) An evolutionarily conserved mechanism delimiting SHR movement defines a single layer of endodermis in plants. *Science* 316(5823): 421-425
- Cui Y, Zhao S, Wu Z, Dai P, Zhou B (2012) Mitochondrial release of the NADH dehydrogenase Ndi1 induces apoptosis in yeast. *Molecular Biology of the Cell* 23(22): 4373-4382
- Da Rocha Correa L, Troleis J, Mastroberti AA, Mariath JE, Fett-Neto AG (2012) Distinct modes of adventitious rooting in *Arabidopsis thaliana*. *Plant Biology* 14(1): 100-109

- De Klerk GJ, Van der Krieken W, De Jong JC (1999) Review the formation of adventitious roots: New concepts, new possibilities. *In Vitro Cellular & Developmental Biology – Plant* 35(3): 189-199
- De Rybel B, Audenaert D, Xuan W, Overvoorde P, Strader LC, Kepinski S, Hoyer R, Brisbois R, Parizot B, Vanneste S, Liu X (2012) A role for the root cap in root branching revealed by the non-auxin probe naxillin. *Nature Chemical Biology* 8(9): 798-805
- De Smet I, Tetsumura T, De Rybel B, Frei dit Frey N, Laplaze L, Casimiro I, Swarup R, Naudts M, Vanneste S, Audenaert D, Inzé D, Bennett MJ, Beeckman T (2007) Auxin-dependent regulation of lateral root positioning in the basal meristem of *Arabidopsis*. *Development* 134(4): 681-690
- De Smet I, Vassileva V, De Rybel B, Levesque MP, Grunewald W, Van Damme D, Van Noorden G, Naudts M, Van Isterdael G, De Clercq R, Wang JY, Meuli N, Vanneste S, Friml J, Hilson P, Jürgens G, Ingram GC, Inzé D, Benfey PN, Beeckman T (2008) Receptor-like kinase ACR4 restricts formative cell divisions in the *Arabidopsis* root. *Science* 322(5901): 594-597
- De Smet I (2012) Lateral root initiation: One step at a time. *New Phytologist* 193(4): 867-873
- De Smet S, Cuypers A, Vangronsveld J, Remans T (2015) Gene networks involved in hormonal control of root development in *Arabidopsis thaliana*: a framework for studying its disturbance by metal stress. *International Journal of Molecular Sciences* 16(8): 19195-19224
- Della Rovere F, Fattorini L, D'Angeli S, Veloccia A, Falasca G, Altamura MM (2013) Auxin and cytokinin control formation of the quiescent centre in the adventitious root apex of *Arabidopsis*. *Annals of Botany* 112(7): 1395-1407
- Della Rovere F, Fattorini L, D'Angeli S, Veloccia A, Del Duca S, Cai G, Falasca G, Altamura MM (2015) *Arabidopsis* SHR and SCR transcription factors and AUX1 auxin influx carrier control the switch between adventitious rooting and xylogenesis in planta and in in vitro cultured thin cell layers. *Annals of Botany* 115(4): 617-28
- Dello Ioio R, Scaglia Linhares F, Scacchi E, Casamitjana-Martinez E, Heidstra R, Costantino P, Sabatini S (2007) Cytokinin determine *Arabidopsis* root-meristem size by controlling cell differentiation. *Current Biology* 17(8): 678-682
- Dello Ioio R, Nakamura K, Moubayidin L, Perilli S, Taniguchi M, Morita MT, Aoyama T, Costantino P, Sabatini S (2008) A genetic framework for the control of cell division and differentiation in the root meristem. *Science* 322(5906): 1380-1384
- Di Laurenzio L, Wysocka-Diller J, Malamy JE, Pysh L, Helariutta Y, Freshour G, Hahn MG, Feldmann KA, Benfey PN (1996) The SCARECROW gene

regulates an asymmetric cell division that is essential for generating the radial organization of the *Arabidopsis* root. *Cell* 86(3): 423-433

- Ding Z and Friml J (2010) Auxin regulates distal stem cell differentiation in *Arabidopsis* roots. *Proceedings of the National Academy of Sciences* 107(26): 12046-12051
- Ditengou FA, Teale WD, Kochersperger P, Flittner KA, Kneuper I, van der Graaff E, Nziengui H, Pinosa F, Li X, Nitschke R, Laux T (2008) Mechanical induction of lateral root initiation in *Arabidopsis thaliana*. *Proceedings of the National Academy of Sciences* 105(48): 18818-18823
- Doerner P, Jorgensen JE, You R, Steppuhn J, Lamb C (1996) Control of root growth and development by cyclin expression. *Nature* 380(6574): 520
- Dolan L, Janmaat K, Willemsen V, Linstead P, Poethig S, Roberts K, Scheres B (1993) Cellular organisation of the *Arabidopsis thaliana* root. *Development* 119(1): 71-84
- Driouch A, Durand C, Cannesan MA, Percoco G, Vicré-Gibouin M (2010) Border cells versus border-like cells: Are they alike?. *Journal of Experimental Botany* 61(14): 3827-3831
- Du F, Ruan G, Liu H (2012) Analytical methods for tracing plant hormones. *Analytical and Bioanalytical Chemistry* 403(1): 55-74
- Dubrovsky JG, Doerner PW, Colón-Carmona A, Rost TL (2000) Pericycle cell proliferation and lateral root initiation in *Arabidopsis*. *Plant Physiology* 124(4): 1648-1657
- Dubrovsky JG, Sauer M, Napsucialy-Mendivil S, Ivanchenko MG, Friml J, Shishkova S, Celenza J, Benková E (2008) Auxin acts as a local morphogenetic trigger to specify lateral root founder cells. *Proceedings of the National Academy of Sciences* 105(25): 8790-8794
- Elhafez D, Murcha MW, Clifton R, Soole KL, Day DA, Whelan J (2006) Characterization of mitochondrial alternative NAD (P) H dehydrogenases in *Arabidopsis*: Intraorganelle location and expression. *Plant & Cell Physiology* 47(1): 43-54
- Emanuelsson O, Nielsen H, Brunak S, von Heijne G (2000) Predicting subcellular localization of proteins based on their N-terminal amino acid sequence. *Journal of Molecular Biology* 300(4): 1005-1016.
- Enders TA and Strader LC (2015) Auxin activity: Past, present, and future. *American Journal of Botany* 102(2): 180–196
- Fahy D, Sanad MN, Duscha K, Lyons M, Liu F, Bozhkov P, Kunz HH, Hu J, Neuhaus HE, Steel PG, Smertenko A (2017) Impact of salt stress, cell death, and

- autophagy on peroxisomes: Quantitative and morphological analyses using small fluorescent probe N-BODIPY. *Scientific Reports* 7:39069
- Fang TK, Donaldson RP, Vigil EL (1987) Electron transport in purified glyoxysomal membranes from castor-bean endosperm. *Planta* 172(1): 1-3
- Fendrych M, Van Hautegeem T, Van Durme M, Olvera-Carrillo Y, Huysmans M, Karimi M, Lippens S, Guérin CJ, Krebs M, Schumacher K, Nowack MK (2014) Programmed cell death controlled by ANAC033/SOMBRERO determines root cap organ size in *Arabidopsis*. *Current Biology* 24(9): 931-940
- Fett-Neto AG, Fett JP, Goulart LW, Pasquali G, Termignoni RR, Ferreira AG (2001) Distinct effects of auxin and light on adventitious root development in *Eucalyptus saligna* and *Eucalyptus globulus*. *Tree Physiology* 21(7): 457-464
- Fletcher JC (2001) The ULTRAPETALA gene controls shoot and floral meristem size in *Arabidopsis*. *Development* 128(8): 1323-1333
- Forzani C, Aichinger E, Sornay E, Willemsen V, Laux T, Dewitte W, Murray JA (2014) WOX5 suppresses CYCLIN D activity to establish quiescence at the center of the root stem cell niche. *Current Biology* 24(16): 1939-1944
- Fu X and Harberd NP (2003) Auxin promotes *Arabidopsis* root growth by modulating gibberellin response. *Nature* 421(6924): 740-743
- Galinha C, Hofhuis H, Luijten M, Willemsen V, Blilou I, Heidstra R, Scheres B (2007) PLETHORA proteins as dose-dependent master regulators of *Arabidopsis* root development. *Nature* 449(7165): 1053-1057
- Gendreau E, Traas J, Desnos T, Grandjean O, Caboche M, Hofte H (1997) Cellular basis of hypocotyl growth in *Arabidopsis thaliana*. *Plant Physiology* 114(1): 295-305
- Gerbling H and Gerhardt B (1987) Activation of fatty acids by non-glyoxysomal peroxisomes. *Planta* 171(3): 386-392
- Gerhardt B (1983) Localization of β -oxidation enzymes in peroxisomes isolated from nonfatty plant tissues. *Planta* 159(3): 238-246
- Gutierrez L, Bussell JD, Păcurar DI, Schwambach J, Păcurar M, Bellini C (2009) Phenotypic plasticity of adventitious rooting in *Arabidopsis* is controlled by complex regulation of AUXIN RESPONSE FACTOR transcripts and microRNA abundance. *The Plant Cell* 21(10): 3119-3132
- Haecker A, Gross-Hardt R, Geiges B, Sarkar A, Breuninger H, Herrmann M, Laux T (2004) Expression dynamics of WOX genes mark cell fate decisions during early embryonic patterning in *Arabidopsis thaliana*. *Development* 131(3): 657-668

- Hamann T, Benková E, Bäurle I, Kientz M, Jürgens G (2002) The Arabidopsis *BODENLOS* gene encodes an auxin response protein inhibiting MONOPTEROS-mediated embryo patterning. *Genes & Development* 16(13): 1610-1615
- He J, Duan Y, Hua D, Fan G, Wang L, Liu Y, Chen Z, Han L, Qu LJ, Gong Z (2012) DEXH box RNA helicase-mediated mitochondrial reactive oxygen species production in Arabidopsis mediates crosstalk between abscisic acid and auxin signaling. *The Plant Cell* 24(5): 1815-1833
- Heidstra R, Welch D, Scheres B (2004) Mosaic analyses using marked activation and deletion clones dissect Arabidopsis *SCARECROW* action in asymmetric cell division. *Genes & Development* 18(16): 1964-1969
- Helariutta Y, Fukaki H, Wysocka-Diller J, Nakajima K, Jung J, Sena G, Hauser M, Benfey PN (2000) The *SHORT-ROOT* gene controls radial patterning of the Arabidopsis root through radial signalling. *Cell* 101(5): 555-567
- Hicks DB and Donaldson RP (1982) Electron transport in glyoxysomal membranes. *Archives of Biochemistry and Biophysics* 215(1): 280-288.
- Hobe M, Müller R, Grünewald M, Brand U, Simon R (2003) Loss of *CLE40*, a protein functionally equivalent to the stem cell restricting signal *CLV3*, enhances root waving in Arabidopsis. *Development Genes and Evolution* 213(8): 371-381
- Huang LC, Kohashi C, Vangundy R, Murashige T (1995) Effects of common components on hardness of culture media prepared with gelrite™. *In Vitro Cellular & Developmental Biology – Plant* 31(2): 84-89
- Inukai Y, Sakamoto T, Ueguchi-Tanaka M, Shibata Y, Gomi K, Umemura I, Hasegawa Y, Ashikari M, Kitano H, Matsuoka M (2005) *Crown rootless1*, which is essential for crown root formation in rice, is a target of an *AUXIN RESPONSE FACTOR* in auxin signaling. *The Plant Cell* 17(5): 1387-1396
- Jackson MB (1985) Ethylene and responses of plants to waterlogging and submergence. *Annual Review of Plant Physiology* 36(1): 145-174
- Jackson MB (2008) Ethylene-promoted elongation: An adaptation to submergence stress. *Annals of Botany* 101(2): 229-248
- Jambunathan N (2010) Determination and detection of reactive oxygen species (ROS), lipid peroxidation, and electrolyte leakage in plants. *Plant Stress Tolerance* 639(Methods and Protocols): 291-297
- Jefferson RA, Kavanagh TA, Bevan MW (1987) *GUS* fusions: Beta-glucuronidase as a sensitive and versatile gene fusion marker in higher plants. *The EMBO Journal* 6(13): 3901-3907

- Jin K, Shen J, Ashton RW, Dodd IC, Parry MA, Whalley WR (2013) How do roots elongate in a structured soil? *Journal of Experimental Botany* 64(15): 4761-4777
- Karuppanapandian T, Moon JC, Kim C, Manoharan K, Kim W (2011) Reactive oxygen species in plants: Their generation, signal transduction, and scavenging mechanisms. *Australian Journal of Crop Science* 5(6): 709-725
- Kende H (1993) Ethylene biosynthesis. *Annual Review of Plant Biology* 44(1): 283-307
- Kende H, Van der Knaap E, Cho H (1998) Deepwater rice: A model plant to study stem elongation. *Plant Physiology* 118(4): 1105–1110
- Kieber JJ, Rothenberg M, Roman G, Feldmann KA, Ecker JR (1993) CTR1, a negative regulator of the ethylene response pathway in Arabidopsis, encodes a member of the Raf family of protein kinases. *Cell* 72(3): 427-441
- Kitomi Y, Ogawa A, Kitano H, Inukai Y (2008) CRL4 regulates crown root formation through auxin transport in rice. *Plant Root* 2: 19-28
- Kitomi Y, Ito H, Hobo T, Aya K, Kitano H, Inukai Y (2011) The auxin responsive AP2/ERF transcription factor CROWN ROOTLESS5 is involved in crown root initiation in rice through the induction of OsRR1, a type-A response regulator of cytokinin signaling. *The Plant Journal* 67(3): 472-484
- Kong X, Lu S, Tian H, Ding Z (2015) WOX5 is shining in the root stem cell niche. *Trends in Plant Science* 20(10): 601-603
- Kumpf RP and Nowack MK (2015) The root cap: A short story of life and death. *Journal of Experimental Botany* 66(19): 5651-5662
- Latrasse D, Benhamed M, Bergounioux C, Raynaud C, Delarue M (2016) Plant programmed cell death from a chromatin point of view. *Journal of Experimental Botany* 67(20): 5887-5900
- Laufs P, Grandjean O, Jonak C, Kiêu K, Traas J (1998) Cellular parameters of the shoot apical meristem in Arabidopsis. *The Plant Cell* 10(8): 1375-1389
- Laux T, Mayer KF, Berger J, Jürgens G (1996) The WUSCHEL gene is required for shoot and floral meristem integrity in Arabidopsis. *Development* 122(1): 87-96
- Lavenus J, Goh T, Roberts I, Guyomarc'h S, Lucas M, De Smet I, Fukaki H, Beeckman T, Bennett M, Laplaze L (2013) Lateral root development in Arabidopsis: Fifty shades of auxin. *Trends in Plant Science* 18(8): 450-458
- Lenhard M, Bohnert A, Jürgens G, Laux T (2001) Termination of stem cell maintenance in Arabidopsis floral meristems by interactions between WUSCHEL and AGAMOUS. *Cell* 105(6): 805-814

- Liu H, Wang S, Yu X, Yu J, He X, Zhang S, Shou H, Wu P (2005) ARL1, a LOB-domain protein required for adventitious root formation in rice. *The Plant Journal* 43(1): 47–56
- Liu S, Wang J, Wang L, Wang X, Xue Y, Wu P, Shou H (2009) Adventitious root formation in rice requires OsGNOM1 and is mediated by the OsPINs family. *Cell Research* 19(9): 1110-1119
- Ljung K, Hull AK, Celenza J, Yamada M, Estelle M, Normanly J, Sandberg G (2005) Sites and regulation of auxin biosynthesis in Arabidopsis roots. *The Plant Cell* 17(4): 1090-1104
- López-Huertas E, Corpas FJ, Sandalio LM, Del Río LA (1999) Characterization of membrane polypeptides from pea leaf peroxisomes involved in superoxide radical generation. *The Biochemical Journal* 337(3): 531-536
- Lorbiecke R and Sauter M (1999) Adventitious root growth and cell-cycle induction in deepwater rice. *Plant Physiology* 119(1):21-30
- Lucas M, Godin C, Jay-Allemand C, Laplaze L (2008) Auxin fluxes in the root apex co-regulate gravitropism and lateral root initiation. *Journal of Experimental Botany* 59(1): 55-66
- Lucas M, Swarup R, Paponov IA, Swarup K, Casimiro I, Lake D, Peret B, Zappala S, Mairhofer S, Whitworth M, Wang J, Ljung K, Marchant A, Sandberg G, Holdsworth MJ, Palme K, Pridmore T, Mooney S, Bennett MJ (2011) SHORT-ROOT regulates primary, lateral and adventitious root development in Arabidopsis. *Plant Physiology* 155(1): 384-398
- Mallory AC, Bartel DP, Bartel B (2005) MicroRNA-directed regulation of Arabidopsis AUXIN RESPONSE FACTOR17 is essential for proper development and modulates expression of early auxin response genes. *The Plant Cell* 17(5): 1360-1375
- Mano S, Nakamori C, Hayashi M, Kato A, Kondo M, Nishimura M (2002) Distribution and characterization of peroxisomes in Arabidopsis by visualization with GFP: Dynamic morphology and actin-dependent movement. *Plant and Cell Physiology* 43(3): 331-341
- Mansfield SG and Briarty LG (1996) The dynamics of seedling and cotyledon cell development in *Arabidopsis thaliana* during reserve mobilization. *International Journal of Plant Sciences* 157(3): 280-295
- Marin E, Jouannet V, Herz A, Lokerse AS, Weijers D, Vaucheret H, Nussaume L, Crespi MD, Maizel A (2010) miR390, Arabidopsis TAS3 tasiRNAs, and their AUXIN RESPONSE FACTOR targets define an autoregulatory network quantitatively regulating lateral root growth. *The Plant Cell* 22(4): 1104-1117
- Masubelele NH, Dewitte W, Menges M, Maughan S, Collins C, Huntley R, Nieuwland J, Scofield S, Murray JAH (2005) D-type cyclins activate division

- in the root apex to promote seed germination in *Arabidopsis*. *Proceedings of the National Academy of Sciences* 102(43): 15694-15699
- Mergemann H, Sauter M (2000) Ethylene induces epidermal cell death at the site of adventitious root emergence in rice. *Plant Physiology* 124(2): 609-14.
- Migliaccio F and Piconese S (2001) Spiralizations and tropisms in *Arabidopsis* roots. *Trends in Plant Science* 6(12): 561–565
- Mittler R (2017) ROS Are Good. *Trends in Plant Science* 22(1): 11-19
- Mizukami Y and Ma H (1992) Ectopic expression of the floral homeotic gene *AGAMOUS* in transgenic *Arabidopsis* plants alters floral organ identity. *Cell* 71(1): 119-131
- Monfared MM, Carles CC, Rossignol P, Pires HR, Fletcher JC (2013) The *ULT1* and *ULT2* *trxG* genes play overlapping roles in *Arabidopsis* development and gene regulation. *Molecular Plant* 6(5): 1564-79
- Monshausen GB and Gilroy S (2009) Feeling green: Mechanosensing in plants. *Trends in Cell Biology* 19(5): 228-235
- Monshausen GB and Haswell E (2013) A force of nature: Molecular mechanisms of mechanoperception in plants. *Journal of Experimental Botany* 64(15): 4663-4680
- Morgan DO (2007) *The cell cycle: Principles of control*. New Science Press
- Murashige T and Skoog F (1962) A revised medium for rapid growth and bioassays with tobacco tissue cultures. *Physiologia Plantarum* 15(3):473-497
- Nakajima K, Sena G, Nawy T, Benfey PN (2001) Intercellular movement of the putative transcription factor *SHR* in root patterning. *Nature* 413(6853): 307-311
- Nieuwland J, Stamm P, Wen B, Randall RS, Murray JAH, Bassel GW (2016) Re-induction of the cell cycle in the *Arabidopsis* post-embryonic root meristem is ABA-insensitive, GA-dependent and repressed by *KRP6*. *Scientific Reports* 6: 23586
- Okamoto T, Tsurumi S, Shibasaki K, Obana Y, Takaji H, Oono Y, Rahman A (2008) Genetic dissection of hormonal responses in roots of *Arabidopsis* grown under continuous mechanical impedance. *Plant Physiology* 146(4): 1651-1662
- Oliva M and Dunand C (2007) Waving and skewing: How gravity and the surface of growth media affect root development in *Arabidopsis*. *New Phytologist* 176(1): 37-43

- Olsen LJ, Ettinger WF, Damsz B, Matsudaira K, Webb MA, Harada JJ (1993) Targeting of glyoxysomal proteins to peroxisomes in leaves and roots of a higher plant. *The Plant Cell* 5(8): 941-952
- Olsen LJ (1998) The surprising complexity of peroxisome biogenesis. *Plant Molecular Biology* 38(1-2): 163-189
- Paz Sanchez M, Aceves-García P, Petrone E, Steckenborn S, Vega-León R, Álvarez-Buylla ER, Garay-Arroyo A, García-Ponce B (2015) The impact of Polycomb group (PcG) and Trithorax group (TrxG) epigenetic factors in plant plasticity. *New Phytologist* 208(3): 684-694
- Péret B, Li G, Zhao J, Band LR, Voß U, Postaire O, Luu D, Da Ines O, Casimiro I, Lucas M, Wells DM, Lazzerini L, Nacry P, King JR, Jensen OE, Schäffner AR, Maurel C, Bennett MJ (2012) Auxin regulates aquaporin function to facilitate lateral root emergence. *Nature Cell Biology* 14(10): 991–998
- Pillitteri LJ, Guo X, Dong J (2016) Asymmetric cell division in plants: Mechanisms of symmetry breaking and cell fate determination. *Cellular and Molecular Life Science: CMLS* 73(22): 4213-4229
- Pires HR, Monfared MM, Shemyakina EA, Fletcher JC (2014) ULTRAPETALA *trxG* genes interact with KANADI transcription factor genes to regulate *Arabidopsis* gynoecium patterning. *The Plant Cell* 26(11):4345-4361
- Poethig RS (2003) Phase change and the regulation of developmental timing in plants. *Science* 301(5631): 334-336
- Pop TI, Pamfil D, Bellini C (2011) Auxin control in the formation of adventitious roots. *Notulae Botanicae Horti Agrobotanici Cluj-Napoca* 39(1): 307-316
- Potocka I, Szymanowska-Pułka J, Karczewski J, Nakielski J (2011) Effect of mechanical stress on *Zea* root apex. I. Mechanical stress leads to the switch from closed to open meristem organization. *Journal of Experimental Botany* 62(13): 4583-4593
- Pu L, Liu MS, Kim SY, Chen LF, Fletcher JC, Sung ZR (2013) EMBRYONIC FLOWER1 and ULTRAPETALA1 act antagonistically on *Arabidopsis* development and stress response. *Plant Physiology* 162(2): 812-830
- Rasmusson AG, Soole KL, Elthon TE (2004) Alternative NAD (P) H dehydrogenases of plant mitochondria. *Annual Review of Plant Biology* 55: 23-39
- Rhoades MW, Reinhart BJ, Lim LP, Burge CB, Bartel B, Bartel DP (2002) Prediction of plant microRNA targets. *Cell* 110(4): 513-520
- Richter GL, Monshausen GB, Krol A, Gilroy S (2009) Mechanical stimuli modulate lateral root organogenesis. *Plant Physiology* 151(4): 1855-1866

- Roeder AHK and Janofsky MF (2006) Fruit development in Arabidopsis. The Arabidopsis Book: e0075
- Rosa S, Ntoukakis V, Ohmido N, Pendle A, Abranches R, Shaw P (2014) Cell differentiation and development in Arabidopsis are associated with changes in histone dynamics at the single-cell level. *The Plant Cell* 26(12): 4821-4833
- Sabatini S, Beis D, Wolkenfelt H, Murfett J, Guilfoyle T, Malamy J, Benfey P, Leyser O, Bechtold N, Weisbeek P, Scheres B (1999) An auxin-dependent distal organizer of pattern and polarity in the Arabidopsis root. *Cell* 99(5): 463-472
- Sabatini S, Heidstra R, Wildwater M, Scheres B (2003) SCARECROW is involved in positioning the stem cell niche in the Arabidopsis root meristem. *Genes & Development* 17(3): 354-358
- Sabelli PA, Liu Y, Dante RA, Lizarraga LE, Nguyen HN, Brown SW, Klingler JP, Yu J, LaBrant E, Layton TM, Feldman M, Larkins BA (2013) Control of cell proliferation, endoreduplication, cell size, and cell death by the retinoblastoma-related pathway in maize endosperm. *Proceedings of the National Academy of Sciences* 110(19): E1827–E1836
- Sablowski R (2007) Flowering and determinacy in Arabidopsis. *Journal of Experimental Botany* 58(5): 899-907
- Santisree P, Nongmaithem S, Vasuki H, Sreelakshmi Y, Ivanchenko MG, Sharma R (2011) Tomato root penetration in soil requires a coaction between ethylene and auxin signaling. *Plant Physiology* 156(3): 1424-1438
- Sarkar AK, Luijten M, Miyashima S, Lenhard M, Hashimoto T, Nakajima K, Scheres B, Heidstra R, Laux T (2007) Conserved factors regulate signalling in *Arabidopsis thaliana* shoot and root stem cell organizers. *Nature* 446(7137): 811–814
- Sato EM, Hijazi H, Bennett MJ, Vissenberg K, Swarup R (2015) New insights into root gravitropic signalling. *Journal of Experimental Botany* 66(8): 2155-2165
- Sauter M and Kende H (1992) Gibberellin-induced growth and regulation of the cell division cycle in deepwater rice. *Planta* 188(3): 362-368
- Sauter M, Mekhedov SL, Kende H (1995) Gibberellin promotes histone H1 kinase activity and the expression of cdc2 and cyclin genes during the induction of rapid growth in deepwater rice internodes. *The Plant Journal* 7(4): 623-632
- Schertl P and Braun HP (2014) Respiratory electron transfer pathways in plant mitochondria. *Frontiers in Plant Science* 5(163): 7
- Schneider CA, Rasband WS, Eliceiri KW (2012) NIH Image to ImageJ: 25 years of image analysis. *Nature methods* 9(7): 671-675

- Sisler EC and Serek M (2003) Compounds interacting with the ethylene receptor in plants. *Plant Biology* 5(5): 473-480
- Sliwinska E, Bassel GW, Bewley JD (2009) Germination of *Arabidopsis thaliana* seeds is not completed as a result of elongation of the radicle but of the adjacent transition zone and lower hypocotyl. *Journal of Experimental Botany* 60(12): 3587-3594
- Sorin C, Bussell JD, Camus I, Ljung K, Kowalczyk M, Geiss G, McKhann H, Garcion C, Vaucheret H, Sandberg G, Bellini C (2005) Auxin and light control of adventitious rooting in *Arabidopsis* require ARGONAUTE1. *The Plant Cell* 17(5): 1343-1359
- Stahl Y, Wink RH, Ingram GC, Simon R (2009) A signaling module controlling the stem cell niche in *Arabidopsis* root meristems. *Current Biology* 19(11): 909-914
- Stahl Y, Grabowski S, Bleckmann A, Kühnemuth R, Weidtkamp-Peters S, Pinto KG, Kirschner GK, Schmid JB, Wink RH, Hülsewede A, Felekyan S, Seidel CAM, Simon R (2013) Moderation of *Arabidopsis* root stemness by CLAVATA1 and ARABIDOPSIS CRINKLY4 receptor kinase complexes. *Current Biology* 23(5): 362–371
- Steffens B and Sauter M (2005) Epidermal cell death in rice is regulated by ethylene, gibberellin and abscisic acid. *Plant Physiology* 139(2): 713-721
- Steffens B, Wang J, Sauter M (2006) Interactions between ethylene, gibberellin and abscisic acid regulate emergence and growth rate of adventitious roots in deepwater rice. *Planta* 223(3): 604-612
- Steffens B and Sauter M (2009) Epidermal cell death in rice is confined to cells with a distinct molecular identity and is mediated by ethylene and H₂O₂ through an autoamplified signal pathway. *The Plant Cell* 21(1): 184-196
- Steffens B, Kovalev A, Gorb SN, Sauter M (2012) Emerging roots alter epidermal cell fate through mechanical and reactive oxygen species signaling. *The Plant Cell* 24(8): 3296-3306
- Steffens B and Rasmussen A (2016) The physiology of adventitious roots. *Plant Physiology* 170 (2): 603-617
- Strader LC and Bartel B (2011) Transport and metabolism of the endogenous auxin precursor indole-3-butyric acid. *Molecular Plant* 4(3): 477-486
- Sukumar P, Maloney GS, Muday GK (2013) Localized induction of the ATP-binding cassette B19 auxin transporter enhances adventitious root formation in *Arabidopsis*. *Plant Physiology* 162(3): 1392-1405
- Swarup K, Benková E, Swarup R, Casimiro I, Péret B, Yang Y, Parry G, Nielsen E, De Smet I, Vanneste S, Levesque MP, Carrier D, James N, Calvo V, Ljung

- K, Kramer E, Roberts R, Graham N, Marillonnet S, Patel K, Jones JDG, Taylor CG, Schachtman DP, May S, Sandberg G, Benfey P, Friml J, Kerr I, Beeckman T, Laplaze L, Bennett MJ (2008) The auxin influx carrier LAX3 promotes lateral root emergence. *Nature Cell Biology* 10(8): 946-954
- Swarup R, Kramer EM, Perry O, Knox K, Leyser HMO, Haseloff J, Beemster GTS, Bhalerao R, Bennett MJ (2005) Root gravitropism requires lateral root cap and epidermal cells for transport and response to a mobile auxin signal. *Nature Cell Biology* 7(11): 1057 - 1065
- Takahashi F, Sato-Nara K, Kobayashi K, Suzuki M, Suzuki H (2003) Sugar-induced adventitious roots in *Arabidopsis* seedlings. *Journal of Plant Research* 116(2): 83–91
- Takatsuka H and Umeda M (2014) Hormonal control of cell division and elongation along differentiation trajectories in roots. *Journal of Experimental Botany* 65(10): 2633-2643
- Thompson MV and Holbrook NM (2004) Root-gel interactions and the root waving behavior of *Arabidopsis*. *Plant Physiology* 135(3): 1822–1837
- Tian H, De Smet I, Ding Z (2014) Shaping a root system: Regulating lateral versus primary root growth. *Trends in Plant Science* 19(7): 426-431
- Tognetti VB, Mühlenbock P, Van Breusegem F (2012) Stress homeostasis - the redox and auxin perspective. *Plant, Cell & Environment* 35(2): 321-333
- Truernit E, Bauby H, Dubreucq B, Grandjean O, Runions J, Barthélémy J, Palauqui J (2008) High-resolution whole-mount imaging of three-dimensional tissue organization and gene expression enables the study of phloem development and structure in *Arabidopsis*. *The Plant Cell* 20(6): 1494-1503
- Turrens JF (2003) Mitochondrial formation of reactive oxygen species. *The Journal of physiology* 552(2): 335-344
- Ulmasov T, Murfett J, Hagen G, Guilfoyle TJ (1997) Aux/IAA proteins repress expression of reporter genes containing natural and highly active synthetic auxin response elements. *The Plant Cell* 9(11): 1963-1971
- Van den Berg, Willemsen V, Hage W, Weisbeek P, Scheres B (1995) Cell fate in the *Arabidopsis* root meristem determined by directional signalling. *Nature* 378(6552): 62-65
- Verbelen JP, De Cnodder T, Le J, Vissenberg K, Baluška F (2006) The root apex of *Arabidopsis thaliana* consists of four distinct zones of growth activities. *Plant Signaling & Behavior* 1(6): 296-304
- Verstraeten I, Schotte S, Geelen D (2014) Hypocotyl adventitious root organogenesis differs from lateral root development. *Frontiers in Plant Science* 5: 495

- Vicré M, Santaella C, Blanchet S, Gateau A, Driouich A (2005) Root border-like cells of *Arabidopsis*. Microscopical characterization and role in the interaction with Rhizobacteria. *Plant Physiology* 138(2): 998-1008
- Voinnet O (2009) Origin, biogenesis, and activity of plant microRNAs. *Cell* 136(4): 669-687
- Wallström SV, Florez-Sarasa I, Araújo WL, Escobar MA, Geisler DA, Aidemark M, Lager I, Fernie AR, Ribas-Carbó M, Rasmusson AG (2014) Suppression of NDA-type alternative mitochondrial NAD (P) H dehydrogenases in *Arabidopsis thaliana* modifies growth and metabolism, but not high light stimulation of mitochondrial electron transport. *Plant and Cell Physiology* 55(5): 881-896
- Wang JW, Wang LJ, Mao YB, Cai WJ, Xue HW, Chen XY (2005) Control of root cap formation by microRNA-targeted auxin response factors in *Arabidopsis*. *The Plant Cell* 17(8): 2204-2216
- Wang W, Fang H, Groom L, Cheng A, Zhang W, Liu J, Wang X, Li K, Han P, Zheng M, Yin J, Wang W, Mattson MP, Kao JPY, Lakatta EG, Sheu SS, Ouyang K, Chen J, Dirksen RT, Cheng H (2008) Superoxide flashes in single mitochondria. *Cell* 134(2): 279-290
- Wang Z, Gerstein M, Snyder M (2009) RNA-Seq: A revolutionary tool for transcriptomics. *Nature Reviews Genetics* 10(1): 57-63
- Weigel D and Glazebrook J (2002) *Arabidopsis: A laboratory manual*. Cold Spring Harbor Laboratory Press
- Weigel D and Jürgens G (2002) Stem cells that make stems. *Nature* 415(6873): 751-754
- Welch D, Hassan H, Blilou I, Immink R, Heidstra R, Scheres B (2007) *Arabidopsis* JACKDAW and MAGPIE zinc finger proteins delimit asymmetric cell division and stabilize tissue boundaries by restricting SHORT-ROOT action. *Genes & Development* 21(17): 2196-2204
- Willemsen V, Bauch M, Bennett T, Campilho A, Wolkenfelt H, Xu J, Haseloff J, Scheres B (2008) The NAC domain transcription factors FEZ and SOMBRERO control the orientation of cell division plane in *Arabidopsis* root stem cells. *Developmental Cell* 15(6): 913-922
- Wojciak JM and Clubb RT (2001) Finding the function buried in SAND. *Nature Structural Biology* 8(7): 568-570
- Wu G, Lewis DR, Spalding EP (2007) Mutations in *Arabidopsis* multidrug resistance-like ABC transporters separate the roles of acropetal and basipetal auxin transport in lateral root development. *The Plant Cell* 19(6): 1826-1837

- Xuan W, Band LR, Kumpf RP, Van Damme D, Parizot B, De Rop G, Opdenacker D, Möller BK, Skorzinski N, Njo MF, De Rybel B, Audenaert D, Nowack MK, Vanneste S, Beeckman T (2016) Cyclic programmed cell death stimulates hormone signaling and root development in Arabidopsis. *Science* 351(6271): 384-387
- Yang L, Zhang J, He J, Qin Y, Hua D, Duan Y, Chen Z, Gong Z (2014) ABA-mediated ROS in mitochondria regulate root meristem activity by controlling PLETHORA expression in Arabidopsis. *PLoS Genetics* 10(12): e1004791
- Zarembinski TI and Theologis A (1993) Anaerobiosis and plant growth hormones induce two genes encoding 1-aminocyclopropane-1-carboxylate synthase in rice (*Oryza sativa* L.). *Molecular Biology of the Cell* 4(4): 363-373
- Zebell SG and Dong X (2015) Cell cycle regulators and cell death in immunity. *Host & Microbe* 18(4): 402–407
- Zhao J, Morozova N, Williams L, Libs L, Avivi Y, Grafi G (2001) Two phases of chromatin decondensation during dedifferentiation of plant cells: Distinction between competence for cell fate switch and a commitment for S phase. *The Journal of Biological Chemistry* 276(25): 22772-22778
- Zhao XY, Su YH, Cheng ZJ, Zhang XS (2008) Cell fate switch during in vitro plant organogenesis. *Journal of Integrative Plant Biology* 50(7): 816-824

10 SUPPLEMENTAL DATA

AtULT1 and to a minor degree AtULT2 are described to control stem cell fate in shoots and flowers through regulation of the key homeotic genes *AGAMOUS* (*AG*) and *APETALA2* (*AP2*) (Carles and Fletcher 2009). In consequence, plants lacking AtULT1 show slower bolting and produce supernumerous flower organs (Fletcher 2001, Carles et al., 2005; Monfared et al., 2013). Increased floral organ number and delayed bolting time was verified for the *ult1-3* and *ult1-3 ult2-1* lines used in this study (Figure S1). Wildtype flowers are composed of 4 whorls. From the outside to the inside the whorls consists of 4 sepals, 4 petals, 6 stamens and 2 carpels fused to a central gynoecium (Figure S1 A and B). The number of carpels was not analysed. Compared to wildtype, stamina number of *ult1-3* and *ult1-3 ult2-1* flowers was more variable. On average 6 stamens were counted in each genotype. An increased number of sepals and petals was observed in *ult1-3* and *ult1-3 ult2-1* flowers. *ult1-3* plants needed 4.4 and *ult1-3 ult2-1* 11.5 more days until bolting (Figure S1 C and D). Wildtype plants started to bolt after 24.1 days.

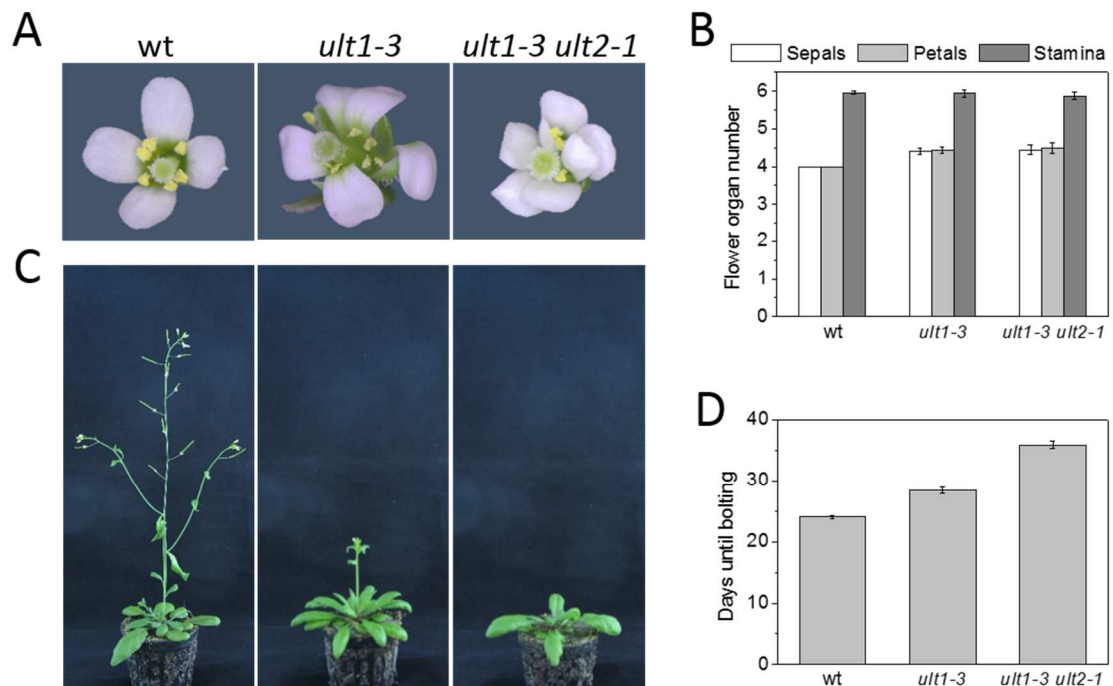


Figure S1: *AtULT1* restricts shoot and floral meristem determination in *Arabidopsis thaliana*.

A and **B** Inflorescences of *ult1-3* and *ult1-3 ult2-1* plants developed extra floral organs. Flower phenotypes of wildtype (wt) and *AtULT1* knockout lines (*ult1-3*, *ult1-3 ult2-1*) are shown (A). Mean numbers (\pm SE; n=41-54) of sepals, petals and stamens were determined in up to 5 of the first flower buds of wildtype (wt), *ult1-3* and *ult1-3 ult2-1* plants (B).

C and **D** *AtULT1* knockout causes delay of flowering time. Phenotypes of 35-day-old wildtype, *ult1-3* and *ult1-3 ult2-1* plants were illustrated and mean number of days to bolt (\pm SE; n=11-17) were calculated.

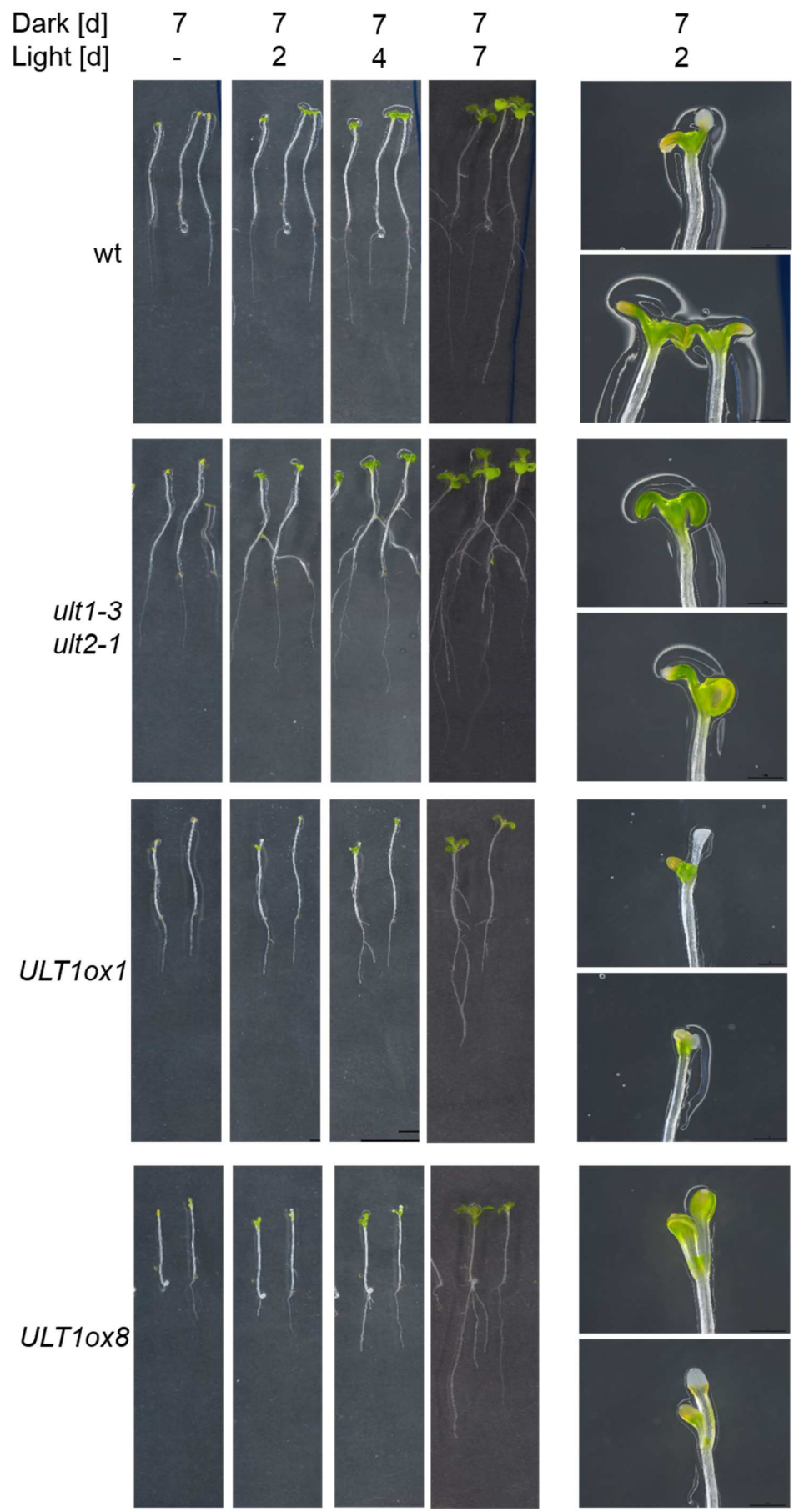


Figure S2: AtULT1 hinders de-etiolation and growth of seedlings experiencing illumination after prolonged darkness.

Development of 7 days dark grown wildtype (wt), *ult1-3 ult2-1* and *AtULT1* overexpressing seedlings (*ULT1ox*) was tracked 0, 2, 4 and 7 days after transfer to light. Constitutive *AtULT1* expression retards root growth, rosette expansion and cotyledon greening.

11 DECLARATION OF AUTHORSHIP

I hereby declare that I authored the presented thesis “Possible roles of ULTRAPETALA in root development” independently and that it is original and the result of my own investigation, with the following exceptions: advice was given by Prof. Dr. Margret Sauter on the manuscript and during experimentation. Experiments in the section 6.1: Sequence and expression analysis of ULTRAPETALA1 and ALTERNATIVE NAD (P) H DEHYDROGENASE A1 were partly performed by Karina Borisova. I did not use any other sources and aids than the indicated references. I declare that, to the best of my knowledge and belief, I followed the rules for Good Scientific Practice as detailed in the recommendations of the Deutsche Forschungsgemeinschaft. This thesis has not been submitted, either in part or whole, at this or any other University.

Kiel,

Melanie Demuth

12 CURRICULUM VITAE

Personal information

Name: Melanie Demuth
Date of birth: 03.07.1985
Place of birth: Erfurt, Germany
Nationality: German

Education

10.2012 – 03.2017 PhD student
Research unit Plant Developmental Biology and
Physiology
Christian-Albrechts-University, Kiel University

08.2011 – 06.2012 Diploma thesis
Research unit Plant Developmental Biology and
Physiology
Christian-Albrechts-University, Kiel University
“Analysen zum epidermalen Zelltod in Reis”

10. 2003 – 05.2012 Undergraduate and graduate studies
in cell biology, microbiology and forensic medicine
Christian-Albrechts-University, Kiel University

08.1995 – 06.2003 Abitur (equivalent to A-level)
Heinrich-Mann Gymnasium Erfurt

Professional experience

11.2011 – 11.2011	Students employee at Botanical Institute Kiel University
08.2011 – 09.2011	Students employee at Botanical Institute, Kiel University
10.2007 – 12.2007	Students employee at Botanical Institute, Kiel University
04.2007 – 07.2007	Students employee at Botanical Institute Kiel University
10.2006 – 12.2006	Students employee at Institute of Phytopathology, Kiel University
04.2006 – 07.2006	Students employee at Botanical Institute, Kiel University

Memberships

German Genetics Society